1994

Pulsed electrochemical detection for the investigation and determination of amine compounds separated by high performance liquid chromatography

David Allen Dobberpuhl
Iowa State University

Order Number 9503546

Pulsed electrochemical detection for the investigation and determination of amine compounds separated by high-performance liquid chromatography

Dobberpuhl, David Allen, Ph.D.

Iowa State University, 1994

U·M·I
300 N. Zeeb Rd.
Ann Arbor, MI 48106

Pulsed electrochemical detection for the investigation and determination of amine compounds separated by high performance liquid chromatography

by

David Allen Dobberpuhl

A Dissertation Submitted to the

Graduate Faculty in Partial Fulfillment of the

Requirements for the Degree of

DOCTOR OF PHILOSOPHY

Department: Chemistry
Major: Analytical Chemistry

Approved:

Signature was redacted for privacy.

In Charge of Major Work

Signature was redacted for privacy.

For the Major Department

Signature was redacted for privacy.

For the Graduate College

Iowa State University
Ames, Iowa

1994

DEDICATION

To my wife, Annie, who has provided me with love, encouragement and support.

TABLE OF CONTENTS

GENERAL INTRODUCTION

Explanation of the dissertation format. In addition to the general introduction and conclusions, this dissertation contains four separate papers. Each paper is to be submitted for publication in a refereed analytical chemistry journal, and each paper follows the general format of the journal in which it is to appear. The four papers are preceded by this general introduction and are followed by the general conclusions and acknowledgements. References cited in the general introduction and general conclusions will follow the general conclusions section.

The research described in this dissertation was performed under the direction of Professor Dennis C. Johnson beginning in December of 1989. Paper 1 describes the pulsed electrochemical detection (PED) of amino alcohols separated by high performance liquid chromatography (HPLC). A multimodal HPLC column permits the separation of alkanolamines based on both reverse-phase and cation-exchange retention mechanisms, and baseline resolution of alkanolamine isomers is demonstrated. The application of HPLC-PED to amines and diamines is the focus of Paper 2, with separations performed using several different columns and mobile phases. Guidelines are provided for selecting the optimum PED waveform for each class of compounds, based upon results from both linear scan (cyclic) and pulsed voltammetry.

Paper 3 describes the application of PED to the ring of a Au rotating ring-disk electrode (RRDE). Since PED at the ring of an RRDE is a novel application of pulsed detection, the first portion of the paper is devoted to validating the technique by

comparing the PED response for ferrocyanide, a compound with well-known voltammetric behavior, to the results from constant potential (DC) detection and RRDE theory. The rest of the paper describes the results obtained when the technique is used to monitor the adsorption of amine compounds at Au as a function of the electrode potential. A qualitative description of adsorption is provided for aliphatic amines, alkanolamines, and an amino acid, glycine. The results are discussed with respect to selecting a PED waveform for the HPLC of aliphatic amines. By designing the PED waveform to maximize adsorption, a ten-fold improvement in the signal-to-noise ratio is obtained.

The electrochemical behavior of ethylamine at Au in alkaline solutions is the subject of Paper 4, which continues development of the technique first described in Paper 3, PED at the ring of an RRDE. Ring response from PED is combined with cyclic voltammetry at the disk to provide a semi-quantitative description of the processes resulting in the oxidation of ethylamine at Au. The results are used to emphasize the contribution of adsorption to the overall anodic signal. Ethylamine is found to undergo two types of adsorption, with one occurring directly to the reduced Au surface, and the other through co-adsorption with hydroxide (OH^-).

Oxidation of aliphatic amines at metal electrodes. Many aliphatic compounds, including amines, traditionally have been considered as being inactive at metal electrodes. Adams [1] stated that "...aliphatic amines are difficult to anodically oxidize in any quantitative fashion" at solid metal electrodes, and Malfoy and Reynaud [2] concluded: "Among the 20 amino acids not containing sulfur atoms, present in the proteins, only tryptophan and tyrosine are selectively oxidizable at solid electrodes." It perhaps was not

coincidental that Malfoy and Reynaud made this comment in a paper studying amino acid oxidation at Au, a noble metal that has no empty d-orbitals to facilitate interaction with the lone-pair electrons of amines and thus promote reactivity.

Despite their apparent lack of reactivity, the oxidation of amine compounds has been studied at various metals, including Cu [3 - 6], Ag [6 - 9], Ni [6, 10, 11], and Co [6, 11, 12]. For these studies, amine reactivity was generally not observed at the reduced metal. However, amine reactivity was attained after a layer of catalytic surface oxide had been formed, often by carefully pre-treating the electrode prior to placing it in solution. Aliphatic amines also were studied at Pt by Mann *et al.*[13, 14], who was one of the first to determine the products of amine oxidation. At Pt, the oxidation of primary amines resulted in the formation of an aldehyde. The following (abbreviated) reaction mechanism was proposed by Mann to account for the experimental findings:

$$RCH_2\dot{\ddot{N}}H_2 \rightarrow RCH_2\dot{N}H_2^+ + e^- \quad (1)$$

$$RCH_2\dot{N}H_2^+ \rightarrow RCH\dot{N}H_2 + H^+ \quad (2)$$

$$RCH\dot{N}H_2 \rightarrow RCH{=}NH_2^+ + e^- \quad (3)$$

$$RCH{=}NH_2^+ + H_2O \rightarrow RCHO + NH_3 + H^+ \quad (4a)$$

with the labile imine formed in Step 3 ultimately resulting in the cleavage of the C-N bond.

Hampson and co-workers determined that the product formed from the oxidation of amines at oxidized Ag depended upon experimental conditions [9]. At high

concentrations of hydroxide (2.0 M or greater) and relatively low electrode potentials (e.g., 0.64 V vs NHE) the major product was an aldehyde. However, under most conditions the primary product was a nitrile. A mechanism was proposed for the experimental findings in which the first steps were similar to the first three steps of Mann's mechanism for the formation of the aldehyde, but then deviating at Step 4 to account for the formation of the nitrile.

$$RCH{=}NH_2^+ \rightarrow RCH{=}\ddot{\dot{N}}H + H^+ \qquad (4b)$$

$$RCH{=}\ddot{\dot{N}}H \rightarrow RCH{=}\dot{N}H^+ + e^- \qquad (5)$$

$$RCH{=}\dot{N}H^+ \rightarrow RCH{=}\dot{N}: + H^+ \qquad (6)$$

$$RCH{=}\dot{N}: \rightarrow RCH{=}N:^+ + e^- \qquad (7)$$

$$RCH{=}N:^+ \rightarrow RC{\equiv}N: + H^+ \qquad (8)$$

And studies at most other metal and metal oxide electrodes have found that the nitrile is the predominant oxidation product for primary amines [15].

There are only a limited number of studies describing the oxidation of aliphatic amine compounds at Au. Warren Jackson, in a paper co-authored with LaCourse, Dobberpuhl and Johnson, studied the voltammetric behavior of alkanolamines in alkaline conditions [16]. Jackson found that anodic current for alkanolamines was derived primarily from the conversion of the alcohol functional group to the carboxylic acid, with the oxidation of ethanolamine resulting in the formation of glycine. The electrochemistry of amino acids at Au has been investigated [2, 17, 18], but the apparent lack of response

for most amino acids has allowed only limited conclusions. Bogdanovskaya *et al.* identified the products of glycylglycine (HGG) oxidation, finding evidence for the formation of dimers resulting from the cleavage of HGG's terminal carboxylate group [17].

In general, with the exception of amino alcohols and amino sugars, the response for the amine compounds at Au is indicative of a reaction that is under kinetic control. More specifically, the oxidation of amines appears to require the concomitant formation of surface oxide. This suggests that amines must adsorb to the electrode surface with the catalytic oxide prior to or during the oxidation process. Such a mechanism has been proposed by Fleishman *et al.* for the reaction of amines in 1.0 M KOH [6]:

$$OH^- + \text{lower oxide} \rightleftharpoons \text{higher oxide} + H_2O + e^- \quad (9)$$

$$(\text{Amine})_{sol} \rightleftharpoons (\text{amine})_{ads} \quad (10)$$

$$(\text{Amine})_{ads} + \text{higher oxide} \xrightarrow{\text{H ABSTRACTION}} \text{radical intermediate} + \text{lower oxide} \quad (11)$$

$$\text{Radical intermediate} \rightarrow \text{product} + (n\text{-}1)\, e^- \quad (12)$$

where n is the total number of electrons transferred in the reaction. The adsorption of amines at noble metals has been the focus of several papers, most notably those of Horanyi and co-workers, who for many years studied the phenomenon at Pt [19 - 22], and more recently at Au [23-25] using radiotracer isotope techniques. Amine compounds were shown to have strong adsorption at Au in basic solutions and little or no adsorption in acidic media. Aliphatic amines and amino alcohols exhibited similar adsorptive behavior, which was cited as evidence that both classes of amines adsorb via the amine

moiety. The surface coverage of amine compounds was determined to be dependent upon electrode potential, and occurring at less positive potentials than where their oxidation takes place at Au. Horányi also found evidence for two different adsorption states, with one attributed to loosely physisorbed species and the other to chemisorbed species resulting from charge transfer [23].

The adsorptive behavior of amines again brings into question the state of the Au surface and its apparent ability to foster adsorption despite having no empty d-orbitals to facilitate the nucleophilic attack of the amine group's lone-pair electrons. Recent studies of Au surfaces have provided some indication as to how amine compounds might interact with the Au surface. Electrochemical and spectroscopic results indicate that, in alkaline solutions, hydroxide adsorption occurs at the Au surface at potentials approximately 0.6 V negative of the onset of oxide formation at Au [26-31]. The exact nature of hydroxide adsorption is still in question, with some authors attributing it to simple physisorption without charge transfer, while others believing it to be chemisorption with at least partial charge transfer. Whatever its nature, hydroxide adsorption, as with other types of anion adsorption, begins when the electrode potential is made positive of the point of zero charge (PZC).

Burke et al. [32-35] was one of the first to suggest that adsorption of hydroxide ion has a catalytic effect on the oxidation of aliphatic compounds at Au, and went on to suggest that this catalytic activity is through facilitated co-adsorption. This idea was supported by Vitt *et al.*[36] who demonstrated that the oxidation of several dissimilar compounds begins at the same potential for a Au electrode in alkaline conditions, and

concluded that the results are indicative of a surface-catalyzed oxidation in which AuOH is a participant. Vitt went on to propose an oxidation mechanism for aliphatic compounds that, like the mechanism of Fleishman [6], begins with the adsorption of OH^-. The catalytic ability of Au for compounds like aliphatic amines apparently is provided by the formation of surface hydrous oxides, which tend to be transient in nature. This perhaps explains the conclusions reached by some authors that Au and other metal electrodes are not electroactive for most amine compounds, since the oxidation of amines requires the continuous regeneration of these transient hydrous oxides. This is also the basis for pulsed electrochemical detection (PED) of amines, in which the conditions necessary to catalyze the oxidation of amines are continuously regenerated with each cycle of the PED waveform, thus allowing for a sensitive and reproducible anodic response.

Detection of amine compounds separated by HPLC. Because of their biological significance, amines are perhaps the subject of more HPLC studies than any other class of compounds. The majority of these studies, for obvious reasons, have been devoted to amino acids, with ensuing applications to other amine compounds often possible with only slight modifications of the separation and detection conditions. The detection of separated amines can be divided broadly into two categories depending upon whether or not derivatization is necessary to obtain reasonable signal. For underivatized amines, electrochemical detection using constant potential detection has been demonstrated at two different electrodes under flow-through conditions. Huber and co-workers used an oxidized Ni electrode for the detection of amino acids [37, 38], and several groups have

used oxidized Cu for the detection of a variety of amine compounds [39 - 41]. Although these electrode materials show that aliphatic amines can be electrochemically active at metal electrodes without derivatization, they have some drawbacks. The electrodes often require careful pre-treatment to achieve the catalytic form of the metal oxide responsible for amine oxidation. Also, the response tends to diminish significantly with continued use as catalytic activity is lost over time. Therefore, the majority of HPLC methods using electrochemical detection of aliphatic amine compounds have relied on pre- or post-column derivatization of the analytes with a electroactive adduct to provide response [42-44].

Because of the popularity of the UV/vis detector in HPLC, photometric detection has far superceded electrochemical and other forms of detection as the most common method of providing signal for amine compounds. Since aliphatic amine compounds are not natural chromophores or fluorophores, pre- or post-column derivatization with a spectroscopically-active adduct is necessary for photometric detection to be feasible. The first widely used derivatizing reagent for amines was ninhydrin [45 - 48], followed in more recent years by fluorescamine [49, 50], *o*-phthalaldehyde [51 - 53], 7-chloro-4-nitrobenzo-2-oxa-1,3-diazole (NBD chloride) [54, 55], phenylisothiocyanate [56 - 58], 5-dimethyl-aminonapthalene-1-sulfonyl (dansyl) chloride [59, 60], and 4-dimethylamino-azobenzene-4′-sulfonyl (dabsyl) chloride [61. 62]. Detection limits in the femtomole region are possible using flourescence detection with several of these reagents, but derivatization tends to introduce its own set of experimental difficulties and uncertainties. The derivatization procedure can be time-consuming and made difficult because different

analytes will complexe with varying efficiencies in different matrices. The derivatized complex is also often labile, so the response can be sensitive to variations in the chromatographic retention times or separation conditions.

The HPLC separation strategy used for aliphatic amine compounds depends on whether the analytes were derivatized prior to the separation procedure. Because aliphatic amines are hydrophilic, the HPLC techniques most commonly used for the separation of underivatized amines are based on ion-exchange or ion-pair chromatography. Normal-phase separations are also possible, but the mobile phases typically used with this type of HPLC often interfere with both electrochemical and photometric detection, thus making this strategy less appealing. With the prevalence of pre-colum derivatization, reverse-phase chromatography has become the predominant separation methods for amines. There are primarily two reasons for this. One, companies have been able to manufacture reverse-phase columns (C18, C8, etc.) of consistent uniformity, so that chromatographic results are highly reproducible. Two, the reagents used to derivatize amines are all large and relatively hydrophobic organic compounds, and so allow for significant retention on reverse-phase columns and thus make separations possible. However, as stated earlier, derivatization does come with some disadvantages, and so direct detection with other separation methods often may be preferrable.

HPLC-PED of amine compounds. Many aliphatic compounds, including amines, have been considered to be electro-inactive at metal electrodes. This is because either the reaction results in the adsorption of species which passivate, or "foul," the electrode

surface, or because the surface oxides which catalyze the reaction providing analytical signal are gradually exhausted with successive determinations. Pulsed electrochemical detection (PED) was introduced in 1983 by Hughes, Meschi and Johnson for the detection of aliphatic compounds separated by HPLC [63, 64]. The ability of PED to detect many compounds traditionally considered electro-inactive is provided by the multi-step potential waveform. This waveform continually regenerates the conditions responsible for providing signal at noble metal electrodes. PED has been shown to provide a reproducible and sensitive response for alcohols, carbohydrates and sulfur compounds, and since HPLC-PED has been the subject of several recent reviews [65 - 67], it will not be reviewed here except as related to the determination of amine compounds.

Polta and Johnson were the first to apply PED for the determination of amine compounds, specifically amino acids and amino sugars at a Pt working electrode [68, 69]. The Pt working electrode has been superceded in more recent years by the Au working electrode [70 - 72], which also has been shown to provide good signal for these compounds. For amino acids, a recent innovation of PED has scanned the detection potential into oxide formation and reduction during the detection step (E_{DET}). By integrating the current generated during the potential scan, better limits of detection have been demonstrated [72]. Vandeberg and Johnson used this derivative of PED, named integrated voltammetric detection (IVD), to specifically improve the response for sulfer-containing compounds, including sulfur-containing amino acids [73].

For alkanolamines, much of the initial work elucidating the voltammetric basis for

their response at Au was performed by a former member of our group, Warren Jackson, and the electrochemistry of alkanolamines was the focus of his dissertation [74] and a paper [16]. During his tenure at Iowa State, Jackson also co-authored a paper describing the PED of alkanolamines with separation provided by ion-pair reverse-phase liquid chromatography [75]. Cambell, Carson and Van Bramer also used HPLC-PED to determine diethanolamine (DEA) and triethanolamine (TEA) in an aluminum etching solution. Unlike the straight-chain alkanolamines studied by Jackson, DEA and TEA were found to be sufficiently hydrophobic to be separated on a reverse-phase polymer-based column without an ion-pair reagent [76].

Of all mono-amine compounds, the aliphatic amines have been the least studied with respect to their suitability for HPLC-PED. Preliminary studies of amines have indicated that they are detectable by PED at both Au and Pt electrodes [77], and a chromatogram showing the separation of two or three different amines has been included in various reviews [66]. However, no references devoted primarily to the HPLC-PED of aliphatic amines or diamines could be found in literature.

PAPER 1

PULSED ELECTROCHEMICAL DETECTION OF ALKANOLAMINES SEPARATED BY MULTIMODAL HIGH PERFORMANCE LIQUID CHROMATOGRAPHY*

*From Dobberpuhl, D. A.; Johnson, D. C. *J. Liq. Chromatogr.*, to be submitted.

ABSTRACT

Pulsed electrochemical detection (PED) is used to determine amino alcohols separated by high performance liquid chromatography (HPLC). A multimodal HPLC column with both cation-exchange and reverse-phase retention modes is used with an acidic mobile phase, so that cationic retention of the alkanolamines is possible. Small alkanolamines can be eluted isocratically without any organic modifier in the mobile phase. Baseline resolution of alkanolamines, including positional isomers, is possible.

Response for a representative alkanolamine, *tris*(hydroxymethyl)aminomethane (TRIS) is shown to be linear over a concentration range of better than three decades. The limit of detection for TRIS is 20 nM (500 fmole in a 25 μL injection) and the standard deviation of the PED response for 10 μM TRIS is better than 0.4%. HPLC-PED is shown to permit the sensitive and precise determination of alkanolamines in both a biological sample (blood) and a commercial formulation (shaving gel), with minimal sample preparation.

INTRODUCTION

Alkanolamines are used extensively by chemical and pharmaceutical industries as lubricants, corrosion inhibitors, emulsifying agents, and as ingredients of various medications. Furthermore, they are often utilized for metal surface finishing, gas purification, and as additives and dyes in cleaning solutions [1-2]. Because alkanolamines are used in many ways, and since they have been identified as pollutants in certain waste water effluents [3], there is a strong need to quantify alkanolamines both sensitively and accurately, and without extensive sample manipulation.

Methods used to determine alkanolamines have included wet chemistry techniques, gas chromatography, thin-layer chromatography, and high performance liquid and ion chromatography (HPLC, HPIC) coupled with spectroscopic, electrochemical or conductivity detection. Wet chemical techniques generally are more precise than other analytical methods, however, their application to complex real-life matrices is made difficult by the need to isolate the analytes from the rest of the sample. Gas chromatography is possible [4-8], but the high polarity of alkanolamines makes them difficult to analyze in this manner. Thin-layer chromatography with photometric detection has been demonstrated for the analysis of β-alkanolamines [9]. However, since alkanolamines possess no natural chromophore or fluorophore, this method requires that the alkanolamines be derivatized with a spectroscopically-active adduct prior to analysis. The same is true for the HPLC techniques utilizing photometric detection [10-14]. Derivatization techniques can be time-consuming, and quantitation sometimes is difficult

because the alkanolamines will derivatize with varying efficiencies in different matrices. Therefore, direct detection is preferable whenever possible. Conductivity detection has been used for the direct detection of alkanolamines separated by HPIC [15-17]. However, the sensitivity of conductivity detection is generally not as good as most other chromatographic detection methods.

Recently, pulsed electrochemical detection (PED) coupled with HPLC has been shown to be a viable method for the determination of alkanolamines. LaCourse *et al.* demonstrated the separation of mono-, di- and tri-alkanolamines using a dodecanesulfonate salt ion-pair reagent and a silica-based C18 reverse-phase column [18]. Though the determination of alkanolamines was possible at the ppb level, relatively long chromatographic run times (1-2 hours) were necessary to obtain reasonable separation. Cambell, Carson and Van Bramer also determined alkanolamines via HPLC-PED, employing the reverse-phase characteristics of a polymer-based column to separate diethanolamine (DEA) and triethanolamine (TEA) in an aluminum etching bath [2]. However, use of the same column (Dionex PAX-500) in our laboratory indicated that the smaller and more hydrophilic alkanolamines were not strongly retained, and often were unresolved from each other and the solvent front peak.

Because of the hydrophilic nature of aliphatic alkanolamines, HPIC seemed to hold greater promise than reverse-phase HPLC as a separation technique for these compounds. However, a column that combines cation-exchange retention properties with reverse-phase retention might prove even more successful for alkanolamine separations, and a recent review of PED included a separation using such a column [19]. Herein we

provide a more complete description of alkanolamine retention on a multimodal column. The separation of alkanolamines is studied as a function of mobile phase composition, with retention measured versus both the pusher ion (Na^+) and organic modifier (acetonitrile) concentration in the eluent. Under optimized separation conditions, multimodal HPLC is shown to provide not only baseline resolution of amino alcohols of different molecular weights, but also of alkanolamine positional isomers. The sensitivity and reproducibility of the PED response is found to be better than previous HPLC-PED determinations of alkanolamines, largely because of chromatographic improvements made possible by the multimodal column. Applications of HPLC-PED for the determination of alkanolamines in both a commercial and a biological sample also are demonstrated.

EXPERIMENTAL

Reagents. All chemicals for the chromatographic eluents were reagent grade or better and were used as received. Sodium acetate (Fisher) was obtained in either anhydrous or trihydrate form. Glacial acetic acid (Fisher) and acetonitrile (Fisher) were HPLC grade. All mobile phases were filtered through a 0.2 μM nylon filter (Whatman) prior to use. Sodium hydroxide used to provide post-column alkalinity in the eluent was obtained by dilution of a commercially available 50% w/w NaOH solution (Fisher) to a concentration of 0.30 M.

Ethanolamine (Fisher) and all other alkanolamines (Aldrich) used as chromatographic standards were of the best grade available. Perchloric acid (Fisher) for the dilution of some of the biological samples was reagent grade. Deionized water used for all mobile phase and standard solutions was obtained from a Milli-Q system (Millipore) after passing through two D-45 deionizing tanks (Culligan).

Voltammetric apparatus and procedures. Pulsed voltammetry was performed at the disk of an AFMT28AUAU rotating ring-disk electrode (RRDE, Pine Instruments). Rotation of the electrode was provided by an AFMSR rotator (Pine). The counter electrode for the electrochemical cell was provided by a coiled Pt wire. Potentials are reported versus a saturated calomel electrode (SCE; Fisher Scientific). The electrochemical cell was made of pyrex, and had porous glass frits separating the individual compartments for the working, reference and counter electrodes. Potential control was maintained with an AFRDE4 bi-potentiostat (Pine) interfaced to a personal

computer (Jameco) via a DT2801-A data acquisition board (Data Translation). The parameters of the pulsed waveform were selected through programming written in ASYST version 4.0 (Keithley/Asyst) software. The electrolyte solutions were deaerated by passing N_2 through the electrochemical cell during the experiments.

Chromatographic apparatus. Unless noted otherwise, all chromatographic equipment was from Dionex Corporation. Separations utilized either a full-sized (4 x 250 mm) or guard (4 x 50 mm) version of the PCX-500 column. Sample injection was provided by a pneumatically activated injector equipped with a 25 μL sample loop. A GPM gradient pump and Pulsed Electrochemical Detector were interfaced to a personal computer (Zenith) through an AI-450 Chromatography Automation System. PED was performed in a flow-through cell consisting of a 1.4 mm diameter Au working electrode and a Ag/AgCl reference electrode. The counter electrode was provided by the upper half of the detection cell, which was made of stainless steel. A solution of 0.30 M NaOH was added post-column through a mixing tee, with constant flow maintained by a Postcolumn Pneumatic Controller. The post-column eluent had a final pH of about 13, providing the alkaline environment necessary for alkanolamine detection at the Au working electrode.

RESULTS AND DISCUSSION

Voltammetry of alkanolamines. Pulsed voltammetric (i-E) results for a representative alkanolamine, *tris*(hydroxymethyl)aminomethane (TRIS), are shown in Figure 1. Pulsed voltammetry, in which the response for a given compound is measured as one of the parameters of a pulsed waveform is systematically varied, has been described previously for optimizing PED response conditions [20]. For Figure 1, the detection potential (E_{DET}) was stepped from -0.80 V to +0.75 V at 10 mV increments, while the oxidative cleaning potential (E_{OXD}) and reductive regeneration potential (E_{RED}) were kept constant at +0.80 V and -0.80 V, respectively. Current was averaged for 50 ms at each detection step after a delay period (t_{DEL}) of 250 ms, and plotted as a function of E_{DET}.

In the absence of analyte (curve **a**), most of the current generated by pulsed voltammetry at the Au working electrode is due to the formation of surface oxide (AuO). This current becomes apparent at about 0.2 V and quickly increases as the detection potential is stepped to more positive values. Current for TRIS (curves **b** - **f**) begins at about -0.4 V and reaches an anodic plateau at more positive potentials. In the plateau region, the TRIS response appears to be a linear function of concentration, which is indicative of a mass-transport limited reaction. The response for other alkanolamines studied, including 2-amino-1-ethanol (ETH), 3-amino-1-propanol (PRO), 4-amino-1-butanol (BUT), and 5-amino-1-pentanol (PEN) was similar to that of TRIS. At potentials greater than 0.2 V, the alkanolamine signal decreases relative to the amount of

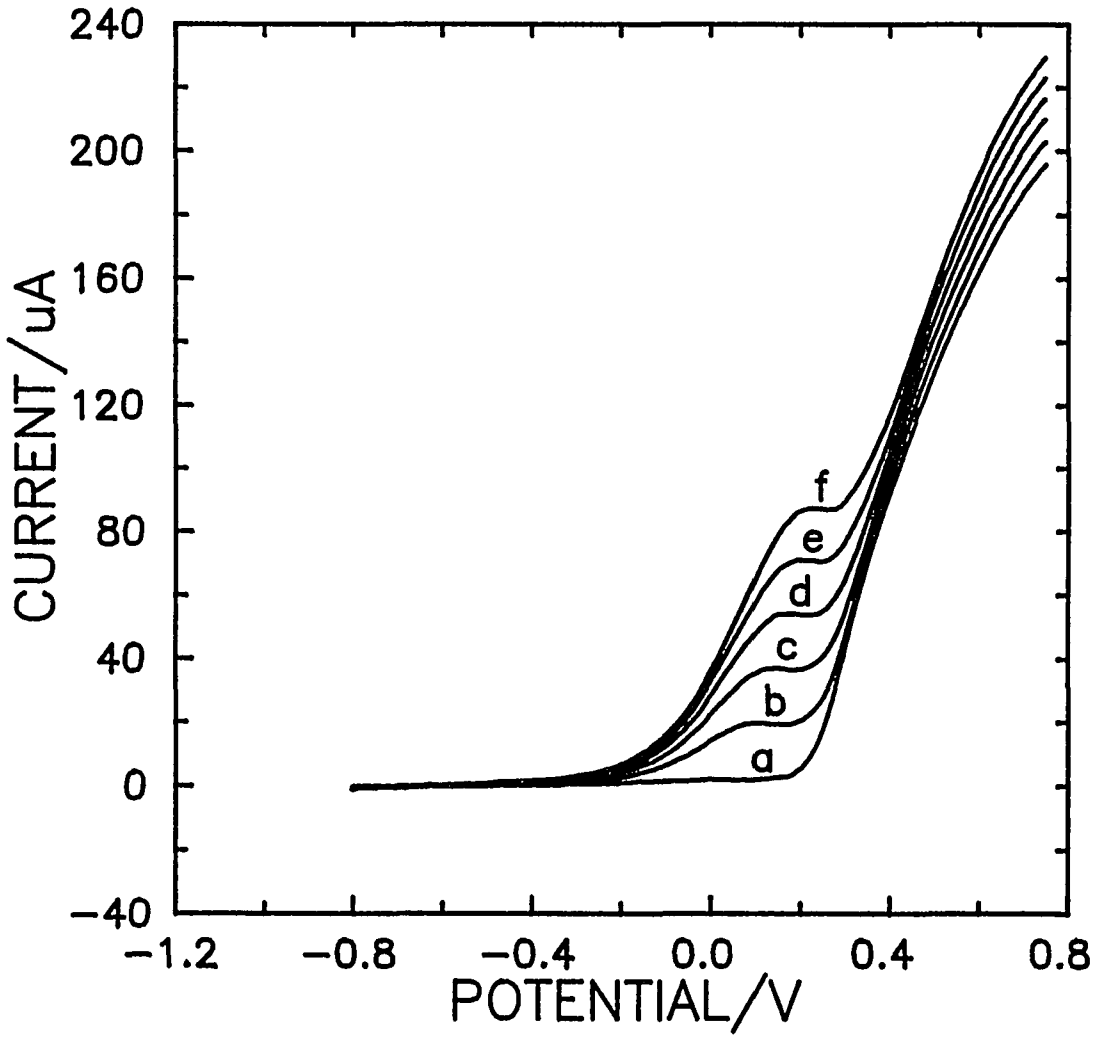

Figure 1. Pulsed voltammetric response of TRIS at a Au disk electrode in 0.1 M NaOH. Rotation rate: 400 rev min^{-1}. Potential waveform: E_{DET} stepped from -0.80 V to 0.75 V at 10 mV increments (t_{DET}= 300 ms, t_{DEL} = 250 ms); E_{OXD} = 0.80 V (t_{OXD} = 120 ms); E_{RED} = -0.80 V (t_{RED} = 380 ms). Curves: (a) 0 μM, (b) 20 μM, (c) 40 μM, (d) 60 μM, (e) 80 μM, and (f) 100 μM TRIS, respectively.

background current generated by AuO formation. Therefore, based upon these results from pulsed voltammetry, the optimum detection potential for alkanolamines is between 0.0 and 0.2 V (vs. SCE) at pH 13. Since the potential for the onset of oxide formation varies with pH, much of the HPLC-PED work was performed at detection potentials between 0.0 and 0.1 V to ensure that slight changes in the eluent pH would not cause large changes in the background.

Optimizing separation conditions. The separation of several alkanolamines using a cation-exchange/reverse-phase multimodal column is shown in Figure 2. The mobile phase was sufficiently acidic to ensure protonation of the amine functional group, thus providing the cationic form of the alkanolamines necessary for retention on the multimodal column. Since there is no response for alkanolamines at a Au electrode in acidic media, post-column addition of NaOH was used to provide the alkaline environment necessary for reasonable PED signal to be obtained. Sodium acetate (NaOAc) in the eluent provided Na^+ as the counter (pusher) ion that was necessary to elute the alkanolamines from the cationic portion of the multimodal column. The order of elution generally is from the most hydrophilic compounds to the least hydrophilic compounds. TRIS, with three alcohol groups, is the most hydrophilic, and therefore has the least retention. With the exception of ETH and PRO, baseline resolution was possible for the terminal amino alcohols under these conditions.

The elution order of alkanolamines is indicative of a separation that would result from reverse-phase retention, but also might be possible with a simple cation-exchange column. To obtain a better understanding of the retention mechanism for alkanolamines

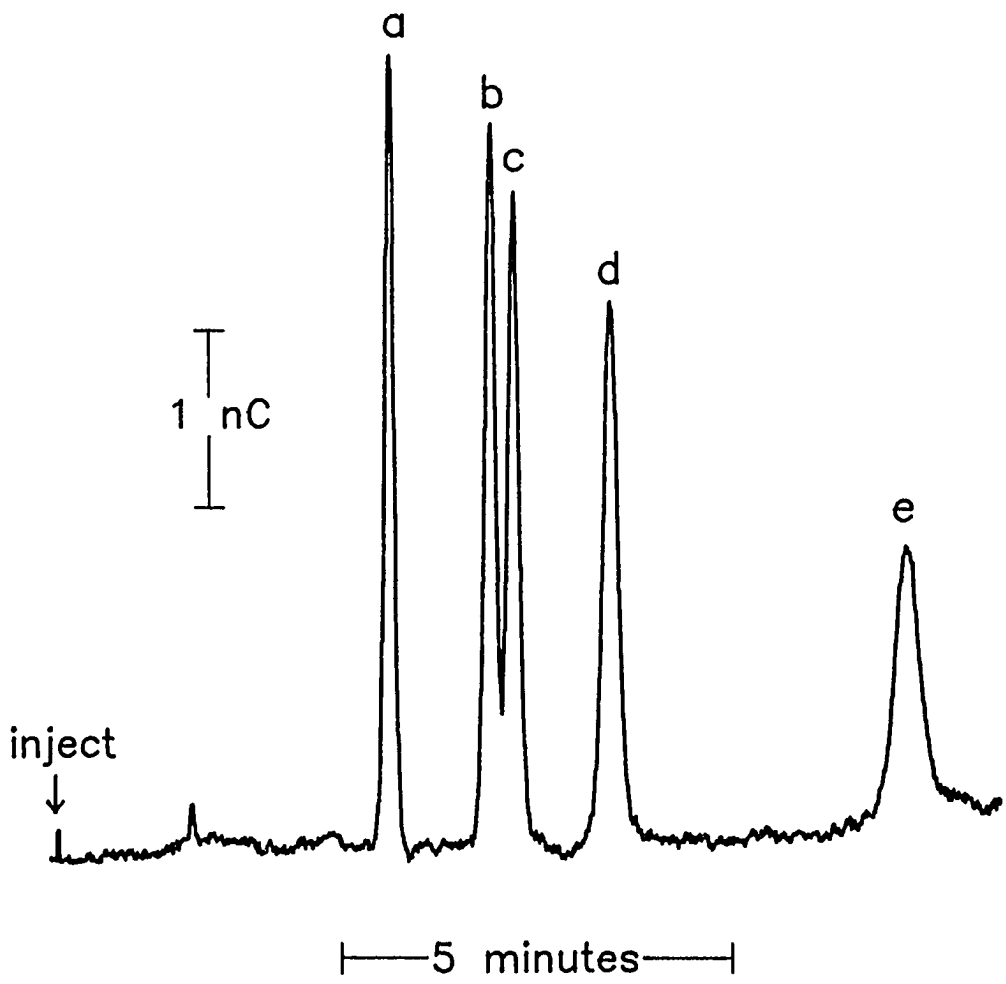

Figure 2. HPLC-PED of five alkanolamines. Column: Dionex PCX-500 (4 x 250 mm). Eluent: 20 mM HOAc/60 mM NaOAc at 1.0 mL min^{-1}. Post-column addition of 0.30 M NaOH at 0.6 mL min^{-1}. PED waveform: E_{DET} = 0.05 V (t_{DET}= 300 ms, t_{DEL} = 250 ms); E_{OXD} = 0.80 V (t_{OXD} = 120 ms); E_{RED} = -0.4 V (t_{RED} = 180 ms). Peaks: (a) 4 μM TRIS, (b) 10 μM ETH, (c) 10 μM PRO, (d) 10 μM BUT, (e) 10 μM PEN.

and to determine the optimum separation conditions) on the multimodal column, the retention factors (*k*) of alkanolamines were measured at various concentrations of organic modifier and pusher ion in the mobile phase. Figure 3 shows the retention factors for five alkanolamines plotted versus the concentration of acetonitrile (AcN) in the eluent. It is evident that the retention factors for the larger and more hydrophobic alkanolamines (e.g., curves **d** - **e**) are most affected by the amount of AcN in the mobile phase. This would be expected for a retention mechanism with a significant reverse-phase component. The eluent AcN concentration, while not having a strong influence on the retention factors of the smaller alkanolamines, is critical to the separation of ETH from PRO (curves **b** and **c**). At AcN concentrations greater than 2% (v/v), there is virtually no difference in the retention factors for ETH and PRO. Instead, the best separation of these two compounds is obtained with no organic modifier in the eluent. Alhough literature supplied with the column indicates that using a mobile phase without an organic solvent may damage the column, we saw no indication of deterioration over several months of operation in this fashion. Larger alkanolamines ($> C_6$) also may be eluted using this separation strategy. However, as the hydrophobicity of the alkanolamine increases, the need for organic modifier in the mobile phase also increases. For example, to obtain reasonable elution times for the C_6 through C_8 alkanolamines on the 25 cm column, a mobile phase containing between 5 and 15% AcN is suggested.

Figure 4 shows alkanolamine retention factors versus the concentration of NaOAc in the mobile phase. NaOAc is used to provide Na^+ as the counter-ion (pusher-ion) for the cation-exchange resin. The results are consistent with an ion-exchange retention

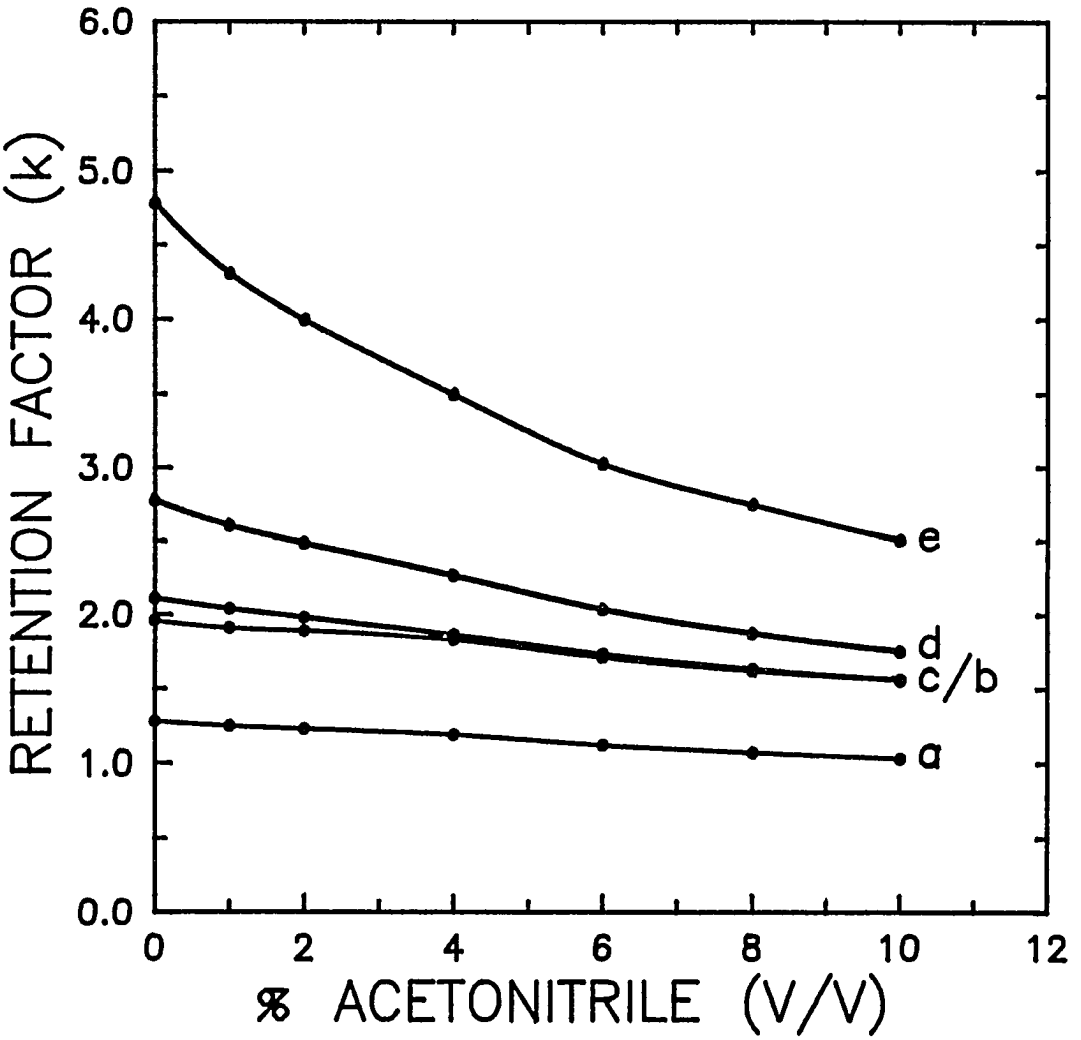

Figure 3. Retention factors (k) plotted versus eluent acetonitrile (AcN) content. Column: Dionex PCX-500 (4 x 250 mm). Eluent: 20 mM HOAc/60 mM NaOAc/variable AcN at 1.0 mL min^{-1}. Post-column addition of 0.30 M NaOH at 0.6 mL min^{-1}. PED waveform: E_{DET} = 0.05 V (t_{DET}= 300 ms, t_{DEL} = 250 ms); E_{OXD} = 0.80 V (t_{OXD} = 120 ms); E_{RED} = -0.4 V (t_{RED} = 180 ms). Curves: (a) TRIS, (b) ETH, (c) PRO, (d) BUT, (e) PEN.

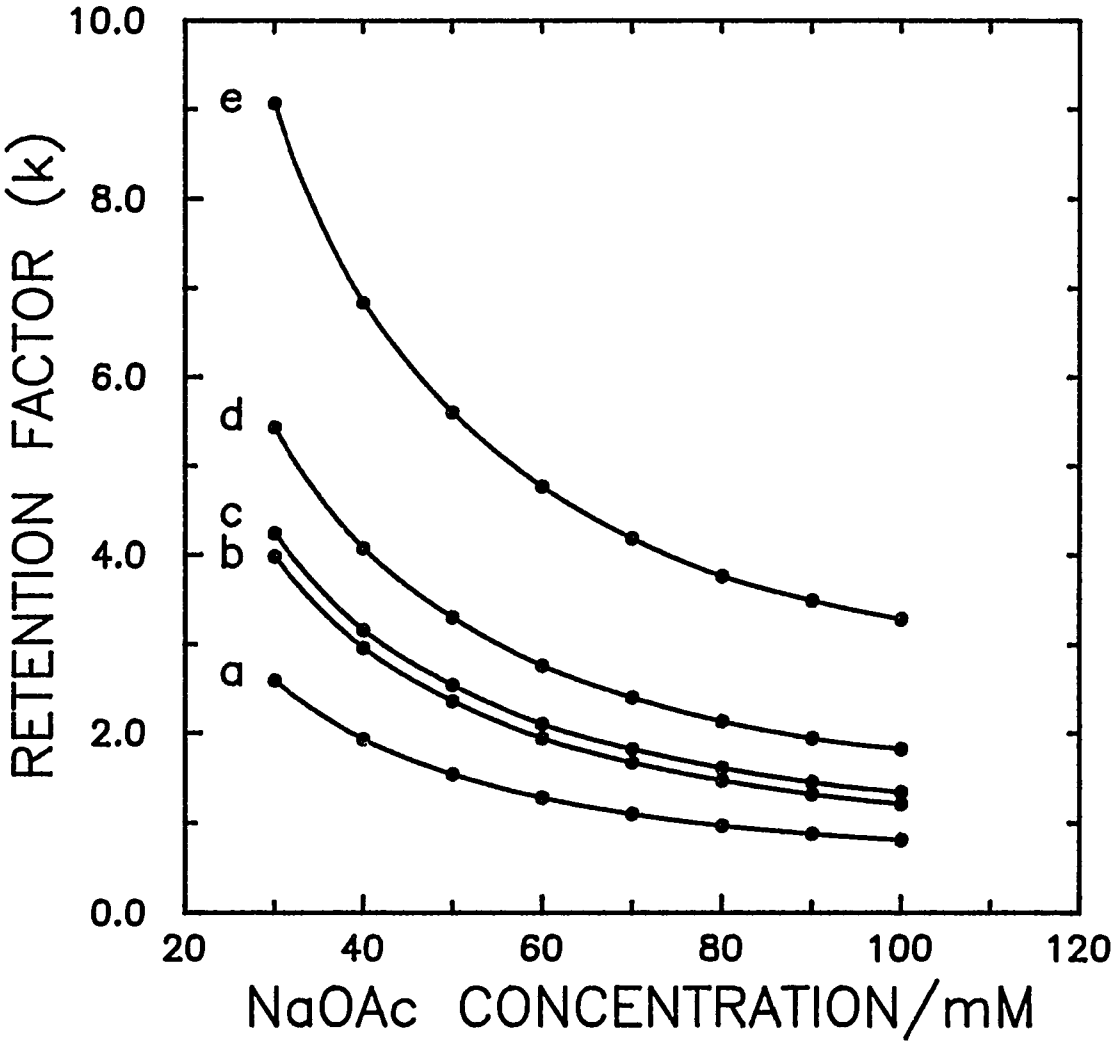

Figure 4. Retention factors (k) plotted versus eluent NaOAc content. Column: Dionex PCX-500 (4 x 250 mm). Eluent: 20 mM HOAc/variable NaOAC at 1.0 mL min^{-1}. Post-column addition of 0.30 M NaOH at 0.6 mL min^{-1}. PED waveform: E_{DET} = 0.05 V (t_{DET}= 300 ms, t_{DEL} = 250 ms); E_{OXD} = 0.80 V (t_{OXD} = 120 ms); E_{RED} = -0.4 V (t_{RED} =180 ms). Curves: (a) TRIS, (b) ETH, (c) PRO, (d) BUT, (e) PEN.

mechanism, with retention factors decreasing as the concentration of Na^+ in the eluent is increased. Retention factors for the various alkanolamines diverge at lower eluent NaOAc concentrations, indicating better separation. However, this trend is offset by increased peak-broadening also seen at lower NaOAc concentrations, making the ideal eluent NaOAC concentration between 40 and 70 mM. The concentration of acetic acid (HOAc) in the eluent had little effect on alkanolamine retention, providing there was sufficient HOAc (greater than 10 mM) to assure protonation of the amine functional group.

Detection limits, linearity and reproducibility. The linear dynamic range was determined for the PED of alkanolamines separated by HPLC, using TRIS as a representative compound. Figure 5 shows the PED response for TRIS concentrations between 50 nM and 100 μM. There is a linear relationship between signal and concentration in this region. Using linear regression analysis, the correlation coefficient (R^2) was calculated as 0.9997 based upon eleven different concentrations. At concentrations greater than 200 μM, the calibration plot begins to roll-over, and at high concentrations ($>$ 2000 μM), the PED signal changes only slightly with increasing alkanolamine concentration. The results shown in Figure 5 were obtained at a detection potential of 0.0 V to minimize the background signal. As the PV results in Figure 1 indicate, mass-transport limited response is more likely at detection potentials between 0.1 and 0.2 V, and so choosing the PED E_{DET} in this region might extend the upper limit of the linear dynamic range. Under the conditions shown in Figure 5, the limit of detection (S/N = 3) for THAM is 20 nM (500 fmol in a 25 μL injection).

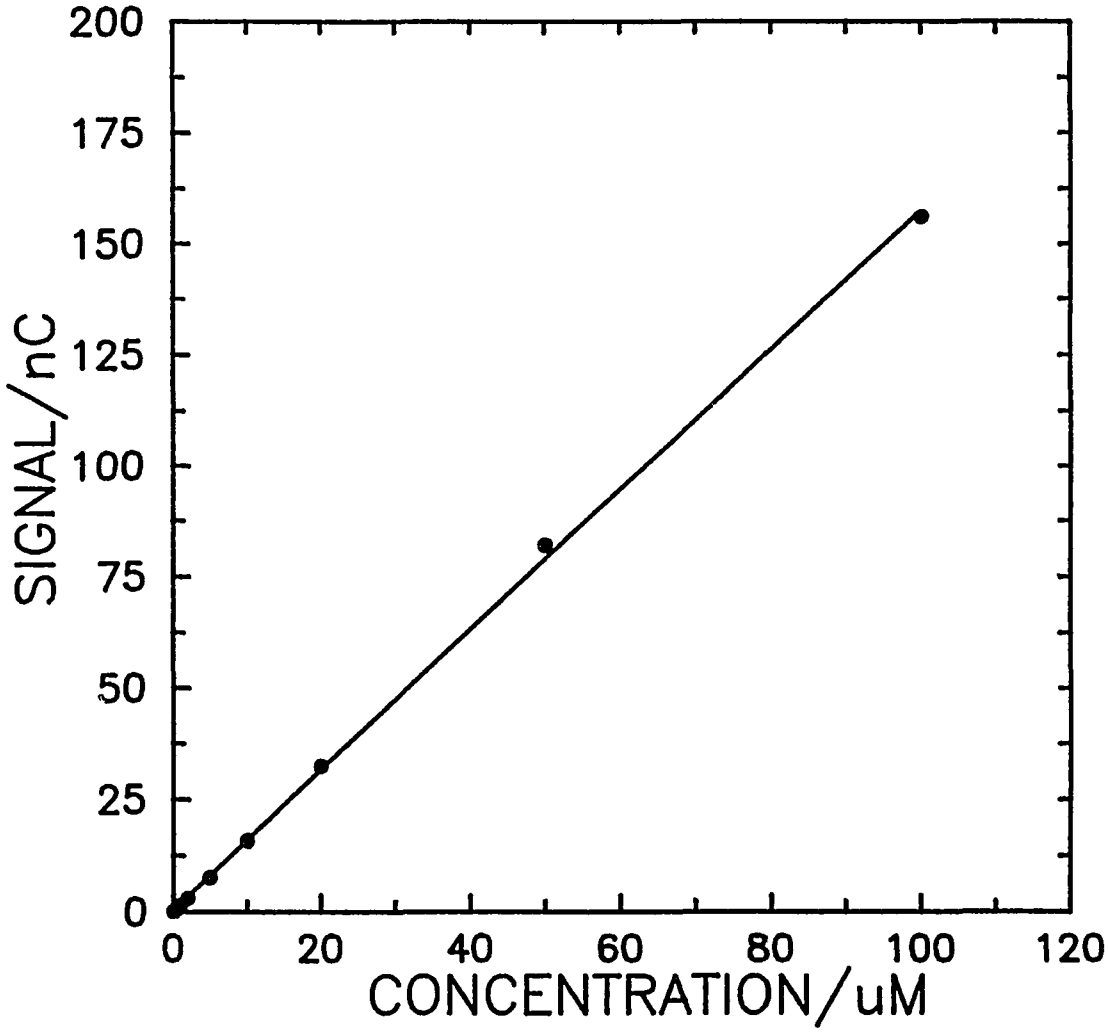

Figure 5. HPLC-PED signal (peak height) as a function of TRIS concentration. Column: PCX-500 (4 x 50 mm). Eluent: 10 mM HOAc/40 mM NaOAc at 1 mL min^{-1}. Post-column addition of 0.30 M NaOH at 0.6 mL min^{-1}. PED Waveform: E_{DET} = 0.00 V (t_{DET}= 300 ms, t_{DEL} = 250 ms); E_{OXD} = 0.80 V (t_{OXD} = 120 ms); E_{RED} = -0.4 V (t_{RED} = 180 ms). TRIS concentrations shown from 50 nM to 100 μM.

Figure 6 shows the HPLC-PED response for ten consecutive injections of 10 μM TRIS. Statistical analysis of peak height data was used to calculate the relative standard deviation (*RSD*), which is less than 0.4% for the ten injections. This indicates that HPLC-PED provides a very reproducible response for alkanolamines.

Isomers and other applications. The separation of alkanolamine isomers is shown in Figure 7. For alkanolamines of identical molecular weights, those with terminal amine groups are eluted before their β-amino analogues. This may be explained by the relative positions of the functional groups. β-alkanolamines have both the amine and the alcohol functional groups near one end of the molecule. As a result, a larger portion of the β-alkanolamines' molecular structure is hydrophobic, resulting in stronger retention on the reverse-phase portion of the multimodal column. The concentration of organic modifier in the mobile phase has a greater effect on the retention of the β-amino alcohols than it does on the retention of the terminal-amino alcohols, which would be the expected result if the β-alkanolamines are more hydrophobic.

The application of multimodal HPLC-PED for the determination of an alkanolamine in a commercial formulation is shown in Figure 8. Minimal preparation of the sample, a shaving gel, was required before analysis. A small portion of the sample was weighed and diluted by approximately 1:10,000 (w/v) in DI water and then injected. The resulting chromatogram exhibits only two peaks, and its simplicity is largely attributable to the value of the detection potential. At 0.05 V, the PED detector is fairly selective for organic compounds with one or more alcohol functional groups, with many

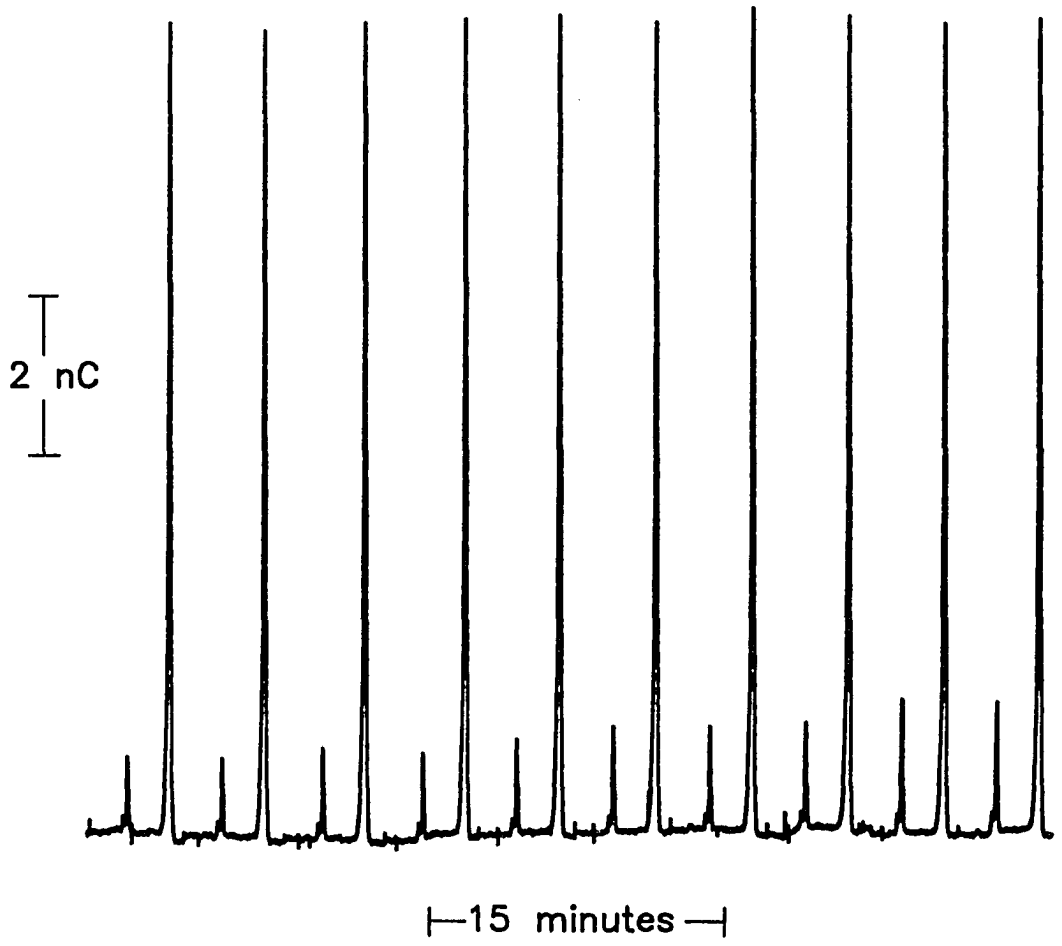

Figure 6. Reproducibility of HPLC response. Column: Dionex PCX-500 (4 x 250 mm). Eluent: 20 mM HOAc/60 mM NaOAc at 1.0 mL min^{-1}. Post-column addition of 0.30 M NaOH at 0.6 mL min^{-1}. PED waveform: E_{DET} = 0.06 V (t_{DET} = 300 ms, t_{DEL} = 250 ms); E_{OXD} = 0.80 V (t_{OXD} = 120 ms); E_{RED} = -0.4 V (t_{RED} = 180 ms). Analyte: 10 μM TRIS.

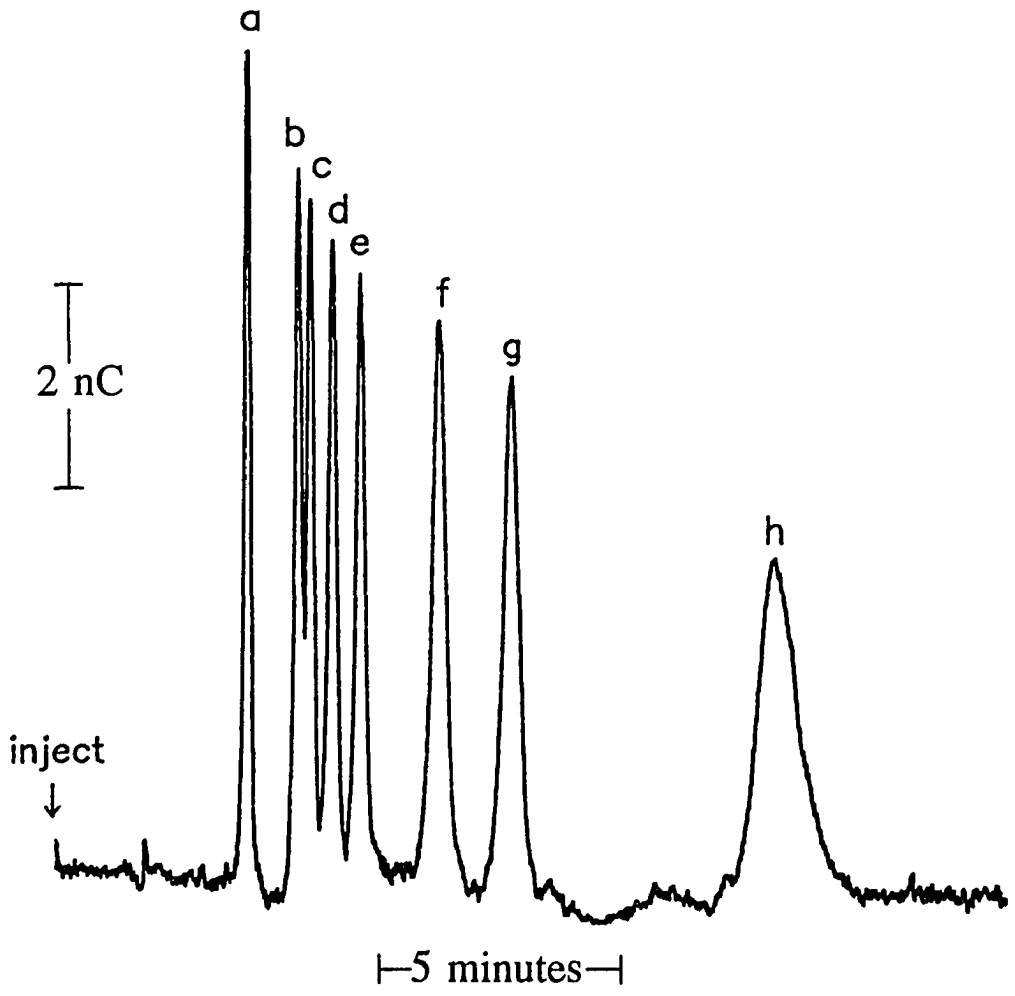

Figure 7. HPLC-PED of alkanolamine isomers. Column: Dionex PCX-500 (4 x 250 mm). Eluent: 20 mM HOAc/70 mM NaOAc at 1.0 mL min^{-1}. Post-column addition of 0.30 M NaOH at 0.6 mL min^{-1}. PED waveform: E_{DET} = 0.05 V (t_{DET}= 300 ms, t_{DEL} = 250 ms); E_{OXD} = 0.80 V (t_{OXD} = 120 ms); E_{RED} = -0.4 V (t_{RED} = 180 ms). Peaks: (a) 8 μM TRIS, (b) 20 μM 2-amino-1-ethanol, (c) 20 μM 3-amino-1-propanol, (d) 20 μM 2-amino-1-propanol, (e) 40 μM 4-amino-1-butanol, (f) 40 μM 2-amino-1-butanol, (g) 40 μM 5-amino-1-pentanol, (h) 80 μM 2-amino-1-pentanol.

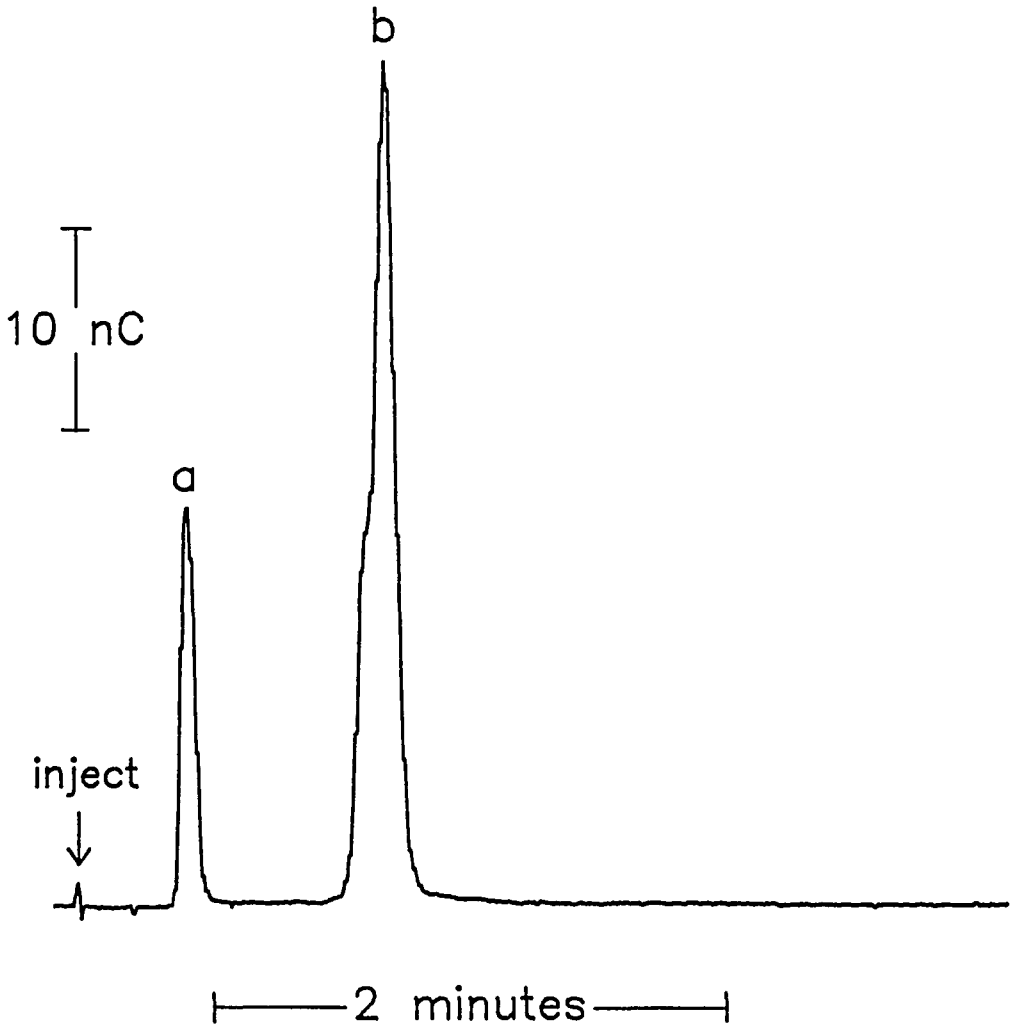

Figure 8. HPLC-PED of commercial shaving gel. Column: Dionex PCX-500 (4 x 50 mm). Eluent: 20 mM HOAc/60 mM NaOAc at 1.0 mL min^{-1}. Post-column addition of 0.30 M NaOH at 0.6 mL min^{-1}. PED waveform: E_{DET} = 0.05 V (t_{DET}= 300 ms, t_{DEL} = 250 ms); E_{OXD} = 0.80 V (t_{OXD} = 120 ms); E_{RED} = -0.4 V (t_{RED} = 180 ms). Peaks: (a) sorbitol, (b) TEA.

possible interferents showing no response at the Au working electrode. The first peak is from sorbitol, one of the ingredients in the shaving gel. The second peak is representative of triethanolamine (TEA). The relative standard deviation for five determinations of TEA was better than 1.0%, thus indicating that even with very little sample preparation, good precision is possible.

We also wanted to demonstrate the use of HPLC-PED for alkanolamines in a biological sample. TRIS, which is known clinically as Tromethamine, is used as a blood buffering agent [21], and recently was discovered by Pollard and co-workers to have possible therapeutic value in the treatment of Alzheimer's Disease [22]. Therefore, the determination of TRIS in a biological matrix might be of some interest. An artificial sample of TRIS in blood was prepared as follows: a 100 μL aliquot of human blood was added to 100 μL of 2.00 mM TRIS. The sample was then diluted to 10.0 mL with either deionized H_2O or 1.0 M $HClO_4$ to give a final TRIS concentration of 20 μM. The solution was mixed thoroughly, centrifuged, and filtered through a 0.22 μm syringe filter prior to injection.

The results for the HPLC-PED of TRIS in blood are shown in Figure 9. The lower chromatogram (**A**) represents the response for a 20 μM TRIS standard. The upper chromatogram (**B**) represents the results obtained for 20 μM TRIS in human blood. The recovery efficiency for TRIS in blood was dependent upon the sample diluent. When the sample was diluted with deionized water, the recovery efficiency was 81.6 $\pm$ 3.1% (n = 4). When 1.0 M perchloric acid was the diluent, the recovery efficiency was 102.0 $\pm$ 2.3% (n = 4). We speculate that the lower recovery efficiency for the sample diluted in

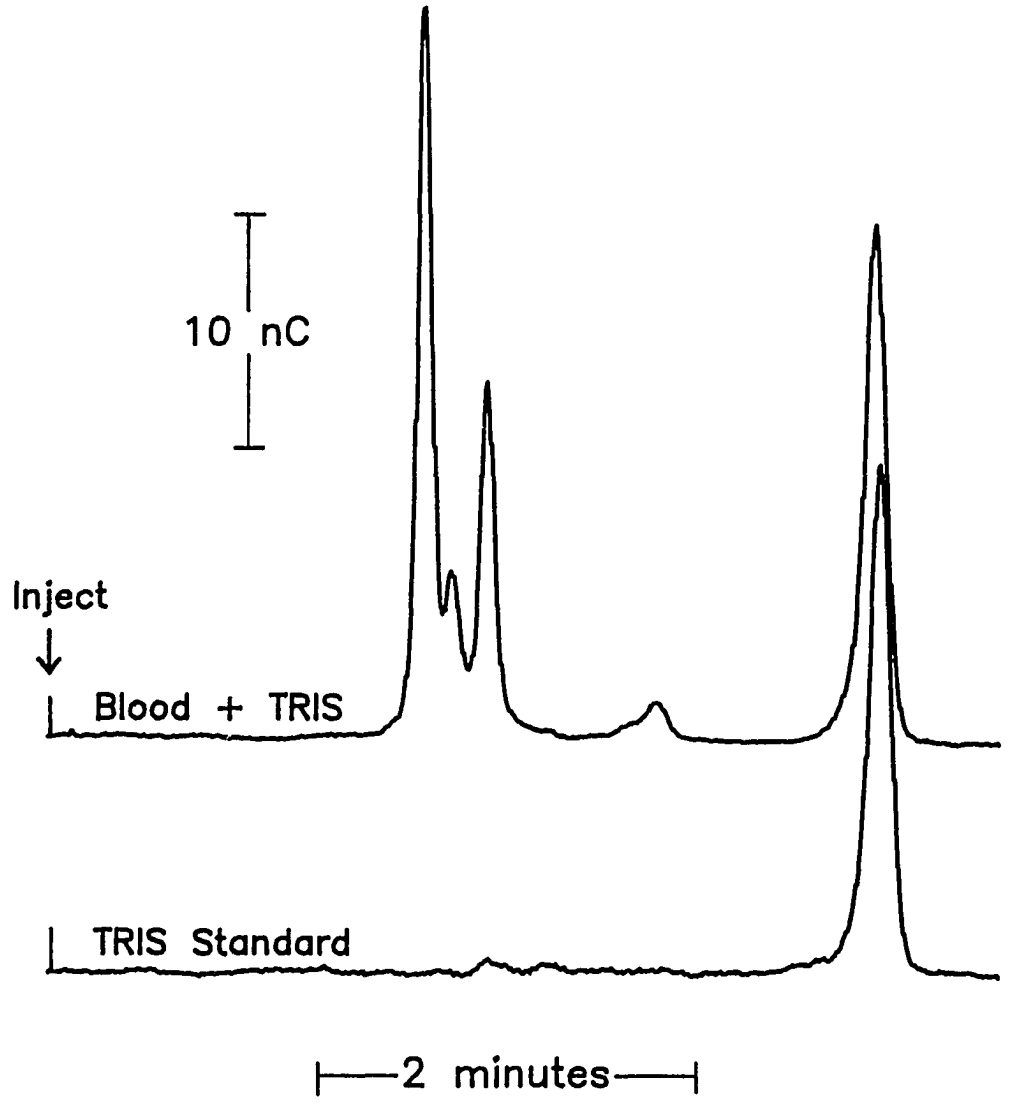

Figure 9. HPLC-PED of TRIS in blood. Column: Dionex PCX-500 (4 x 250 mm). Eluent: 20 mM HOAc/60 mM NaOAc at 1.0 mL min^{-1}. Post-column addition of 0.30 M NaOH at 0.6 mL min^{-1}. PED waveform: E_{DET} = 0.05 V (t_{DET}= 300 ms, t_{DEL} = 250 ms); E_{OXD} = 0.80 V (t_{OXD} = 120 ms); E_{RED} = -0.4 V (t_{RED} = 180 ms). Upper chromatogram: human blood spiked with TRIS, diluted to a final concentration of 20 μM. Lower chromatogram: 20 μM TRIS standard.

water is the result of TRIS being complexed either intra- or extra-cellularly by the blood proteins. This caused the apparent HPLC-PED response to be reduced, either by changing the chromatographic behavior of the TRIS bound by the proteins, or by changing the PED response for the complexed TRIS at the Au electrode. By diluting the samples in acid, the blood cells were lysed and the proteins were ionized, thus releasing the bound TRIS and allowing complete recovery. Another benefit of using acid as the sample diluent relates to sample stability. Injections could be made several days after the sample was diluted with acid without any discernible decrease in the recovery efficiency. Other peaks in the blood sample have not been identified conclusively, except for the first peak, which is due to normal levels of blood sugar (glucose).

CONCLUSIONS

The separation of alkanolamines was shown using multimodal high performance liquid chromatography. The separation relies upon both cation-exchange and reverse-phase retention mechanisms of the mixed-bed column, and the strategy provides baseline resolution of alkanolamine isomers using isocratic elution. When coupled with pulsed electrochemical detection, the determination of alkanolamines was shown to be sensitive and reproducible. The limits of detection were in the nanomolar region, and a linear dynamic range greater than three decades. The method has the advantage of being rugged, with minimal sample preparation required to successfully analyze alkanolamines in both commercial and biological samples.

ACKNOWLEDGEMENTS

This work was supported by a grant from Dionex Corporation.

REFERENCES

1. *The Merck Index*, Merck, Rahway, NJ, 11th Ed., 1991, pp 588, 1521, 1536-1537.
2. D. L. Cambell, S. Carson and D. Van Bramer, *J. Chromatogr.*, 546 (1991) 381.
3. R. B. Butwell, D. J. Kubek and P. W. Sigmund, *Hydrocarbon Processing*, March, 1982, Gulf Publishing Co. 108-116.
4. O. F. Dawodu and A. Meisen, *J. Chromatogr.*, 629 (1993) 297.
5. O. F. Dawodu and A. Meisen, *J. Chromatogr.*, 587 (1991) 237.
6. N. C. Saha, S. K. Jain and R. K. Dua, *Chromatographia*, 10 (1977) 368.
7. S. Beneva and N. Dimov, *Chromatographia*, 14 (1981) 601.
8. G. Vincent, M. Desage, F. Comet, J. L. Brazier and D. LeCompte, *J. Chromatogr.*, 295 (1984) 248.
9. M. Nishikata, *J. Chromatogr.*, 408 (1987) 449.
10. N. P. J. Price, J. L. Firmin and D. O. Gray, *J. Chromatogr.*, 598 (1992) 51.
11. J. A. Grunau and J. M Swiader, *J. Chromatogr.*, 594 (1992) 165.
12. A. J. Bourque and I. S. Krull, *J. Chromatogr.*, 537 (1991) 123.
13. J. F. Davey and R. S. Ersser, *J. Chromatogr.*, 528 (1990) 9.
14. A. R. Hayman, D. O. Gray and S. V. Evans, *J. Chromatogr.*, 325 (1985) 462.
15. J. Krol, P. G. Alden, J. Morawski and P. E. Jackson, *J. Chromatogr.*, 626 (1992) 165.
16. J. Gorham, *J. Chromatogr.*, 362 (1986) 243.
17. H. Small, T. S. Stevens and W. C. Bauman, *Anal. Chem.*, 47 (1975) 1801.

18. W. R. LaCourse, W. A. Jackson and D. C. Johnson, *Anal. Chem.*, 61 (1989) 2466.

19. D. C. Johnson and W. R. LaCourse, *Electroanalysis*, 4 (1992) 367.

20. W. R. LaCourse and D. C. Johnson, *Anal. Chem.*, 65 (1993) 50.

21. G. G. Nahas, *Pharmacol. Rev.*, 14 (1962) 447.

22. N. Arispe, E. Rojas and H. B. Pollard, *Proc. Natl. Acad. Sci. USA*, 90 (1993) 567.

PAPER 2

PULSED ELECTROCHEMICAL DETECTION OF AMINES AND DIAMINES SEPARATED BY HIGH PERFORMANCE LIQUID CHROMATOGRAPHY*

*From Dobberpuhl, D. A.; Hoekstra, J. C.; Johnson, D. C. *Anal. Chem.*, to be submitted.

ABSTRACT

Pulsed electrochemical detection (PED) is used to determine aliphatic amines and diamines separated by high performance liquid chromatography (HPLC). The PED detection potentials are selected based upon results obtained from both cyclic and pulsed voltammetry. The optimum detection potential for amines is approximately 0.2 V (vs. SCE) in alkaline conditions, whereas for diamines it is between 0.4 V and 0.6 V.

Aliphatic amines are separated on a high-capacity "multimodal" column that permits both cation-exchange and reverse-phase retention of analytes. The protonated form of the amines, necessary for cationic retention, is obtained by using an acidic mobile phase. Diamines, which are divalent in acidic eluents, are separated using a low-capacity cation-exchange column. The retention factors for both amines and diamines are measured against several different mobile phase parameters to find the optimum eluent composition, and to evaluate the chromatographic basis for the respective separation strategies.

HPLC-PED is shown to be both an accurate and sensitive method for the determination of amine compounds. Limits of detection for 25 μL injections are 100 nM (2.5 pmol) for amines and 200 nM (5.0 pmol) for diamines. The relative standard devation (RSD) for eight successive injections of 100 μM ethylamine is 0.32%, indicating good reproducibilty.

INTRODUCTION

Aliphatic amines serve as precursors in dyes and pharmaceuticals, and are used as stabilizers, emulsifiers and corrosion inhibitors in various formulations [1]. In addition, amines are found in biological systems as products of amino acid metabolism. Diamines also are biogenic, and their concentrations are indicative of specific carcinomas. In organ transplant recipients, the concentration of some diamines is a measure of how strongly the body is rejecting the tranplanted tissue [2 - 4]. They are also a measure of spoilage in food stuffs, and are especially important in determining the freshness of seafood and other meats [5 - 7]. Therefore, there is a strong need to quantify amines and diamines accurately, reproducibly, and without extensive sample manipulation.

Amines and diamines have been determined by many methods including wet chemical techniques [8, 9], thin-layer chromatography [10], gas chromatography [11 - 13] and recently capillary electrophoresis with indirect UV detection [14]. High performance ion chromatography (HPIC) also has been employed with conductometric detection [15 - 17]. However, the most common method for the determination of amine compounds is high performance liquid chromatography (HPLC) with either fluorescence [18 - 21] or UV/vis detection [22 - 24]. Because amines are not naturally chromophoric or fluorophoric, most photometric detection methods rely on the derivatization of the analytes with a spectroscopically-active adduct. Although this is what makes photometric detection practical, there are several potential drawbacks. The derivatization procedure can be time-consuming, and problematic because analytes will complex with varying

efficiencies in different matrices. In addition, the derivatizing agents are often quite toxic and, therefore, necessitate additional consideration in the disposal of chromatographic waste. Finally, derivatization often results in a complex that is labile, so that variations in separation conditions or retention times can alter the response. With all of these possible complications, we believe that direct detection is preferable whenever possible.

In our laboratories, pulsed electrochemical detection (PED) at noble metal electrodes has been used with HPLC to determine many aliphatic compounds, including amino acids, amino sugars, and amino alcohols [25 - 29]. The multi-step PED waveform continuously cleans and reactivates the working electrode, thus providing for continuous detection of aliphatic compounds previously considered inactive at noble metal electrodes. In this paper, PED is applied to aliphatic amines and diamines separated by HPLC. Several different columns and mobile phases are used. Amines are separated on both a silica-based C18 column and a polymer-based multimodal reverse-phase/cation-exchange column, and the chromatographic basis for each method is evaluated. Diamines are separated on a low-capacity cation-exchange column. For all separations, the mobile phase is made sufficiently acidic to assure protonatation of the amine functional group. With the C18 column, acidic conditions reduce the interaction between the amines and the uncapped silanol groups of the silica support, thus improving the peak shapes. For multimodal and cation-exchange columns, the acidic eluent generates the ionized form of amines and diamines necessary for reasonable retention. Post-column addition of sodium hydroxide provides the alkaline environment necessary for PED signal at a Au working

electrode. The method is shown not only to be both accurate and sensitive, but also reproducible.

EXPERIMENTAL

Reagents. All reagents were used as received. Acetonitrile (Fisher) and glacial acetic acid (Fisher) were HPLC grade. Sodium acetate, sodium nitrate and nitric acid (Fisher) were reagent grade or better. Deionized water used in the preparation of eluents and standard solutions was obtained from a Milli-Q system (Millipore) after passing through two D-45 deinionizing tanks (Culligan). All mobile phases were filtered through a 0.2 μm nylon filter (Whatman) prior to use. Sodium hydroxide used for the supporting electrolyte in the voltammetric experiments and also to provide post-column alkalinity in the HPLC eluents was obtained by dilution of a commercially available 50% w/w NaOH solution (Fisher). Methylamine (Fisher), and ethylamine (Kodak, Sigma) were practical grades of 40% and 70% w/V solutions in water, respectively. All other amines (Aldrich, Chem Service) were of the highest concentration available, as were the diamines (Aldrich).

Voltammetric apparatus and procedures. Cyclic and pulsed voltammetry were done at the disk of an AFMT28AUAU rotating ring-disk electrode (RRDE, Pine Instruments), with rotation of the electrode provided by an AFMSR rotator (Pine). The electrochemical cell was made of pyrex, and had porous glass frits connecting the separate chambers for the working, reference and counter electrodes. The counter electrode for the electrochemical cell was provided by a coiled Pt wire, and all potentials are measured versus a saturated calomel electrode (SCE; Fisher Scientific). Voltammetric data was obtained using an AFRDE4 bi-potentiostat (Pine) interfaced to a

personal computer (Jameco) via a DT2801-A data acquisition board (Data Translation). For cyclic voltammetry, potential control was maintained solely through the potentiostat. For pulsed voltammetry, the potentiostat was placed under computer-control. ASYST version 4.0 (Keithley/Asyst) software was used to write the programs that determined the parameters of the pulsed waveforms. All solutions were deaerated before and during the experiment by bubbling N_2 throught the electrochemical cell's working electrode compartment.

HPLC system and procedures. Amines were separated on either a 3.9 x 150 mm C18 reverse-phase column (Phenomenex) or with either the guard version (4 x 50 mm) or full-sized version (4 x 250 mm) of the PCX-500 column (Dionex). Diamines were separated on a 4 x 250 mm CS-14 column (Dionex) Sample injection was provided by a pneumatically-controlled injector with a 25 μL sample loop. A GPM gradient pump and Pulsed Electrochemical Detector (Dionex) were interfaced to a personal computer (Zenith) through an AI-450 Chromatography Automation System (Dionex). The flow-through detection cell consisted of a 1.4 mm diameter Au working electrode and an Ag/AgCl reference electrode. The counter electrode was provided by the stainless steel upper-half of the detection cell. A Postcolumn Pneumatic Controller (Dionex) was used to regulate the post-column addition of sodium hydroxide.

RESULTS AND DISCUSSION

Voltammetry of amines and diamines. To determine the optimum detection potential (E_{DET}) for the PED of amines and diamines, cyclic and pulsed voltammetry were performed at the disk of a rotating ring-disk electrode. Figure 1 shows the current versus potential (*i-E*) for ethylamine at a Au working electrode in 0.1 M NaOH. Curve **a** is the residual, and represents the response of the Au electrode in the absence of analyte. The residual has several features. As the potential is scanned positive of 0.1 V, anodic current is obtained for the formation of surface oxide (AuO). Oxide formation continues to the positive scan limit, where there is additional anodic current from oxygen evolution occurring through solvent electrolysis. Upon initiation of the negative scan at 0.7 V, the response at the Au electrode quickly decays to near zero. As the potential is scanned negative of 0.1 V, the residual shows a large cathodic peak resulting from the stripping of surface oxide that was formed on the positive scan.

Curves **b** through **d** represent the voltammetric response for different concentrations of ethylamine. Anodic current for ethylamine is generated concurrently with the formation of AuO, and formation of surface oxide is believed to catalyze the amine oxidation. Current for ethylamine is seen throughout the entire oxide formation region, but the signal is maximized relative to the background at a potential of about 0.2 V, at the onset of oxide formation. There is some correlation between amine signal and concentration, though the amount of current generated by the oxidation of ethylamine indicates that the reaction is not mass-transport limited. Instead the reaction appears to

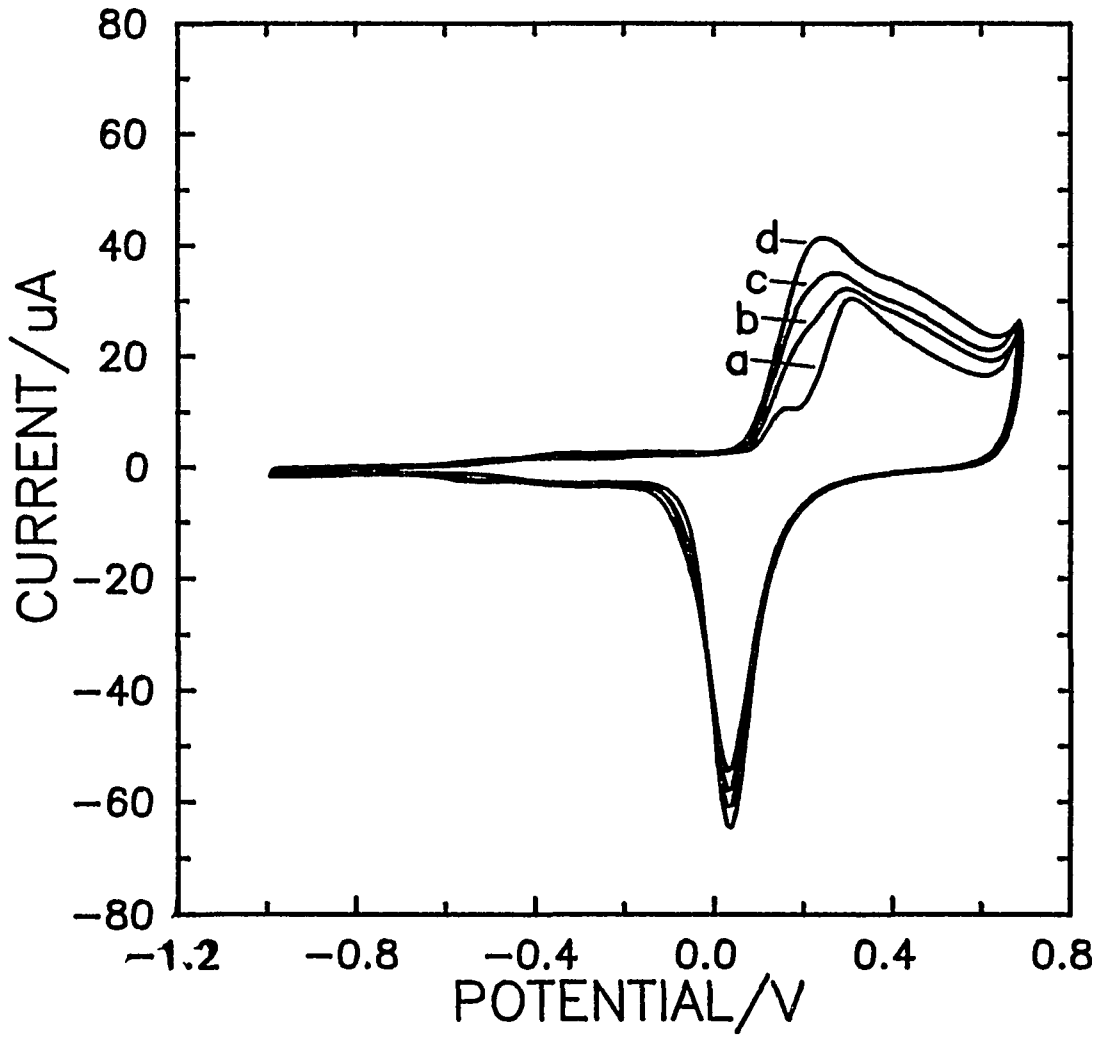

Figure 1. Cyclic voltammetric response of ethylamine at Au RDE in 0.10 M NaOH. Rotation speed: 400 RPM. Scan rate: 100 mV s^{-1}. Curves: (a) residual; (b) 20 μM ethylamine; (c) 40 μM ethylamine; (d) 80 μM ethylamine.

be primarily under surface-control, which would be expected for a reaction catalyzed by the formation surface oxide.

The response for ethylenediamine (EDA) using cyclic voltammetry is shown in Figure 2. Relative to ethylamine, EDA exhibits greater anodic current per unit concentration throughout the entire oxide formation region. The response for EDA, like ethylamine, appears to be dependent upon the formation of surface oxide, with the largest signal-to-background ratios obtained at potentials less than 0.2 V. However, in this region, EDA response shows almost no dependence upon concentration, and so a more positive PED detection potential provide better results for diamines.

Results from pulsed voltammetry (PV), shown in Figure 3, provide further support for using a more positive detection potential with diamines. An experimental design for using PV to optimize PED waveforms has been described previously [30]. To perform the PV experiment, the detection potential was stepped from -0.80 V to +0.75 V at 10 mV increments. The oxidative cleaning potential (E_{OXD}) and reductive regeneration potential (E_{RED}) were -0.80 V and +0.80 V, respectively. At each detection step, the current was measured during the sampling time (t_{INT}) after a delay period (t_{DEL}). Unlike the CV experiments, the PV experiment was done in a supporting electrolyte containing 15% acetonitrile (AcN) to simulate typical HPLC conditions. The PV results (Figure 3) indicate that the presence of AcN severely attentuates the response for EDA at the Au working electrode at potentials less than 0.2 V. However, there is still good response at potentials between 0.4 V and 0.6 V, and so a PED detection potential in this region is much more effective for diamines with AcN present in solution.

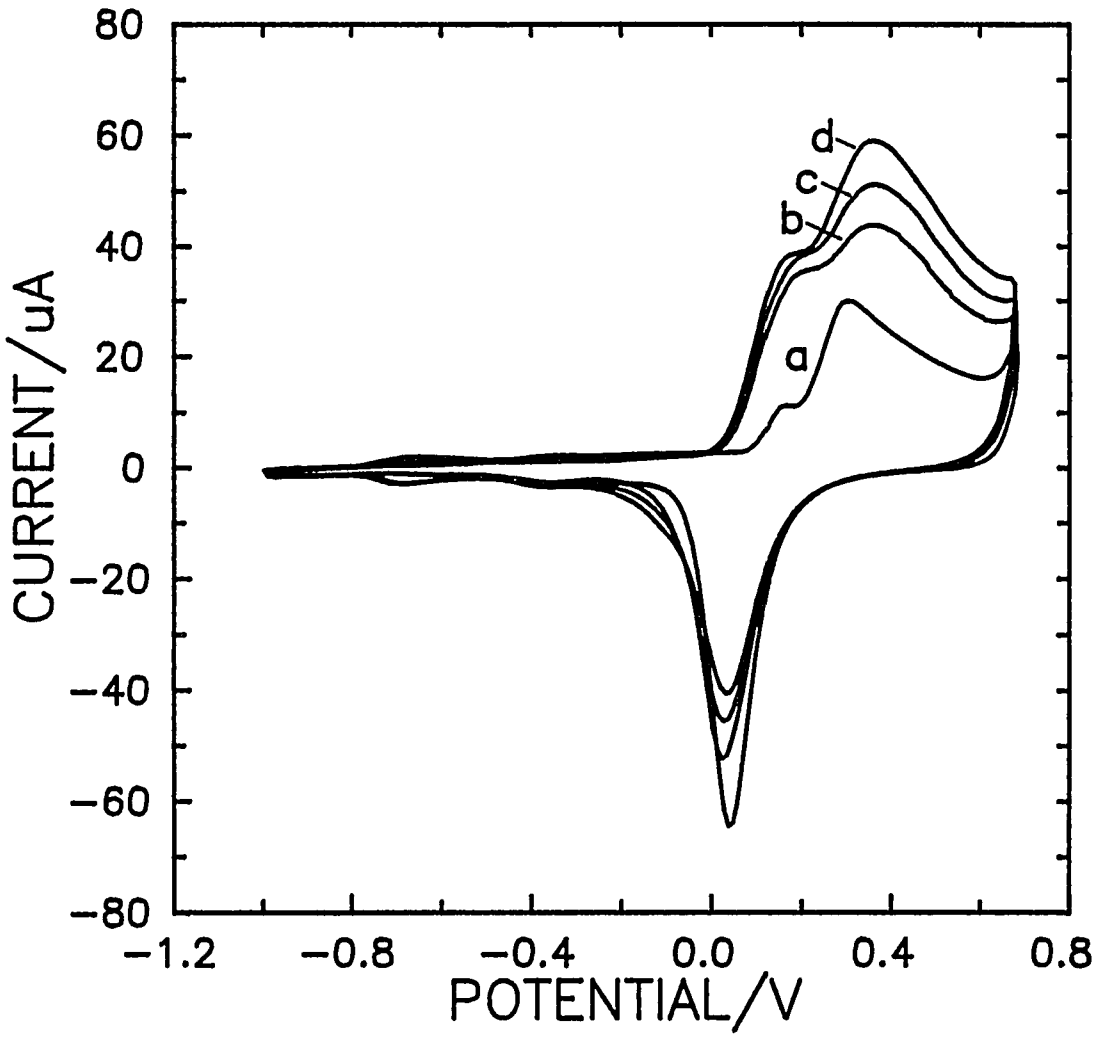

Figure 2. Cyclic voltammetric response of ethylenediamine (EDA) at Au RDE in 0.10 M NaOH. Rotation speed: 400 RPM. Scan rate: 100 mV s^{-1}. Curves: (a) residual; (b) 20 μM EDA; (c) 40 μM EDA; (d) 80 μM EDA.

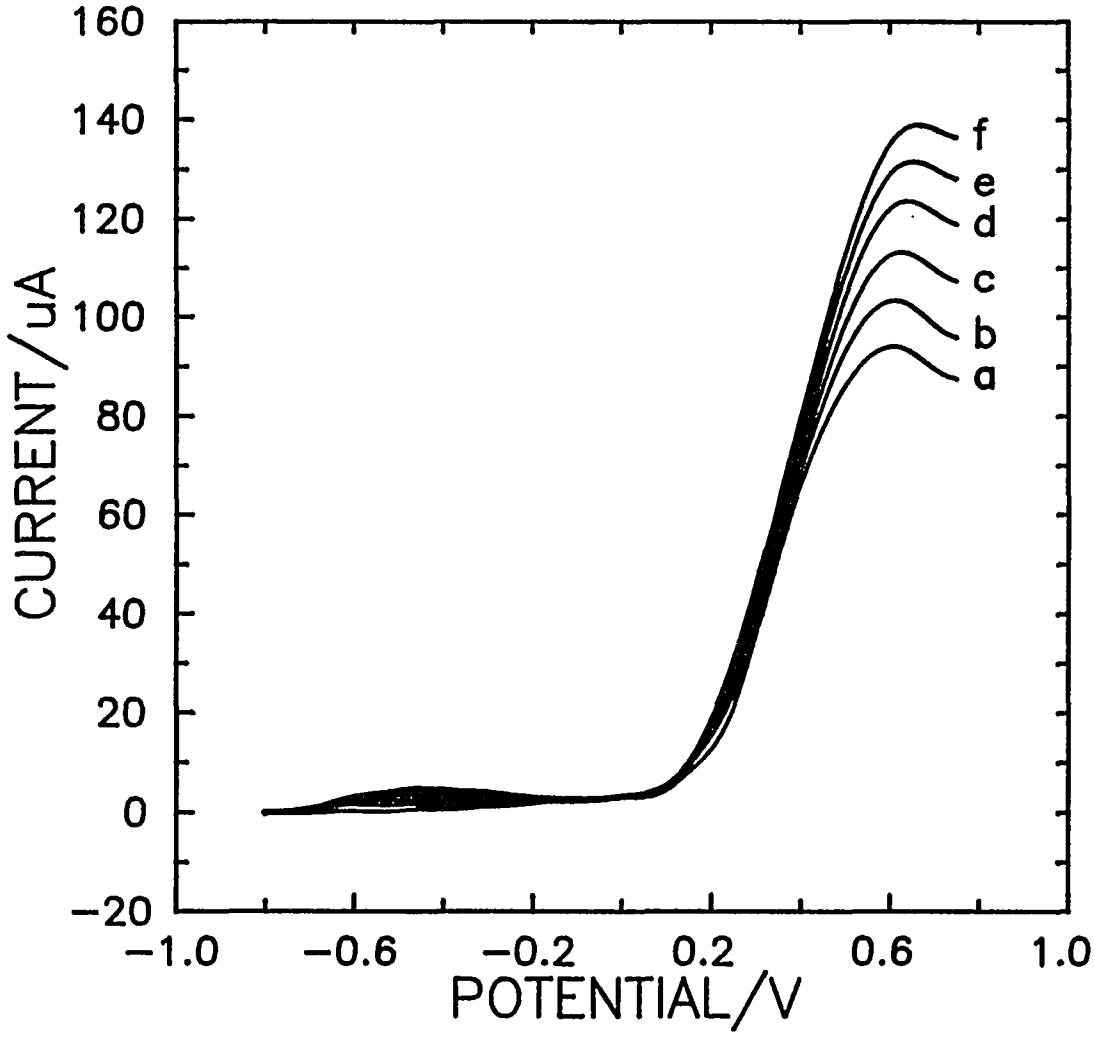

Figure 3. Pulsed voltammetric response of EDA at Au RDE in 0.10 M NaOH/15% acetonitrile (AcN). Rotation rate: 400 rev min^{-1}. Pulsed waveform: E_{DET} stepped from -0.80 V to 0.75 V at 10 mV increments (t_{DET}= 300 ms, t_{DEL} = 250 ms, t_{INT} = 50 ms); E_{OXD} = 0.80 V (t_{OXD} = 120 ms); E_{RED} = -0.80 V (t_{RED} = 380 ms). Curves: (a) 0 μM, (b) 20 μM, (c) 40 μM, (d) 60 μM, (e) 80 μM, and (f) 100 μM EDA, respectively.

Pulsed voltammetry of ethylamine was also performed in supporting electrolytes containing various concentrations of AcN, and, as with EDA, AcN attenuated the amine response at $E_{DET} \leq 0.2$ V. However, the separations described required less AcN for amines than for diamines, and the results will indicate that reasonable response is possible for amines when using a detection potential of 0.2 V. When using mobile phases containing high concentrations of an organic modifier, a detection potential in the 0.4 V to 0.6 V region is more suitable for obtaining optimum PED response for amines.

Separation of aliphatic amines on a C18 column. The first attempt to separate aliphatic amines was made using a silica-based C18 column, and initial results were not very promising. Most analytes eluting with the system peak (void volumn) with only the largest amines ($> C_6$) showing any retention whatsoever. Though not desirable, this lack of retention was expected, since the small hydrophilic aliphatic amines had not been derivatized with a hydrophobic adduct prior to their separation, nor had any ion-pair reagent been included in the eluent. After several week of using the C18 column, the results in Figure 4 were obtained. The separation of several amines was possible, though resolution of the methylamine, ethylamine and n-propylamine peaks was still not achieved. A mobile phase containing small amounts of acetic acid significantly improved peak shapes in comparison to neutral or slightly alkaline eluents. It was concluded that the acidic mobile phase protonated the amine functional group, thus minimizing unwanted interaction between the analytes and the uncapped silanol groups of the silica-based column. The retention times of the amines shown in Figure 4 continued to increase with successive chromatographic runs, and examination of results from earlier separations on

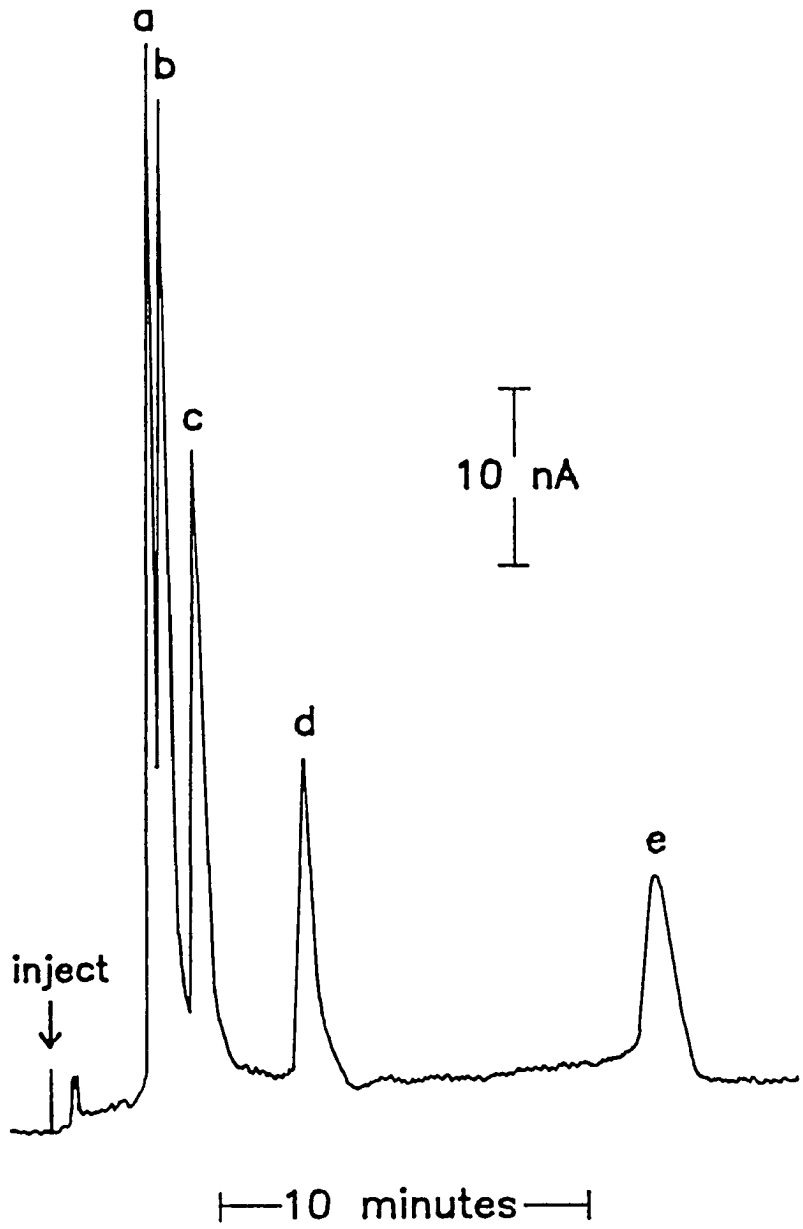

Figure 4. HPLC-PED of aliphatic amines using a silica-based reverse-phase column. Column: Phenomenex Bondclone C18 (3.9 x 150 mm). Eluent: 0.15% HOAc at 0.8 mL min^{-1}. Post-column addition of 0.30 M NaOH at 0.4 mL min^{-1}. PED waveform: E_{DET} = 0.20 V (t_{DET}= 300 ms, t_{DEL} = 250 ms, t_{INT} = 50 ms); E_{OXD} = 0.80 V (t_{OXD} = 120 ms); E_{RED} = -1.0 V (t_{RED} = 180 ms). Peaks: (a) 10 μM ethylamine, (b) 10 μM n-butylamine, (c) 10 μM n-pentylamine, (d) 10 μM n-hexylamine, (e) 10 μM n-heptylamine.

the same column indicated that the migration of retention times had been occurring continuously with column use. Eventually, even the smallest amines began to elute as broad peaks with retention times of several minutes, and the experiments soon were discontinued. The behavior exhibited by the amines on the silica-based column is indicative of gradual hydrolysis of the C18 stationary phase, which caused an increase in the interaction between the amines and the exposed uncapped silanol groups. Therefore, the separation shown in Figure 4 may not be so much be the consequence of reverse-phase retention on the C18 stationary phase, but instead be the result of normal-phase type retention on the silica support.

Attempts were made to duplicate the results shown in Figure 4 with a new silica-based column. Almost no retention was obtained for any of the aliphatic amines. Use of a polymer-based reverse-phase column also resulted in little or no retention for most aliphatic amines. The experiments tend to support the conclusions that the retention of amines on the older silica-based column were not through reverse-phase interaction. The experiments also conclusively showed that a reverse-phase separation of underivatized aliphatic amines was not practical, because they are too hydrophilic to have sufficient retention on the hydrophobic stationary phase.

Separation of amines on a multimodal column. Since simple reverse-phase separation of underivatized amines was not feasible, other separation methods were considered. Previous work had shown that the separation of alkanolamines was possible using a Dionex PCX-500 column [31], which has a multimodal stationary phase with both reverse-phase and cation-exchange retention capabilities. The separation of several small

amines on the PCX-500 column is shown in Figure 5. The mobile phase again was made acidic to ensure protonation of the amine function group, thus permitting cationic retention in addition to reverse-phase retention on the multimodal column. With the exception of methylamine and ethylamine, baseline resolution is possible for all n-amines, using only a 5.0 cm column. Amines larger than those shown in Figure 5 could be eluted by increasing the concentration of organic modifier in the mobile phase.

To determine optimum separation conditions, amine retention factors (*k*) were measured under different eluent conditions. Figure 6 shows k for several amines plotted versus the percentage of organic modifier (AcN) in the mobile phase. Retention factors for all amines were dependent on the concentration of organic modifier and, as expected for a separation with a significant reverse-phase component, the AcN content had a greater effect on the retention of the larger, more hydrophobic, analytes. An AcN concentration of 10% was concluded to provide the best separation of the compounds shown in Figure 6. At AcN concentrations greater than 10%, the capacity factors for the small amines were too similiar to provide for sufficient resolution. At AcN concentrations less than 10%, larger amines were retained too strongly on the column, and therefore required excessive chromatographic run times in order to be eluted.

Figure 7 shows the retention factors for the same series of amines versus the amount of sodium acetate (NaOAc) in the mobile phase. The NaOAc provided Na^+ as the eluent counter-ion (pusher ion) required for the cation-exchange mode of the column. Increasing the NaOAc concentration resulted in decreasing k, indicating that the separation has a significant cation-exchange component. The ideal NaOAc content in the

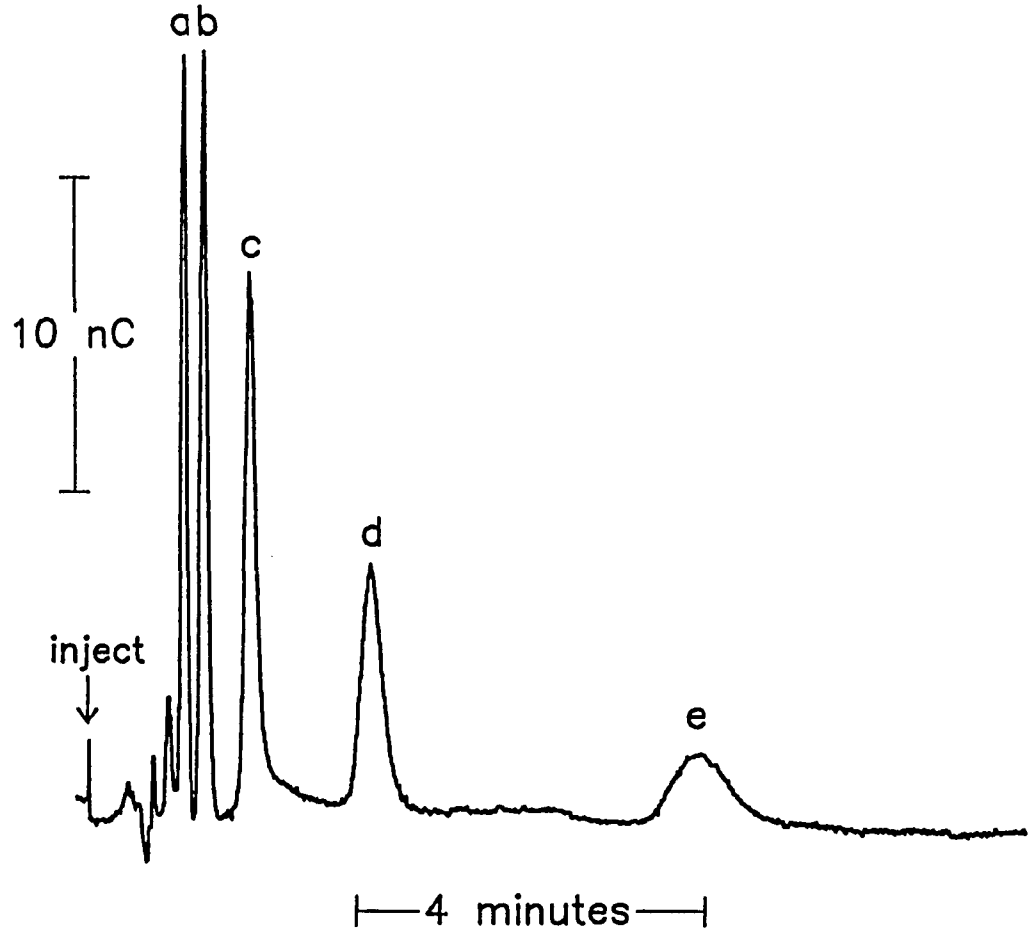

Figure 5. HPLC-PED of aliphatic amines using a multimodal column. Column: Dionex OmniPac PCX-500 (4 x 50 mm). Eluent: 30 mM HOAc/80 mM NaOAc/10% AcN at 1.0 mL min^{-1}. Post-column addition of 0.30 M NaOH at 0.6 mL min^{-1}. PED waveform: E_{DET} = 0.20 V (t_{DET}= 300 ms, t_{DEL} = 250 ms, t_{INT} = 50 ms); E_{OXD} = 0.80 V (t_{OXD} = 120 ms); E_{RED} = -0.4 V (t_{RED} = 380 ms). Peaks: (a) 50 μM ethylamine, (b) 50 μM n-propylamine, (c) 50 μM n-butylamine, (d) 50 μM n-pentylamine, (e) 50 μM n-hexylamine.

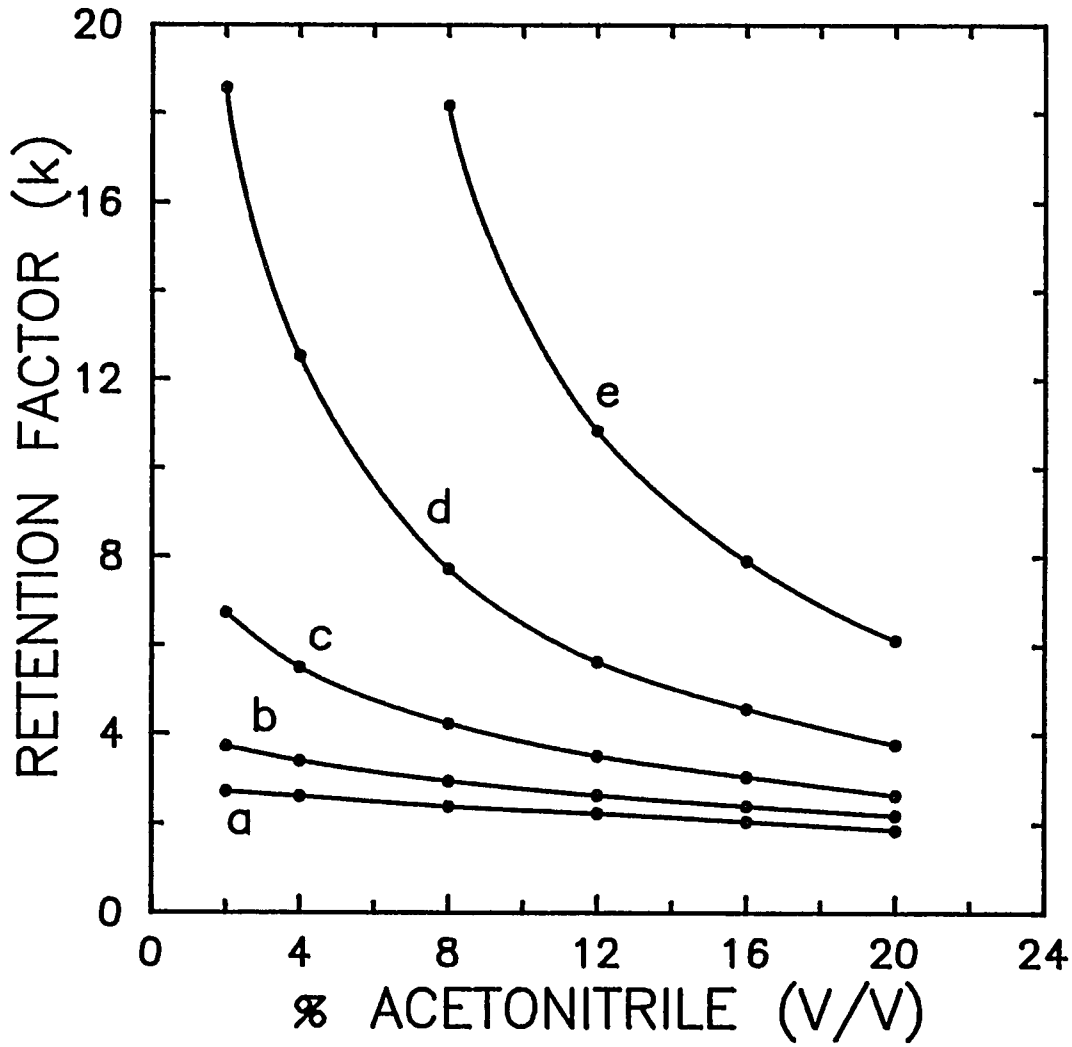

Figure 6. Amine retention factors (k) plotted versus the amount of acetonitrile (AcN) in eluent. Column: Dionex OmniPac PCX-500 (4 x 50 mm) Mobile phase: 30 mM HOAc/80 mM NaOAc/variable AcN at 1.0 mL min^{-1}. Post-column addition of 0.30 M NaOH at 0.6 mL min^{-1}. PED waveform: E_{DET} = 0.20 V (t_{DET}= 300 ms, t_{DEL} = 250 ms, t_{INT} = 50 ms); E_{OXD} = 0.80 V (t_{OXD} = 120 ms); E_{RED} = -0.4 V (t_{RED} = 380 ms). Curves: (a) ethylamine, (b) n-propylamine, (c) n-butylamine, (d) n-pentylamine, (e) n-hexylamine.

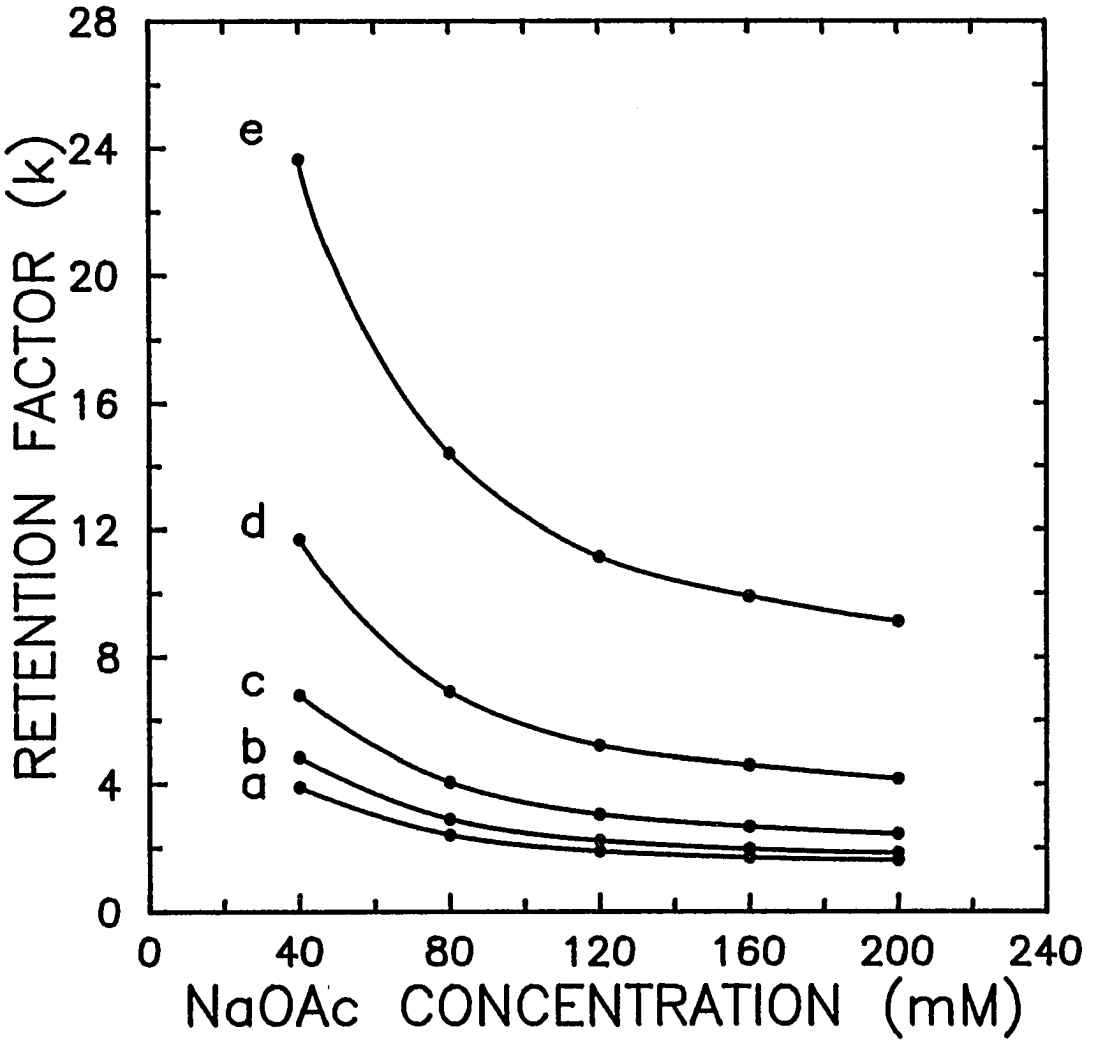

Figure 7. Amine retention factors (k) plotted versus the concentration of NaOAc in eluent. Column: Dionex OmniPac PCX-500 (4 x 50 mm). Mobile phase: 30 mM HOAc/variable NaOAc/10% AcN at 1.0 mL min^{-1}. Post-column addition of 0.30 M NaOH at 0.6 mL min^{-1}. PED waveform: E_{DET} = 0.20 V (t_{DET}= 300 ms, t_{DEL} = 250 ms, t_{INT} = 50 ms); E_{OXD} =0.80 V (t_{OXD} = 120 ms); E_{RED} = -0.4 V (t_{RED} = 380 ms). Curves: (a) ethylamine, (b) n-propylamine, (c) n-butylamine, (d) n-pentylamine, (e) n-hexylamine.

mobile phase was between 40 mM and 80 mM, for the same reasons as cited earlier for AcN. At less than 40 mM, larger amines are retained too strongly on column, and at concentrations greater than 80 mM, the retention times of the smaller amines are too similar to achieve baseline resolution.

The relationship between PED signal and amine concentration is shown in Figure 8. The response is not linear except over a narrow concentration range near the limits of detection. Such a result could be expected from the voltammetric data which also showed that the response for amines was not a linear function of concentration. Instead the response for amines, whether using voltammetry or PED, appears to be derived from species that have undergone adsorption to the electrode surface, and which are oxidized concurrently with the formation of AuO. Whether the response is under surface-control, mass-transport control, or a combination of both, a linear relationship is expected between inverse signal ($1/i$) and inverse concentration ($1/C$) [32]. As shown in Figure 9, such a relationship does exist for amines ($R^2 > 0.997$ for 10 concentrations ranging from 200 nM to 200 μM), and so calibration plots can be made in this manner.

To determine the method's reproducibility, signal was measured for eight consecutive injections of a 100 μM ethylamine standard, shown in Figure 10. The response is very consistent, with a relative standard deviation of 0.32%. Under the conditions of Figure 10, the limit of detection (S/N = 3) for the HPLC-PED of amines was about 100 nM (2.5 pmol in a 25 μL injection).

A separation of a more complex mixture of aliphatic amines is shown in Figure 11, this time using the 25 cm version of the PCX-500 column. By using the full-sized

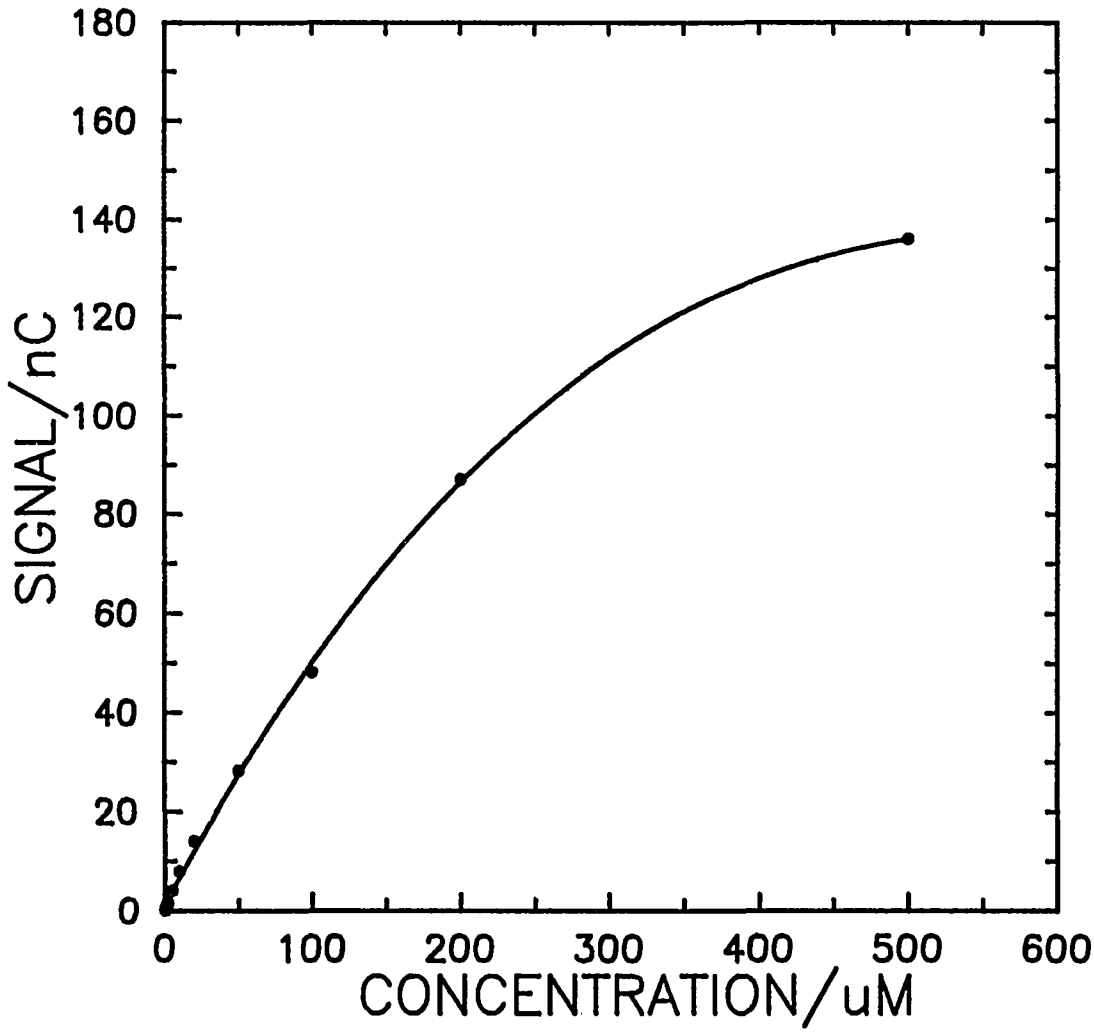

Figure 8. HPLC-PED signal versus concentration. Analyte: methylamine. Column: Dionex OmniPac PCX-500 (4 x 50 mm) Mobile phase: 40 mM HOAc/80 mM NaOAc/10% AcN at 1.0 mL min^{-1}. Post-column addition of 0.30 M NaOH at 0.6 mL min^{-1}. PED waveform: E_{DET} = 0.20 V (t_{DET}= 300 ms, t_{DEL} = 250 ms, t_{INT} = 50 ms); E_{OXD} = 0.80 V (t_{OXD} = 120 ms); E_{RED} = -0.4 V (t_{RED} = 380 ms).

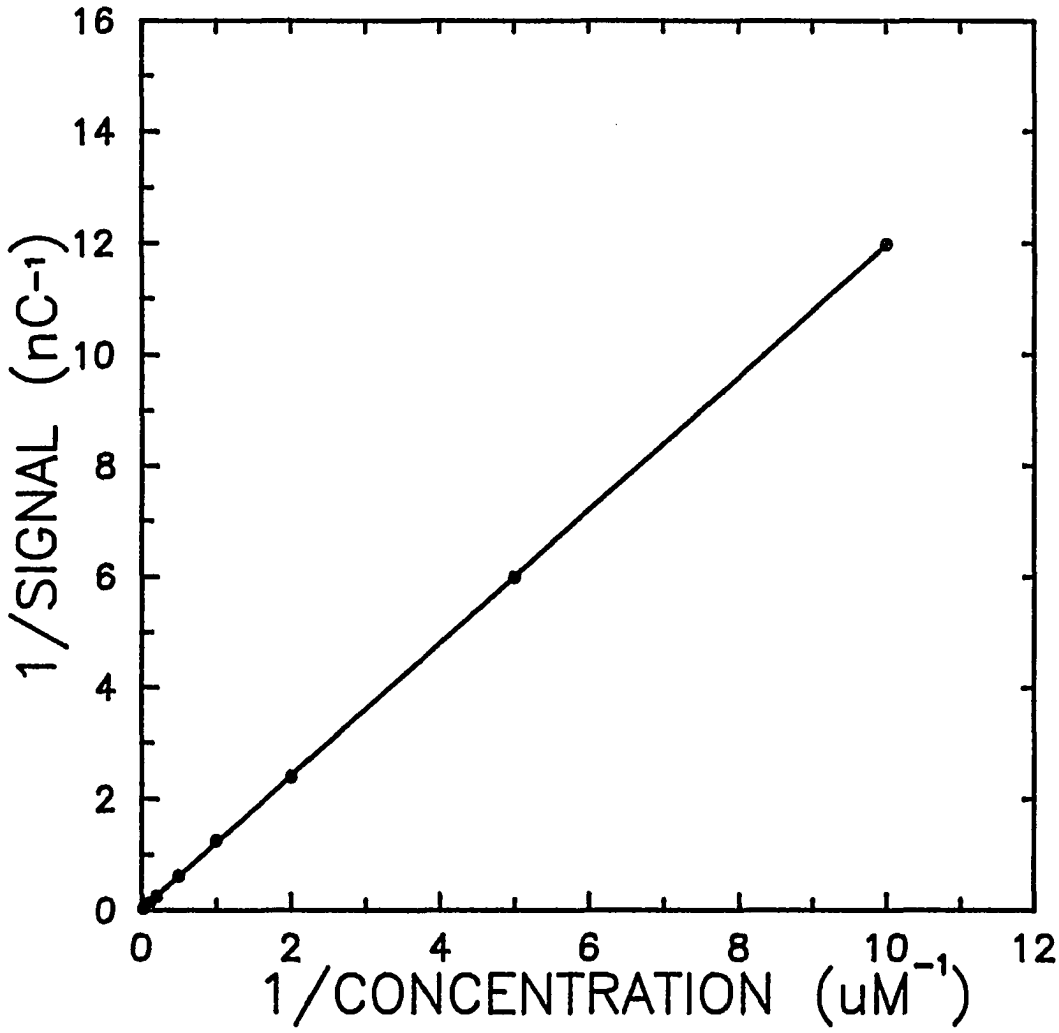

Figure 9. Calibration curve for HPLC-PED. Analyte: methylamine. Column: Dionex OmniPac PCX-500 (4 x 50 mm) Mobile phase: 40 mM HOAc/80 mM NaOAc/10% AcN at 1.0 mL min^{-1}. Post-column addition of 0.30 M NaOH at 0.6 mL min^{-1}. PED waveform: E_{DET} = 0.20 V (t_{DET}= 300 ms, t_{DEL} = 250 ms, t_{INT} = 50 ms); E_{OXD} = 0.80 V (t_{OXD} = 120 ms); E_{RED} = -0.4 V (t_{RED} = 380 ms).

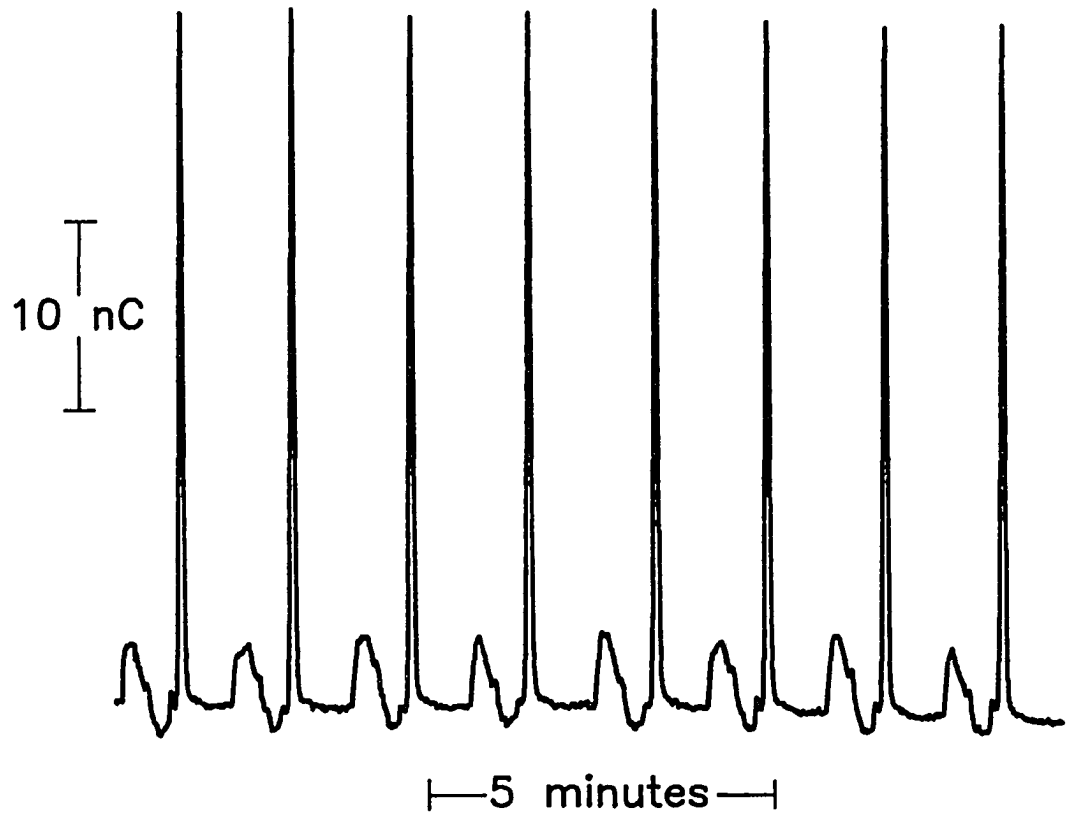

Figure 10. Reproducibility of HPLC-PED response for amines: Analyte 100 μM ethylamine. Column: Dionex OmniPac PCX-500 (4 x 50 mm) Mobile phase: 40 mM HOAc/80 mM NaOAc/10% AcN at 1.0 mL min^{-1}. Post-column addition of 0.30 M NaOH at 0.6 mL min^{-1}. PED waveform: E_{DET} = 0.20 V (t_{DET}= 300 ms, t_{DEL} = 250 ms, t_{INT} = 50 ms); E_{OXD} = 0.80 V (t_{OXD} = 120 ms); E_{RED} = -0.4 V (t_{RED} = 380 ms).

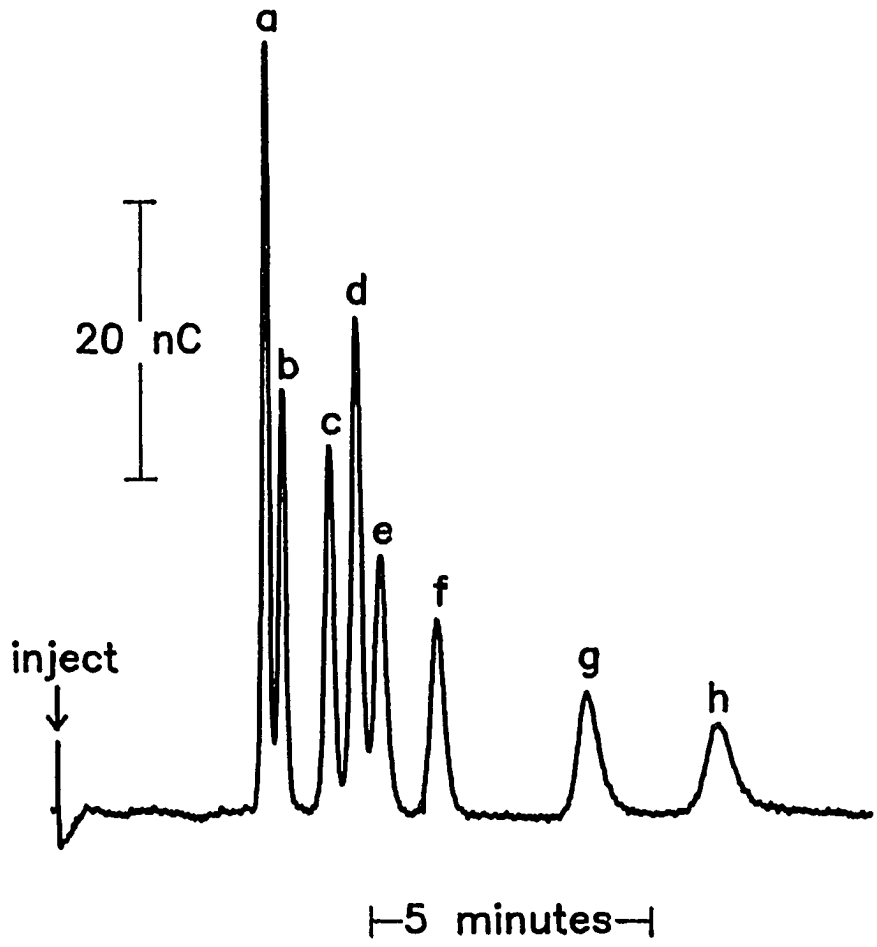

Figure 11. HPLC-PED of aliphatic amines on a full-sized multimodal column. Column: Dionex OmniPac PCX-500 (4 x 250 mm) Mobile phase: 30 mM HOAc/100 mM NaOAc/10% AcN at 1.0 mL min^{-1}. Post-column addition of 0.30 M NaOH at 0.6 mL min^{-1}. PED waveform: E_{DET} = 0.60 V (t_{DET}= 300 ms, t_{DEL} = 250 ms, t_{INT} = 50 ms); E_{OXD} = 0.80 V (t_{OXD} = 120 ms); E_{RED} = -0.4 V (t_{RED} = 380 ms). Peaks (100 μM): (a) methylamine; (b) ethylamine; (c) n-propylamine; (d) pyrrolidine; (e) isobutylamine; (f) n-butylamine; (g) isopentylamine; (h) n-pentylamine.

column, baseline resolution is achieved under isocratic conditions for methylamine and ethylamine, a result that was not possible using the 5 cm column. The separation of positional isomers also is demonstrated. Unlike the separations shown above, the response in Figure 11 was generated using a E_{DET} = 0.6 V. Since this potential is well into the oxide formation region for the Au working electrode, there is a larger background signal and, ultimately, more noise apparent in the PED response.

HPLC-PED of diamines. Attempts to separate diamines on the PCX-500 column proved unsuccessful. Most of the diamines would not elute even with large concentrations of pusher ion and organic modifier in the mobile phase, indicating extremely strong interaction with the stationary phase. This is perhaps because, in acidic media, the divalent state of diamines causes excessive affinity for the cation-exchange sites on the multimodal column. Using eluents that included divalent pusher ions did not noticeably reduce diamine retention, and so other chromatographic columns were considered.

The separation of diamines was possible on a Dionex CS-14 column, as shown in Figure 12. The CS-14 column contains a polymer-based stationary phase functionalized with a low-capacity carboxylic acid. Relative to the sulfonic acid of the PCX-500 column, the carboxylic acid is a much weaker cation-exchange material, and so diamines exhibit significantly less retention on the CS-14 column. The CS-14 column also is not designed specifically to promote hydrophobic interaction, as reflected by the diamine elution order. Straight-chain diamines are eluted from largest to smallest, and their relative retentions may be attributed to the charge densities. Cadavarine

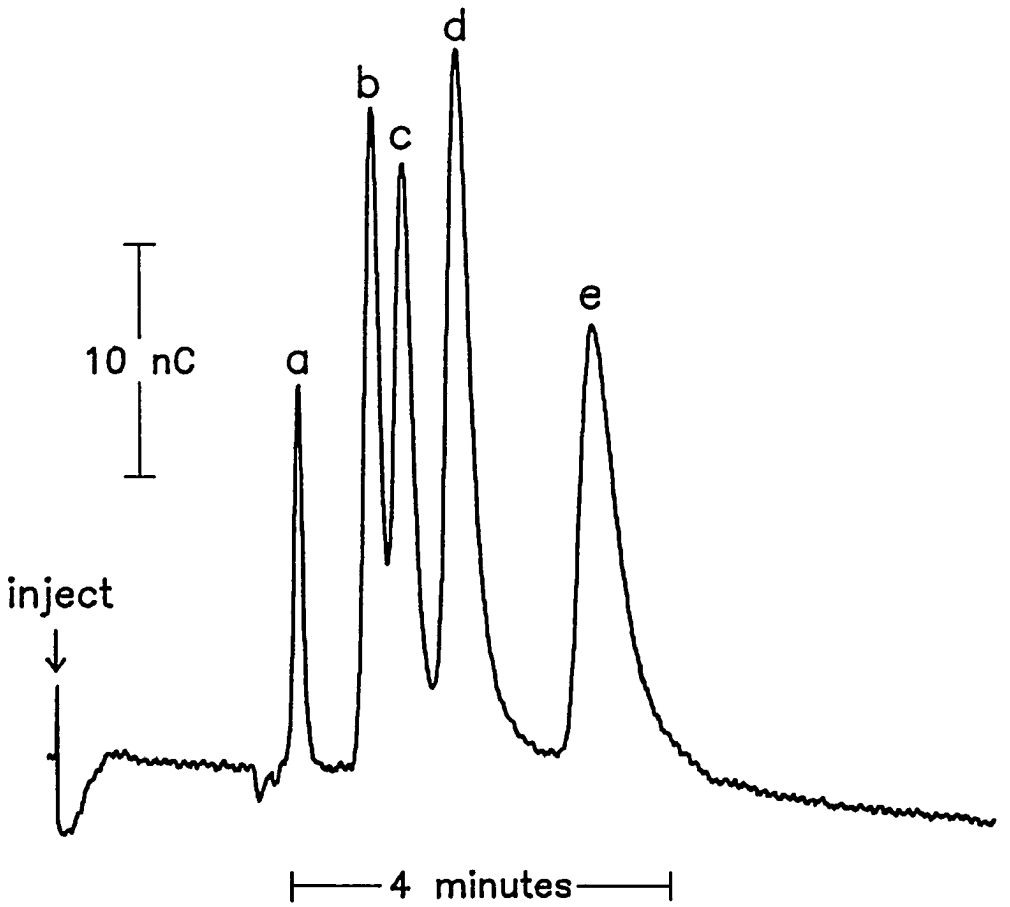

Figure 12. HPLC-PED of aliphatic diamines. Column: Dionex IonPac CS-14 (4 x 250 mm). Eluent: 50 mM HNO_3/30 mM NaOAc/15% AcN at 1.0 mL min^{-1}. Post-column addition of 0.30 M NaOH at 0.6 mL min^{-1}. PED waveform: E_{DET} = 0.40 V (t_{DET}= 300 ms, t_{DEL} = 250 ms, t_{INT} = 50 ms); E_{OXD} = 0.80 V (t_{OXD} = 120 ms); E_{RED} = -0.8 V (t_{RED} = 380 ms). Peaks: (a) 100 μM imdidazole, (b) 100 μM 1,5-diaminopentane (cadavarine), (c) 100 μM 1,4- diaminobutane (putrescine), (d) 100 μM 1,3-diaminopropane (PDA), (e) 100 μM 1,2-diaminoethane (EDA).

(1,5-diaminopentane) has the smallest charge-to-mass ratio, and so is the first to be eluted. Only imidazole, a cyclic diamine, elutes before cadavarine. This perhaps is due to imidazole's structure preventing both amine functional groups from interacting effectively with the cation-exchange sites of the stationary phase.

For the separation shown in Figure 12, the PED detection potential was chosen to be 0.4 V. As illustrated by the cyclic and pulsed voltammetry results discussed earlier, this is within the range of optimum detection potentials for diamines in solutions containing AcN. Because this potential is well into oxide formation at the Au working electrode, there is a relatively large background signal. Therefore, detection limits for diamines are not as good as those for amines. The LOD for diamines under the conditions described in Figure 12 is 200 nM (5 pmole in a 25 μL injection).

The effect of $NaNO_3$ eluent concentration on diamine retention is shown in Figure 13. The concentration of sodium pusher ion has a much smaller effect on diamine retention with the CS-14 column than it has on amine retention with the PCX-500 column. This is attributed to the different ion-exchange materials for each of the columns, and their relative affinities for sodium. The sulfonic acid of the PCX-500 column has a higher affinity for Na^+ than does the carboxylic acid of the CS-14 column. Because it is a weak acid, the CS-14 stationary phase instead has a preference for hydronium ion. Hence, small changes in $[H^+]$ can shift retention times significantly, as illustrated by Figure 14, in which diamine retention factors are plotted versus the concentration of HNO_3 in the mobile phase. Relative to $NaNO_3$, eluent HNO_3 concentration has a much larger effect on diamine retention. To obtain the best

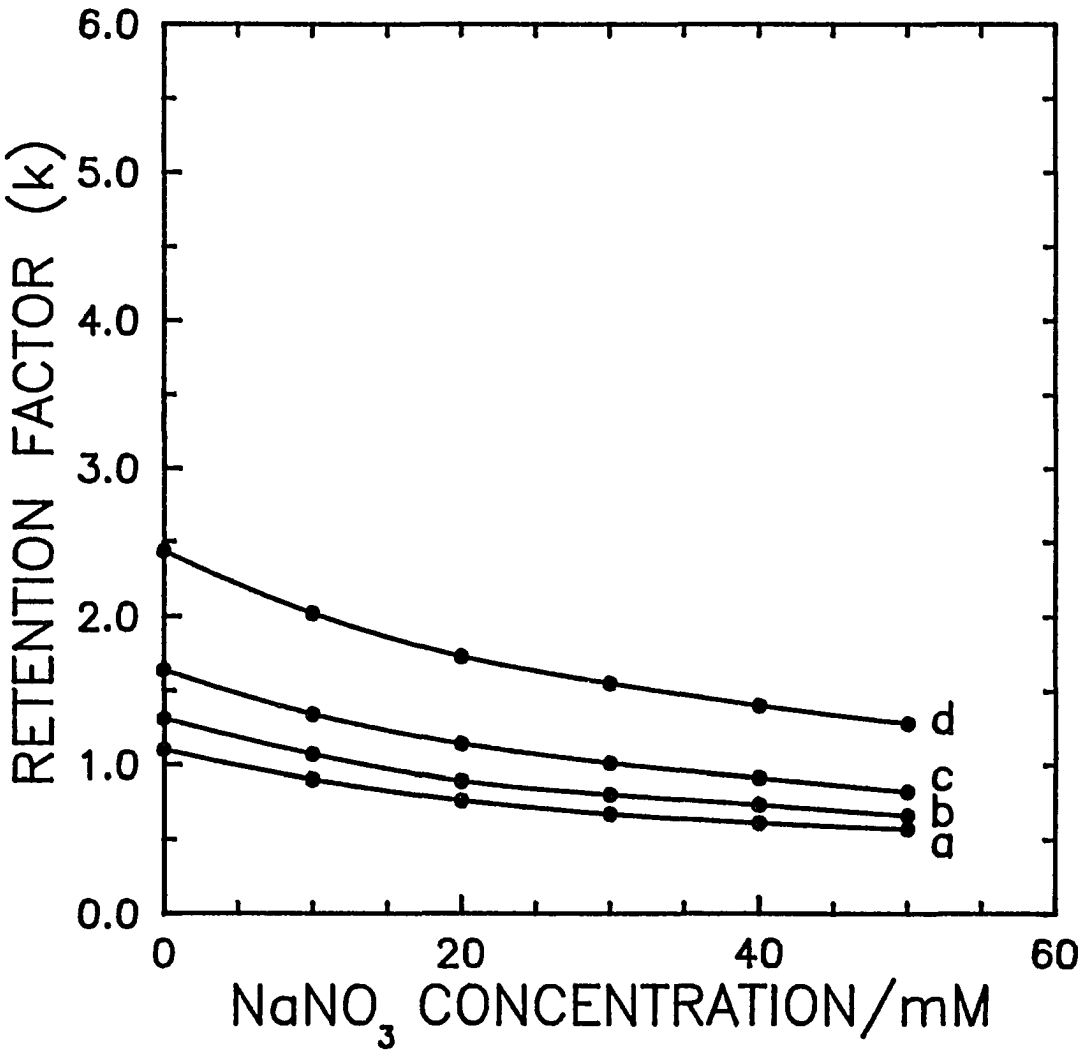

Figure 13. Diamine retention factors (k) plotted versus the concentration of $NaNO_3$ in eluent. Column: Dionex IonPac CS-14. Mobile phase: 25 mM HNO_3/variable $NaNO_3$/15% AcN at 1.0 mL min^{-1}. Post-column addition of 0.30 M NaOH at 0.6 mL min^{-1}. PED waveform: E_{DET} = 0.40 V (t_{DET}= 300 ms, t_{DEL} = 250 ms, t_{INT} = 50 ms); E_{OXD} = 0.80 V (t_{OXD} = 120 ms); E_{RED} = -0.8 V (t_{RED} = 380 ms). Curves: (a) cadavarine, (b) putrescine, (c) PDA, (d) EDA.

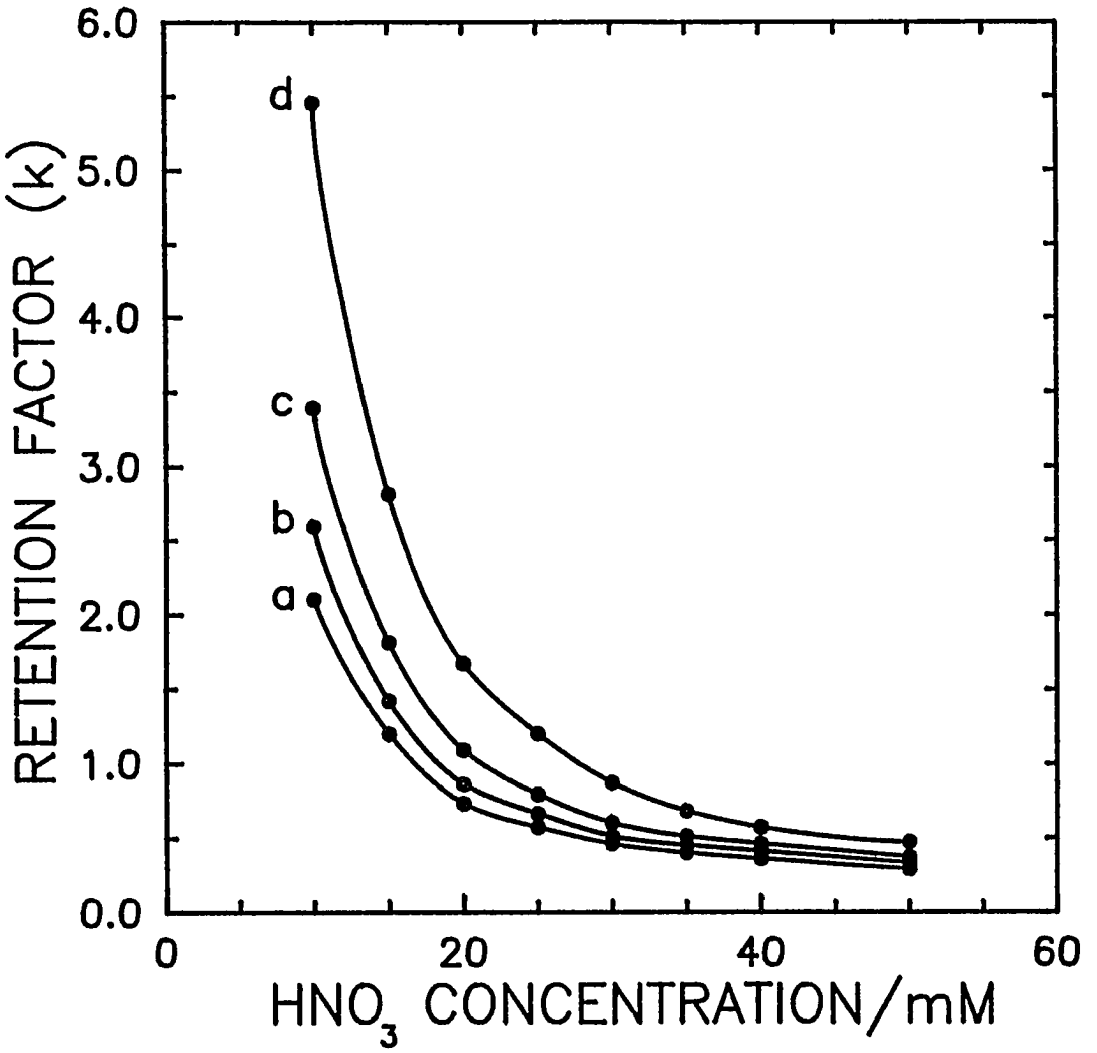

Figure 14. Diamine retention factors (k) plotted versus the concentration of HNO_3 in eluent. Column: Dionex IonPac CS-14. Mobile phase: variable HNO_3/25 mM $NaNO_3$/15% AcN at 1.0 mL min^{-1}. Post-column addition of 0.30 M NaOH at 0.6 mL min^{-1}. PED waveform: E_{DET} = 0.40 V (t_{DET}= 300 ms, t_{DEL} = 250 ms, t_{INT} = 50 ms); E_{OXD} = 0.80 V (t_{OXD} = 120 ms); E_{RED} = -0.8 V (t_{RED} = 380 ms). Curves: (a) cadavarine, (b) putrescine, (c) PDA, (d) EDA.

separation of the C_2 - C_5 diamines, the mobile phase concentration of HNO_3 should be about 20 mM.

The effect of hydronium ion concentration on diamine retention is further illustrated by Figure 15, which shows the retention factors for diamines plotted versus increasing HNO_3/NaOAc ratios. Like the carboxylate stationary phase, acetate in the mobile phase has a strong affinity for $[H^+]$. Therefore, even though the ionic concentration of the mobile phase is being varied, the HNO_3 concentration is always 20 mM greater than the NaOAc concentration. As a result, the pH is kept constant for all different HNO_3/NaOAc values, and so diamine retention factors remain fairly consistent as the eluent's total ionic strength is varied. This is indicative of the dominant role that eluent acidity plays in controlling cationic retetention on the CS-14 column.

It is possible to separate diamine positional isomers under the conditions of Figure 12. However, a more impressive demonstration of the CS-14 column's capabilities is shown in Figure 16, in which two stereoisomers are separated. Though complete baseline resolution was not achieved for the *cis* and *trans* isomers of 1,2-diaminocyclohexane, the results are still quite impressive.

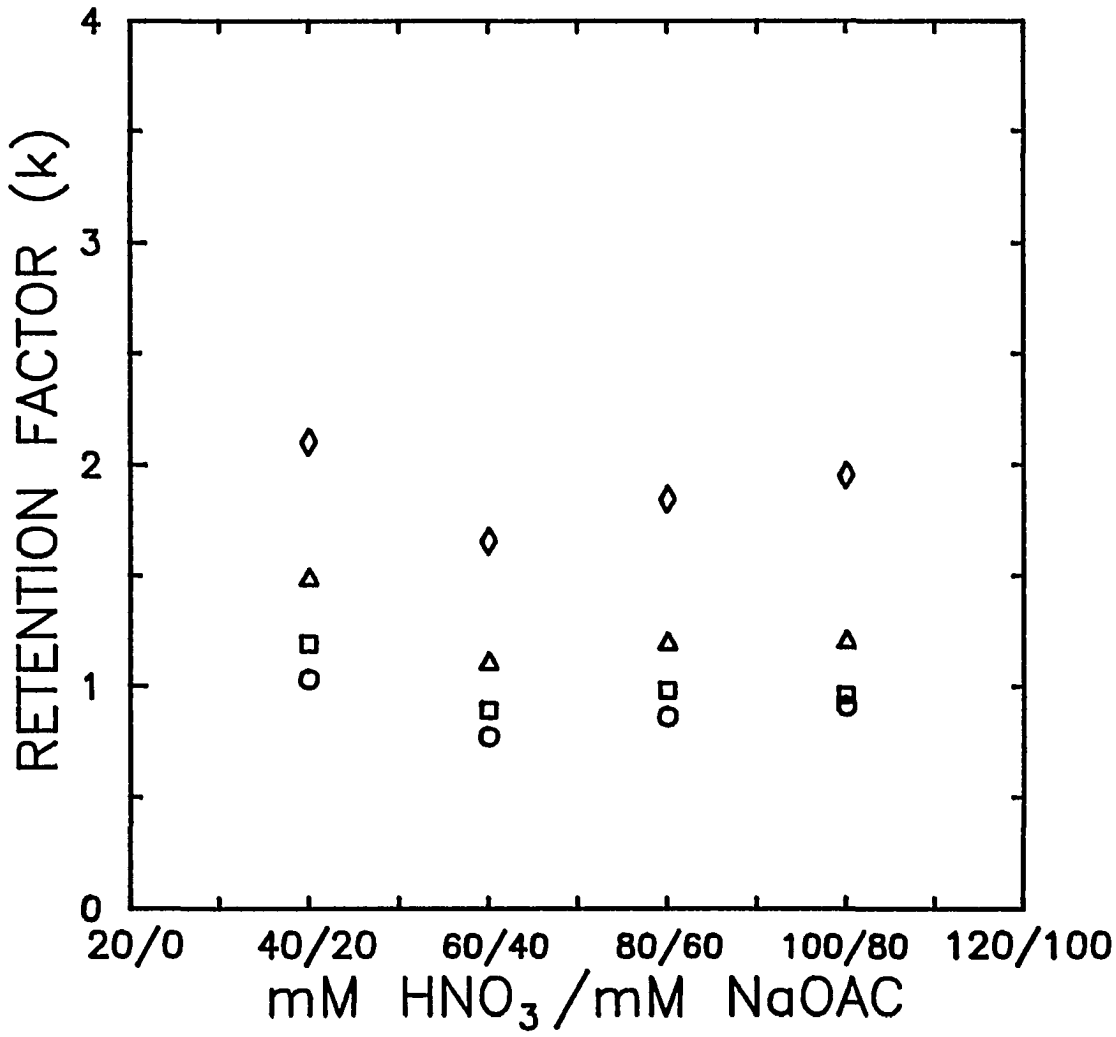

Figure 15: Diamine retention factors (k) plotted versus HNO_3/NaOAc in the eluent. Column: Dionex IonPac CS-14. Mobile phase: variable HNO_3/variable NaOAc/15% AcN at 1.0 mL min^{-1}. Post-column addition of 0.30 M NaOH at 0.6 mL min^{-1}. PED waveform: E_{DET} = 0.40 V (t_{DET}= 300 ms, t_{DEL} = 250 ms, t_{INT} = 50 ms); E_{OXD} = 0.80 V (t_{OXD} = 120 ms); E_{RED} = -0.8 V (t_{RED} = 380 ms). Curves: (○) cadavarine, (□) putrescine, (△) PDA, ( ) EDA.

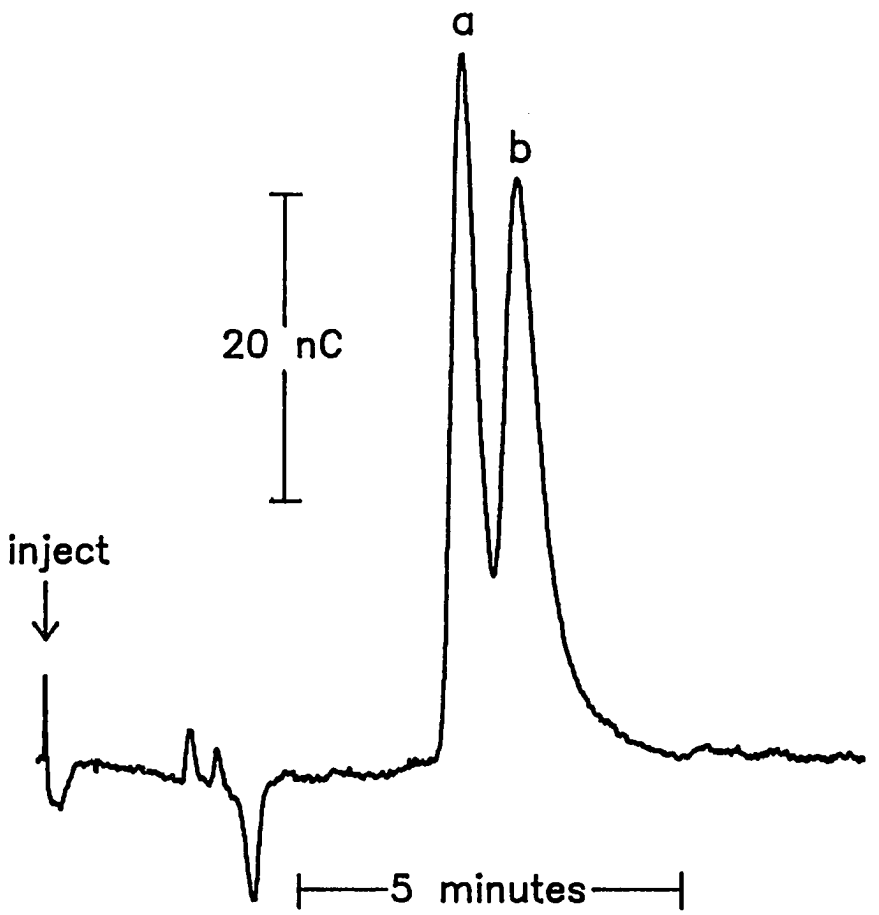

Figure 16: HPLC-PED of diamine stereoisomers. Column: Dionex IonPac CS-14 (4 x 250 mm). Eluent: 25 mM HNO_3/25 mM $NaNO_3$/15% AcN at 1.0 mL min^{-1}. Post-column addition of 0.30 M NaOH at 0.6 mL min^{-1}. PED waveform: E_{DET} = 0.60 V (t_{DET}= 300 ms, t_{DEL} = 250 ms, t_{INT} = 50 ms); E_{OXD} = 0.80 V (t_{OXD} = 120 ms); E_{RED} = -0.8 V (t_{RED} = 380 ms). Peaks: (a) *cis*-1,2-diaminocyclohexane, (b) *trans*-1,2-diaminocyclohexane.

CONCLUSIONS

The application of HPLC-PED to aliphatic amines and diamines was demonstrated. The optimumn PED detection potentials for amines and diamines were determined voltammetrically. For the amines, cyclic voltammetry showed that the optimum E_{DET} is *ca.* 0.2 V. For diamines, cyclic and pulsed voltammetry indicated that a more positive E_{DET} of between 0.4 V and 0.6 V is warranted, especially in solutions containing greater than 10% acetonitrile.

Different separation methods were employed for amines and diamines. A multimodal column combining cation-exchange and reverse-phase retention proved to be most effective for separating amines. Both cation-exchange and reverse-phase retention contributed to the separation of amines on the multimodal column, as indicated by plots of retention factors versus both the concentration of organic modifier and pusher ion in the mobile phase. The LOD for HPLC-PED of amines was 100 nM, and the relative standard deviation for successive injections of methylamine was 0.32%. The multimodal column was not capable of eluting diamines. The inability to elute diamines was attributed to their divalency in acidic eluents, which caused excessive adsorption on the high-capacity multimodal stationary phase. Therefore, a low-capacity cation-exchange column functionalized with a carboxylic acid was used instead. The elution order of the straight-chain diamines was from largest to smallest, with a LOD of 200 nM.

ACKNOWLEDGMENTS

This work was supported by grants from Dionex Corporation and the Merck Chemical Company. The authors wish to acknowledge helpful discussions with William R. LaCourse, University of Maryland, Baltimore County.

REFERENCES

1. *The Merck Index*, Merck, Rahway, NJ, 11th Ed., 1991, pp 236, 594, 1264.
2. Tabor, C. W.; Tabor, H. *Ann. Rev. Biochem.* **1976**, *45*, 285-306.
3. Jänne, J.; Pösö, H.; Raina, A. *Biochim. Biophys. Acta* **1978**, *473*, 241-293.
4. Russel, D. H.; Durie, B. G. *Polyamines as Biochemical Markers of Normal and Malignant Growth*, Raven Press: New York, 1978.
5. Yamanaka, H. *Food Rev. Int.* **1990**, *6*, 591-602.
6. Yamanaka, H.; Shiiomi, K.; Kikuchi, T. *J. Food Sci.* **1987**, *52*, 936-938.
7. Niwa, E.; Yamamoto, M.; Yamanaka, H; Matsumoto, M.; Yano, Y. *Shokuhin Eiseigaku Zasshi* **1989**, *30*, 401-405.
8. Bhavani, T. K.; Chenchu; Naidu, P. R. *Egypt. J. Pharm. Sci.* **1986**, *27*, 369-371.
9. Selig, W. *Microchem. J.* **1982**, *27*, 200-209.
10. Price, N. P. J.; Gray, D. O. *J. Chromatogr.* **1993**, *635*, 165-170.
11. Zhang, A. Q.; Mitchell, S. C.; Ayesh, R.; Smith, R. L. *J. Chromatogr.* **1992**, *584*, 141-145.
12. Avery, M. J.; Junk, G. A. *J. Chromatogr.* **1987**, *420*, 379-384.
13. Cooper, S. W.; Jayanty, R. K. M.; Knoll, J. E.; Midgett, M. R. *J. Chromatogr. Sci.* **1986**, *24*, 204-209.
14. Beck, W.; Engelhardt, H. *Chromatographia* **1992**, *33*, 313-316.
15. Bag, S. P. *Talanta* **1985**, *32*, 779-794.
16. Gilbert, R.; Rioux, R.; Saheb, S. E. *Anal. Chem.* **1984**, *56*, 106-109.

17. Buechele, R. C.; Reutter, D. J. *Anal. Chem.* **1982**, *54*, 2114-2115.

18. Tricard, C.; Cazabeil, J. M.; Salagoity, M. H. *Analusis* **1991**, *19*, M53-M55.

19. Suzuki, S.; Kobayashi, K.; Noda, J.; Suzuki, T.; Takama, K. *J. Chromatogr.* **1990**, *508*, 225-228.

20. Hayman, A. R.; Gray, D. O.; Evans, S. V. *J. Chromatogr.* **1990**, *508*, 225-228.

21. Murray, G. M.; Sepaniak, M. J. *J. Liq. Chromatogr.* **1983**, *6*, 931-938.

22. Danner, R. M.; Reddy, T. V.; Guion, C. W. *LCGC* **1994**, 12, 244-248.

23. Vuorela, H.; Lehtonen, P.; Hiltunen, R. *J. Liq. Chromatogr.* **1991**, *14*, 3181-3195.

24. Lamarre, C.; Gilbert, R.; Gendron, A. *J. Chromatogr.* **1989**, 467, 249-258.

25. Polta, J. A.; Johnson, D. C. *J. Liquid Chromatogr.* **1983**, *6*, 1727-1743.

26. Welch, L. E.; LaCourse, W. R.; Mead, Jr., D. A.; Johnson, D. C.; Hu, T. *Anal. Chem.* **1989**, *61*, 555-559.

27. LaCourse, W. R.; Jackson W. A.; Johnson, *D. C. Anal. Chem.* **1989**, *61*, 2466-2471.

28. Johnson, D. C.; LaCourse, W. R. *Anal. Chem.* **1990**, *62*, 589A-597A.

29. Johnson, D. C.; Dobberpuhl D.; Roberts, R.; Vandeberg, P. *J. Chromatogr.* **1993**, *640*, 79-96.

30. LaCourse, W. R.; Johnson, *D. C. Anal. Chem.* **1993**, *65*, 50-55.

31. Dobberpuhl, D. A.; Johnson, D. C. *J. Chromatogr.*, to be submitted.

32. Austin, D. S.; Polta, J. A.; Polta, T. Z.; Tang, A. P. -C.; Cabelka, T. D.; Johnson, D. C. *J Electroanal. Chem.* **1984**, *168*, 227 -248.

PAPER 3.

APPLICATION OF PULSED ELECTROCHEMICAL DETECTION TO A RING-DISK STUDY OF AMINE ADSORPTION AT A GOLD ELECTRODE*

*From Dobberpuhl, D. A.; Johnson, D. C. *Anal. Chem.*, to be submitted

ABSTRACT

A new application of pulsed electrochemical detection (PED) is demonstrated in which PED is applied to the ring of a Au-Au rotating ring-disk electrode (RRDE). The technique is validated experimentally by comparing the ring response for PED to that for constant potential (DC) detection using ferrocyanide as a model compound. Results indicate that PED response at the ring electrode is in good agreement with both experimental and theoretical values derived from conventional ring-disk voltammetry. Pulsed detection at the ring of an RRDE then is used to monitor the adsorptive behavior of aliphatic amine compounds at the disk electrode. Simple amines (RNH_2) are shown to exhibit potential-dependent adsorption and desorption in alkaline solutions. The behavior of amino alcohols is similar, suggesting that the adsorption of simple amines and alkanolamines is controlled exclusively by the amine moiety. The RRDE results for an amino acid, glycine are unlike those of other amine compounds studied. It is concluded that glycine's different behavior is due to the influence of the carboxylate moiety in the adsorption process.

The potential dependence of amine adsorption is discussed as it applies to selecting a PED waveform for aliphatic amines separated by high performance liquid chromatography (HPLC). Specifically, the reduction potential of a PED waveform is modified to promote amine adsorption, thus enhancing the analytical signal obtained during the detection step. The separation of several simple amines is demonstrated, with

the response from a typical PED waveform compared to that for the PED waveform designed to promote amine adsorption.

INTRODUCTION

The adsorption of amines on metal substrates strongly influences their overall behavior at these surfaces. Understanding this surface interaction therefore is important for many industrial and biological applications. For example, amines are often part of formulations designed to prevent corrosion or improve adhesion. In each application, it is the adsorptive behavior of amines that predominantly determines their utility. A thorough understanding of adsorption also advances knowledge of how amine reactions are catalyzed at metal electrodes. This would benefit techniques such as the synthesis of biologically useful peptides at metal surfaces, and in the so-called "electro-incineration" of amine compounds.

With respect to analytical chemistry, understanding how amines adsorb at metal electrodes has strong significance for electrochemical detection methods. Since adsorption is believed to precede the electrochemical reaction providing analytical signal, electrode materials and applied potentials often are chosen based upon their ability to promote interaction between surface and analyte. This is of strong interest in our laboratories, where pulsed electrochemical detection (PED) is used with high performance liquid chromatography (HPLC) for the determination of aliphatic amines, amino acids, amino alcohols and amine sugars at noble metal working electrodes [1 - 4]. A more complete characterization of amine interaction with the electrode surface should enhance the fundamental understanding of processes responsible for the electrochemical signal. With reference to PED, this means that the parameters of the pulsed potential waveform

might be chosen to maximize surface coverage, and thus increase the signal obtained for amine compounds separated by HPLC.

The adsorption of aliphatic amine compounds at metal surfaces has been studied by several methods. Techniques used to investigate the process under vacuum conditions include secondary-ion mass spectrometry (SIMS) [5], Auger electron spectroscopy (AES) [5, 6], thermal desorption spectroscopy (TDS) [6], low energy electron diffraction spectroscopy (LEEDS) [6], ultraviolet photoelectron spectroscopy (UPS) [6, 7], x-ray photoelectron spectroscopy(XPS) [8 - 10], and internal reflection-adsorption spectroscopy (IRAS) [8 - 11]. In all cited studies, the use of vacuum obviously prevented monitoring the adsorptive behavior in-situ, and so the results may not be applicable to electrochemical detection techniques. In addition, the experimental design does not permit adsorption to be monitored as a function of applied potential, which is important in optimizing electrochemical detection strategies. Other methods have allowed amine adsorption to be monitored while the metal substrate was in solution. Surface enhanced Raman spectroscopy (SERS) has been used to study the effect of amino acid adsorption on Ag [12]. Despite the excellent promise of this technique for measuring analyte interaction with a metal surface, no other application of SERS for monitoring amine adsorption was found. Voltammetry [13 - 16] and voltammetry combined with radiotracer isotopes [17 - 23] are in-situ techniques that have been proven successful for monitoring amine adsorption as a function of electrode potential. By design, these studies have proven the most valuable for determining the electrochemical behavior of amines, with the radiotracer isotope work by Horányi and coworkers [18 - 23] being most

impressive. Radiotracer isotopes were used to study adsorption of amines and amino acids at both Pt and Au, in acid and alkaline solutions, and as a function of both time and applied potential. The only difficulty with applying these results to electrochemical detection is that radiotracer measurements typically are made over a period of minutes or even hours, whereas signal generally is measured at a frequency of 1 Hz or more in flow-through systems.

Another experimental method which has been suggested for monitoring adsorption of compounds at metal surfaces is the rotating ring-disk electrode (RRDE) [24]. In a typical RRDE experiment, the ring is set at a constant potential where the analyte of interest is known to be electroactive. Current then is monitored at both ring and disk as the disk potential is scanned or stepped between selected cathodic and anodic potential limits. Since the ring electrode encircles the disk electrode, some of the analyte reaching the ring first must pass by the disk, and thus the ring electrode is essentially downstream from the disk electrode. If the disk is not producing or consuming analyte, the ring current should remain constant. However there are several processes which can occur at the disk that will change the flux of analyte to the ring. For example, if analyte is adsorbed at the disk, then the flux of analyte to the ring is reduced and the adsorption process can be measured by the resulting decrease in the ring current. Conversely, if analyte adsorbed at one disk potential is desorbed as the disk is scanned to a second potential, the subsequent elevation in analyte flux results in an increase in ring signal. Assuming that there is no attenuation of the ring response for the analyte, then adsorption and desorption at the disk can be monitored effectively by changes in ring current. The

RRDE may be especially useful when the interaction of the analyte with the electrode surface is not apparent from the disk response (e.g., adsorption without charge transfer), because the adsorption or desorption process is evident by the ring response.

Examples of previous work using the RRDE to monitor adsorption include studies of copper on Au [24], bromide [25] and iodide [26] on Pt, and hydrogen on Pt [27]. In all cited studies, constant potential detection (CPD) was used at the ring while the disk potential was varied. It therefore seemed possible to use the ring of a Au RRDE to monitor the adsorptive behavior of aliphatic amines at the disk. However, using CPD at the ring is not effective for monitoring amine compounds, because the signal for aliphatic amines (and many other aliphatic compounds) quickly decays to negligible values when a constant potential is applied to noble metal electrodes [1 - 4]. Hence, for the ring to be capable of monitoring amine behavior at the disk, the conditions responsible for amine signal at the ring would have to be regenerated continuously. PED previously has been shown to maintain conditions necessary to catalyze the oxidation of amine compounds on Au, thus providing a sensitive and reproducible signal for these compounds separated by HPLC. By applying PED to the ring of a RRDE, it should be possible to monitor amine behavior at the disk as a function of the applied potential.

Since this is the first application of PED to the ring of a RRDE, the response of the system first will be characterized using ferrocyanide, a compound with well-know voltammetric behavior, before extending the method to amine compounds. The ring response for ferrocyanide with PED will be compared to the response from CPD, and to the theoretical response calculated for the particular ring-disk geometry. PED at the ring

of the RRDE then will be shown to permit characterization of the electrochemical behavior for several small amine compounds at the Au disk under alkaline conditions. Adsorption of amines will be monitored as a function of the applied disk potential, and the results applied towards optimizing a potential waveform for the HPLC-PED of aliphatic amines.

EXPERIMENTAL SECTION

Reagents. All chemicals were used as received. Potassium ferrocyanide (Fisher Scientific), ethanolamine (Fisher Scientific) and glycine (Sigma) were reagent grade or better. Ethylamine (Kodak, Aldrich) was a practical grade of 70% (w/w) in water. N-propylamine, n-butylamine, n-pentylamine and n-hexylamine (Aldrich) were reagent grade, as were the glacial acetic acid and sodium acetate (Fisher). HPLC grade acetonitrile (Fisher) was used for the chromatographic eluent. Deionized water for all standard solutions and chromatographic eluents was purified in a Milli-Q system (Millipore) after passing through two D-45 deionizing tanks (Culligan). Sodium hydroxide solutions were prepared from a commercially available 50% w/w NaOH solution (Fisher Scientific). All solutions used in the voltammetric experiments were deaerated with nitrogen gas for several minutes prior to use. Chromatographic eluents were pre-filtered through a 0.2 μm nylon filter (Whatman).

Voltammetric apparatus. All RRDE data were obtained using a AFRDE4 bi-potentiostat, AFMSR rotator, and AFMT28AUAU gold ring-disk electrode (Pine Instrument). The disk had an outer radius of 2.29 mm. The ring had an inner radius of 2.46 mm and outer radius of 2.69 mm. The counter electrode was a coiled Pt wire. All potentials are reported versus a saturated calomel electrode (SCE; Fisher Scientific). The electrochemical cell was made of pyrex, and had porous glass frits separating individual compartments for the working, reference and counter electrodes. The potentiostat was interfaced to a personal computer (Jameco) via a DT2801-A data acquisition board (Data

Translation) and ASYST version 4.0 software (Keithley/Asyst).

Voltammetric procedure. Prior to the experiment, the gold ring-disk electrode was polished on microcloth (Buehler) using a paste of 0.05 μM alumina (Buehler) in H_20. The electrode then was placed in the electrolyte solution, and the potential cycled between oxygen and hydrogen evolution until a consistent signal for oxide formation was obtained at both the disk and ring. Potential control of the ring circuit then was placed under computer control to initiate PED. Computer programming allowed selection of the PED parameters (Figure 1) that determined the potential waveform applied to the ring. The detection potential (E_{DET}), oxidative cleaning potential (E_{OXD}), and reduction potential (E_{RED}) all could be chosen independently, as could their corresponding times, t_{DET}, t_{OXD} and t_{RED}. The detection time could be divided further into a delay time (t_{DEL}), and a data sampling time (t_{INT}). The delay time allowed the decay of current from both double layer charging and oxide formation, and thus reduced the magnitude of the background signal. During t_{INT}, the disk current, disk potential and ring current were sampled through the computer interfaced to the bi-potentiostat. The time necessary for one complete PAD waveform determined how often data was taken by the computer. For a typical PAD waveform with a total time of 500 msec, the data acquisition frequency was 2 Hz. During each detection step, signal was sampled several times during t_{INT} and then averaged to help discriminate against random noise. A variable resistor set between 1000 and 2000 Ω was placed in series with the ring electrode to further reduce the effect of system noise upon the ring signal.

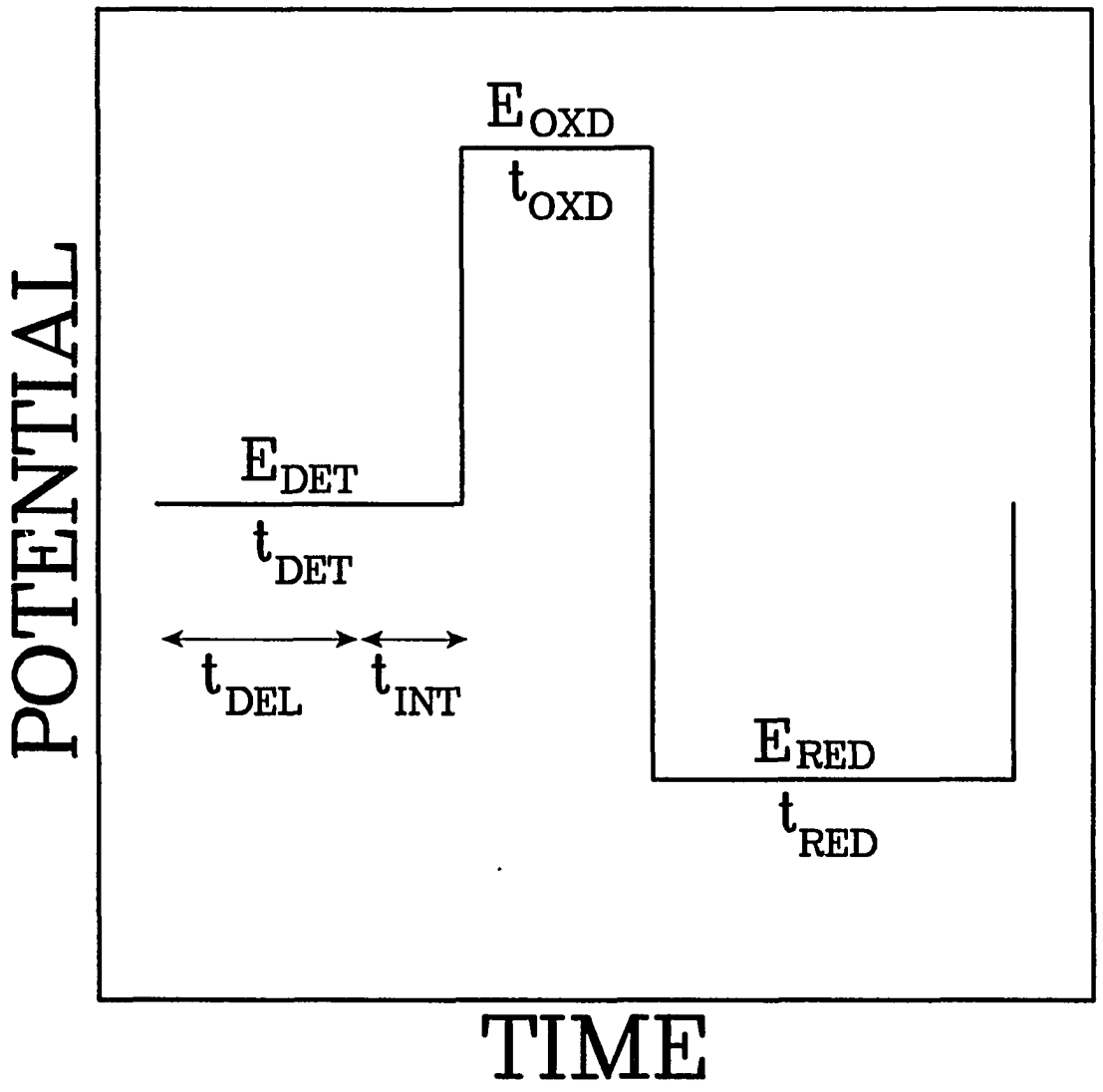

Figure 1. Potential-time (E-t) waveform for Pulsed Electrochemical Detection (PED). E_{DET} = detection potential, t_{DET} = detection period, t_{DEL} = delay period, t_{INT} = current integration (or averaging) period; E_{OXD} = oxidation potential, t_{OXD} = oxidation period; E_{RED} = reduction potential, t_{RED} = reduction period.

Chromatographic system. All chromatographic equipment was from Dionex unless noted otherwise. A GPM gradient pump and Pulsed Electrochemical Detector were interfaced to a personal computer (Zenith) through an AI-450 Chromatography Automation System. The electrochemical detection cell was a commercially available flow-through type, and consisted of a 1.4 mm diameter Au working electrode and a Ag/AgCl reference electrode. The counter electrode was provided by the upper half of the detection cell, which was made of stainless steel. Separations were performed on a PCX-500 column (4 x 50 mm). Sodium hydroxide was added post-column through a mixing tee, with constant flow maintained by a Postcolumn Pneumatic Controller™. Final concentration of NaOH in the post-column eluent was approximately 0.1 M, providing a sufficiently alkaline environment for amine oxidation to occur at the Au working electrode.

RESULTS AND DISCUSSION

Characterization of PED response at the ring with ferrocyanide. The rotating disk electrode (RDE) is one of the most successful hydrodynamic electrodes used in modern electrochemistry for determining the kinetics and mechanisms of reactions occurring at solid electrodes [28, 29]. The RDE benefits from the relative ease with which a controlled hydrodynamic flow is maintained solely through rotation of the electrode body, allowing a rigorous and quantitative treatment of the mass-transport process. Levich showed that the limiting current for a rotating disk electrode ($i_{d,l}$, amps) can be calculated as [30, 31]

$$i_{d,l} = 0.62nFAD^{2/3}\omega^{1/2}\nu^{-1/6}C^{b} \qquad (1)$$

where n is the number of electrons passed in the reaction (eq/mol), F is Faraday's constant (C/eq), A is the area of the electrode (cm^2), ω is the electrode's rate of rotation (rad/s), ν is the kinematic viscosity of solution (cm^2/s), and C^b is the concentration of the analyte in solution (mol/cm^3). Equation 1, referred to as the Levich equation, predicts that current for a mass-transport limited reaction will be proportional to the concentration of analyte and to the square root of electrode rotation rate.

The RRDE is an extension of the RDE in which the disk electrode is encircled by a ring electrode. In the absence of any reaction occurring at the disk, the limiting current at the ring electrode is given by [32]

$$i_{r,l} = 0.62nF\pi(R_3^3 - R_2^3)^{2/3}D^{2/3}\omega^{1/2}\nu^{-1/6}C^{b} \quad (2)$$

where R_3 and R_2 represent the outer and inner radii of the ring electrode, respectively. As with the disk electrode, the limiting current for the ring electrode is proportional to $\omega^{1/2}$. If the formula for the area of a disk is substituted into Equation 1, then the ratio of ring current to disk current ($\beta^{2/3}$) under mass transport-limited conditions can be derived by dividing Equation 2 into Equation 1 to yield

$$\beta^{2/3} = \frac{i_{r,l}}{i_{d,l}} = \frac{(R_3^3 - R_2^3)^{2/3}}{R_1^2} = \left[\left(\frac{R_3}{R_1}\right)^3 - \left(\frac{R_2}{R_1}\right)^3\right]^{2/3} \quad (3)$$

where R_1 is the radius of the disk electrode.

Near the surface of a RRDE, the radial flow of solution outward from the center results in the ring electrode effectively being downstream from the disk electrode, and so some of the analyte reaching the ring must first pass by the disk. The fraction of species produced at the disk which is capable of being detected by the ring is referred to as the theoretical collection efficiency (N). As with $\beta^{2/3}$, N is a function of the ring-disk geometry, and is given by [33 - 34]

$$N = 1 - F(\alpha/\beta) + \beta^{2/3}[1 - F(\alpha)] - (1 + \alpha + \beta)^{2/3}[1 - F(1 + \alpha + \beta)] \quad (4)$$

where

$$\alpha = \left(\frac{R_2}{R_1}\right)^3 - 1 \tag{5}$$

and

$$F(x) = \frac{3^{1/2}}{4\pi} \ln \frac{1+x}{(1+x^{1/3})^3} + \frac{3}{2\pi} \arctan \frac{2x^{1/3}-1}{3^{1/3}} + \frac{1}{4} \tag{6}$$

Choosing an analyte with fast reaction kinetics allows the RRDE's response to be compared with the theoretical results derived from the above equations. For example, Equations 1 and 2 predict that the limiting current for a mass-transfer limited reaction should be proportional to $\omega^{1/2}$ at both the ring and the disk electrodes. Additionally, the experimental values of $\beta^{2/3}$ and N for a given RRDE geometry should be consistent with those calculated from Equations 3 - 6. Since pulsed detection at the ring of a RRDE is a novel application, the technique was first characterized using a compound with known electrochemical behavior. Ferrocyanide, which undergoes a one-electron oxidation to ferricyanide, was chosen as the model compound because of its quasi-reversible kinetics and well-defined electrochemical response at noble metal electrodes [35 - 38]. If the experimental results for ferrocyanide agreed with the expected response for a mass-transport limited analyte, then PED could be extended to compounds such as aliphatic amines that had not been characterized as thoroughly in previous studies.

Figure 2 shows the voltammetric response for Au in 0.1 M NaOH supporting electrolyte, with and without ferrocyanide present. Arrows on the curves indicate scan

direction. Curve **a** is the residual and represents the current from the Au disk electrode as potential is scanned with only supporting electrolyte present in solution. The two most prominent features of the Au residual are the formation of surface oxide (AuO) on the positive scan at potentials greater than 0.1 V, and the subsequent dissolution of surface oxide on the negative scan, seen as a cathodic peak also beginning at about 0.1 V. Curve **b** of Figure 2 shows the response of the disk electrode with 1.00 mM ferrocyanide in solution. The oxidation of ferrocyanide takes place during both scan directions, so long as the disk potential is positive of *ca.* 0.1 V. As the similar shapes of curves **a** and **b** suggest, ferrocyanide oxidation occurs concurrently with oxide formation, although the formation of AuO is not required for the ferrocyanide reaction [35, 36]. If the residual response is subtracted from the response with ferrocyanide in solution (i.e., if curve **a** is subtracted from curve **b**), then the remainder would represent current due only to the reaction of ferrocyanide. Curves **a** and **b** of Figure 2 show that the ferrocyanide response would appear as a current plateau, and this is indicative of a reaction that is mass-tranport limited. Therefore, the oxidation of ferrocyanide to ferricyanide is not limited kinetically under these conditions, and so the reaction is an excellent choice for characterizing RRDE behavior.

Curve **c** of Figure 2 shows the ring current (i_r) plotted versus disk potential (E_d) with 1.00 mM ferrocyanide in solution and CPD applied to the ring. As in all other cyclic voltammograms, the ring response is shown ten times (10x) its actual value for clarity. A potential of 0.5 V was applied to the ring, which was sufficient to oxidize

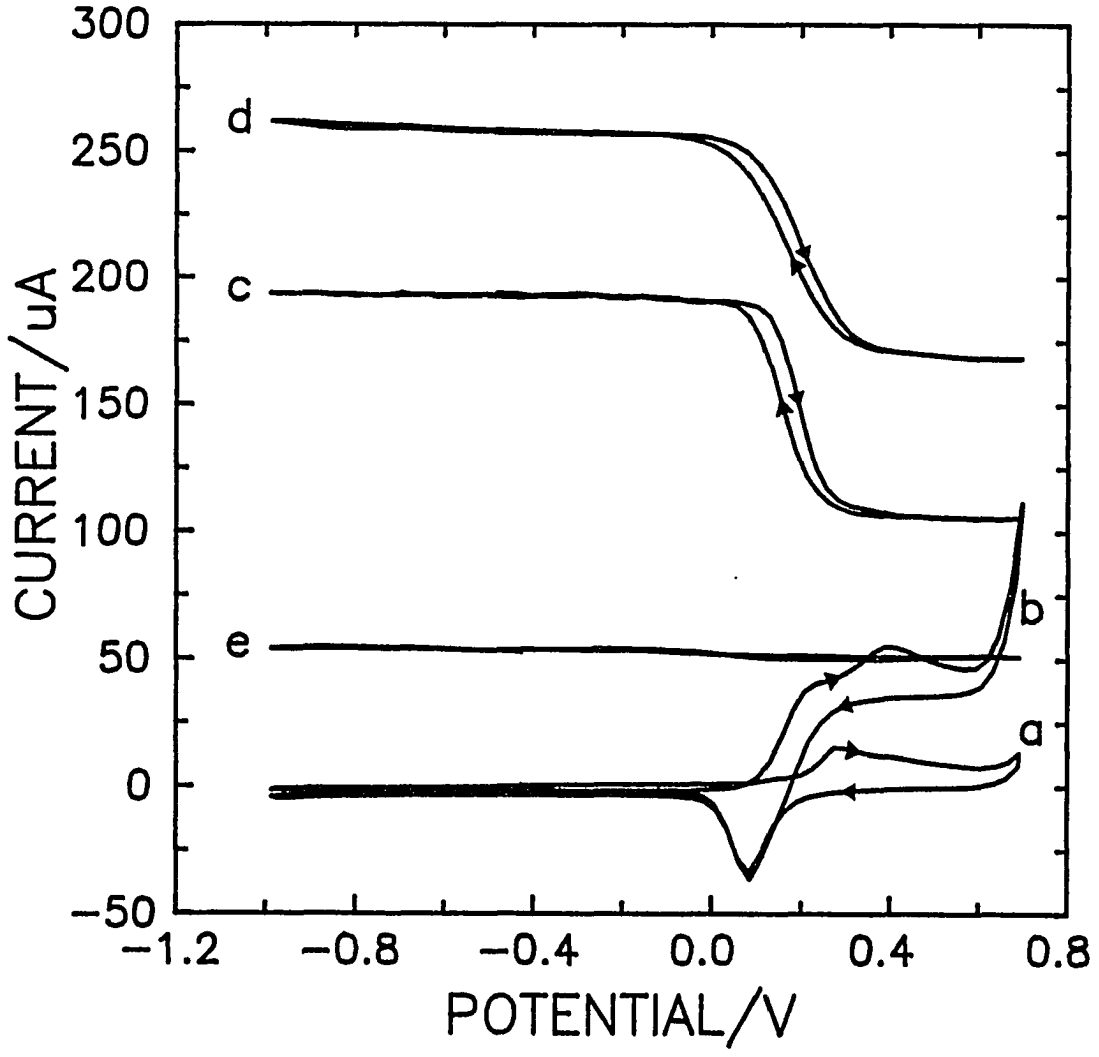

Figure 2. Voltammetric response for 1.00 mM ferrocyanide at Au RRDE in 0.1 M NaOH. Rotation rate: 225 rev min^{-1}. Disk scan rate: 50 mV s^{-1}. Curves: (a) disk, residual, (b) disk, 1.00 mM ferrocyanide, (c) ring (10x), 1.00 mM ferrocyanide; PED waveform: E_{DET} = 0.5 V, t_{DET} = 350 ms, t_{DEL} = 300 ms; E_{OXD} = 0.8 V, t_{OXD} = 60 ms; E_{RED} = -0.8 V, t_{RED} = 90 ms, (d) ring (10x), 1.00 mM ferrocyanide; CPD at a potential of 0.5 V, (e) ring, residual (10x), PED waveform identical to that in (c).

ferrocyanide at a mass-transport limited rate. There are two plateaus of ring response as the disk potential is scanned. When the disk potential is less than 0.1 V, no oxidation of ferrocyanide occurs at the disk. Since the ring is not shielded by the disk, and ring current is at maximum in this potential region. When the disk potential is positive of 0.1 V, ferrocyanide is oxidized at the disk and makes less available to the ring, thus resulting in the smaller current plateau evident at $E_d > 0.2$ V.

Curve **d** of Figure 2 represents the response for ferrocyanide with PED applied to the ring electrode. The PED waveform detection potential (E_{DET}) was chosen to be 0.5 V to facilitate comparison to the CPD response shown in curve **c**. The ring response with PED is qualitatively similar to that using CPD. The most apparent difference is about 5 μA of additional current generated with the PED waveform. As is evident from curve **e**, which shows the ring response for the same PED waveform with no analyte in solution, most of this excess current is attributable to a higher background resulting from the generation of surface oxide during the detection step of the PED waveform. Unlike CPD, the ring potential is not constant during the entire experiment, and so the AuO being generated continuously with each PED cycle results in anodic current that does not completely decay before the ring response is measured during E_{DET}. If the residual current (curve **e**) is subtracted from the PED signal with ferrocyanide present (curve **d**), then there is almost no difference between the PED and CPD response for ferrocyanide.

According to Equation 2, there should be a linear correlation between ring current and the square root of rotation speed for a reaction with fast kinetics. Figure 3 shows plots of i_r versus $\omega^{1/2}$ for ferrocyanide using both CPD and PED. For both sets of data,

the response in the absence of analyte (residual response) has been subtracted. As predicted by the Levich equation, there is a linear relationship ($R^2 > 0.999$) for both CPD and PED at the ring electrode. The intercept of the line representing the PED response is slightly larger than that for CPD, which can be attributed to imperfect correction for the large background current. In the presence of ferrocyanide, there is a small shift in the current for oxide formation at $E_d > 0.2$ V, so that a small offset is seen when the ring residual (background signal) is subtracted from the response with ferrocyanide in solution. The discrepancy should not detract from the fact that, as Figure 3 shows, there is a linear relationship between i vs $\omega^{1/2}$ for both sets of data, and that PED is in good agreement with CPD.

Further validation of PED at the ring of the RRDE was made by measuring the ratio ($\beta^{2/3}$) of the ring current to disk current under mass-transport limited conditions, and comparing the values to those from CPD and theory. The comparison for three electrode rotation speeds is shown in Table 1. The theoretical values ($\beta^{2/3}_{CAL}$) were calculated using Equation 3 and the respective radii of the ring and disk electrodes. The experimental values ($\beta^{2/3}_{PED}$, $\beta^{2/3}_{CPD}$) were determined from the response of 1.00 mM

Table 1: Comparison of calculated and experimental[a] $\beta^{2/3}$ values

Rotation Speed (RPM)	$\beta^{2/3}_{CAL}$	$\beta^{2/3}_{PED}$	$\beta^{2/3}_{CPD}$
400	0.526	0.545 ± 0.018	0.523 ± 0.006
900	0.526	0.537 ± 0.016	0.523 ± 0.006
1600	0.526	0.534 ± 0.016	0.524 ± 0.005

[a]Experimental values of $\beta^{2/3}$ determined using 1.00 mM ferrocyanide in 0.1 M NaOH. Experimental uncertainties measured using the standard deviation of four trials.

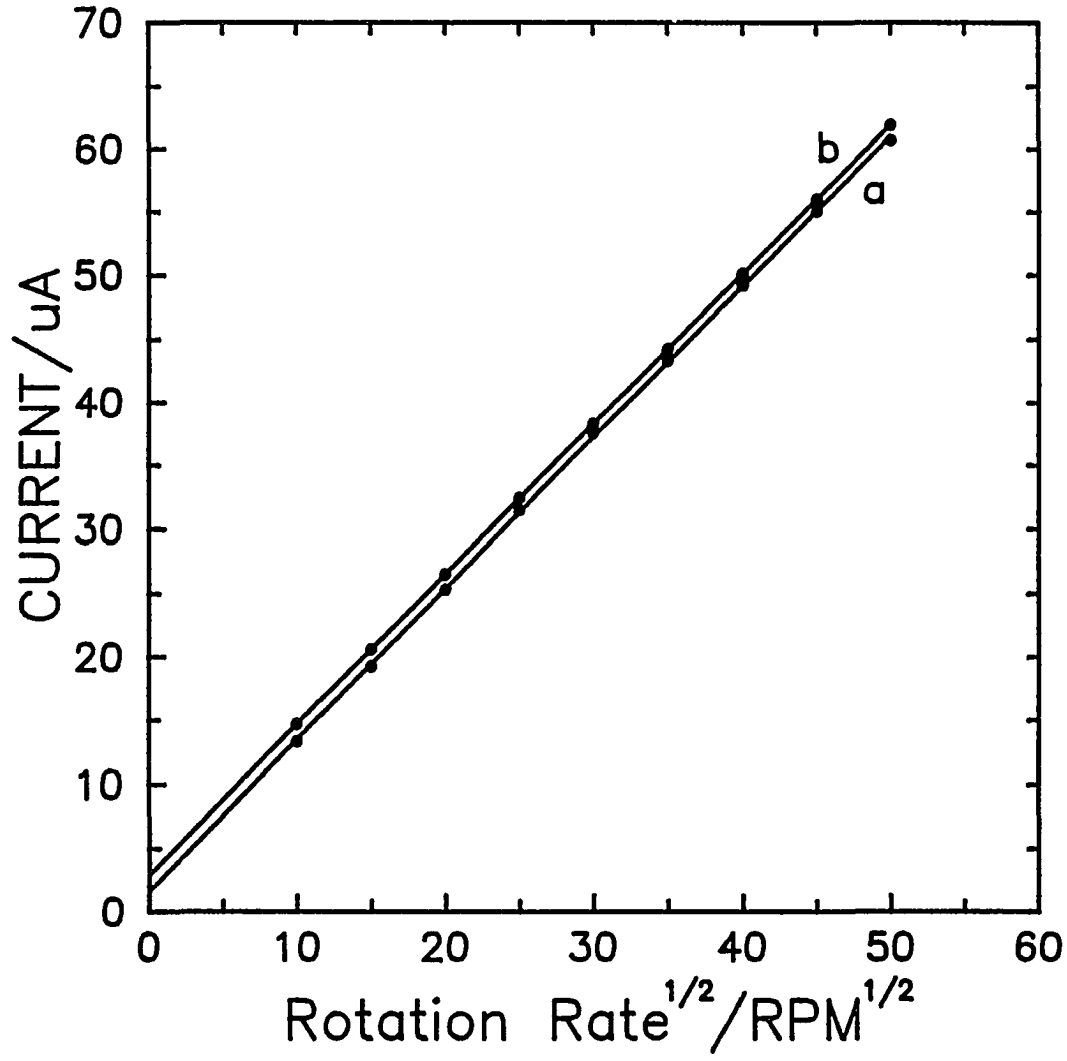

Figure 3. Current versus square root of rotation speed for 1.00 mM ferrocyanide at Au in 0.1 M NaOH. Curves: (a) ring response using CPD at a detection potential of 0.5 V; (b) ring response using PED. Waveform: E_{DET} = 0.5 V, t_{DET} = 350 ms, t_{DEL} = 300 ms; E_{OXD} = 0.8 V, t_{OXD} = 60 ms; E_{RED} = -0.8 V, t_{RED} = 90 ms. The data is shown with the residual current subtracted for both CPD and PED.

ferrocyanide at a potential of 0.5 V. As with the plots of i vs $\omega^{1/2}$, the residual current was subtracted from the response with ferrocyanide in solution. The experimental values of $\beta^{2/3}$ from PED do not conform to the theoretical values as well as do those from CPD. The disparity can be attributed to imperfect correction for background current in the absence of ferrocyanide, which is more evident at the slower rotation speeds where the flux of analyte to the electrode surface is smallest, and the relative error introduced by background subtraction is largest.

A final test of how well PED correlates with CPD and theory is shown in Table 2, which compares collection efficiencies at the three rotation speeds. The theoretical collection efficiency was calculated using Equations 4-6. The experimental N values were determined using:

$$N = -\frac{i_r}{i_d} \qquad (7)$$

which is applicable to a ring reaction that is identical to, but in the reverse direction of, the reaction at the disk. For the experimental values of N shown in Table 2, the disk current was measured at a disk potential of 0.5 V, and the ring current measured at a ring potential of -0.5 V. Thus, the disk reaction was the oxidation of ferrocyanide to ferricyanide, whereas the reaction at the ring was the reverse, with ferricyanide reduced back to ferrocyanide. The waveform used for the PED results was the same as that in Figure 2, with the exception of the detection potential, which was -0.5 V. The PED data

Table 2. Comparison of calculated and experimental[a] collection efficiencies.

Rotation Speed (RPM)	N_{CAL}	N_{PED}	N_{CPD}
400	0.220	0.230 ± 0.016	0.232 ± 0.013
900	0.220	0.227 ± 0.015	0.229 ± 0.010
1600	0.220	0.229 ± 0.012	0.228 ± 0.008

[a]Experimental collection efficiencies determined using 1.00 mM ferrocyanide in 0.1 M NaOH. Uncertainties measured using the standard deviation of four trials.

shows good agreement with RRDE theory and with CPD data, providing further evidence that PED is comparable to CPD.

The similar results obtained by PED and CPD for ferrocyanide, as well as the apparent adherence of PED results to RRDE theory, demostrate that PED can be applied successfully at the ring to monitor analytes which have mass-transport limited response. However, there is no intrinsic advantage for PED over CPD for compounds like ferrocyanide that are electroactive under constant potential conditions. The benefit of PED at the ring of an RRDE is realized for compounds that do not remain electroactive when CPD is used. In the next section, PED at the ring electrode is used to monitor the electrochemical behavior of analytes show little response with CPD. Specifically, PED at the ring electrode will be used to determine the adsorptive behavior of amines at the Au disk electrode.

Monitoring amine behavior using PED at the ring of an RRDE. The electrochemical behavior of amine compounds was studied using PED at the ring and linear-sweep voltammetry at the disk of an RRDE. The results are shown in Figure 4.

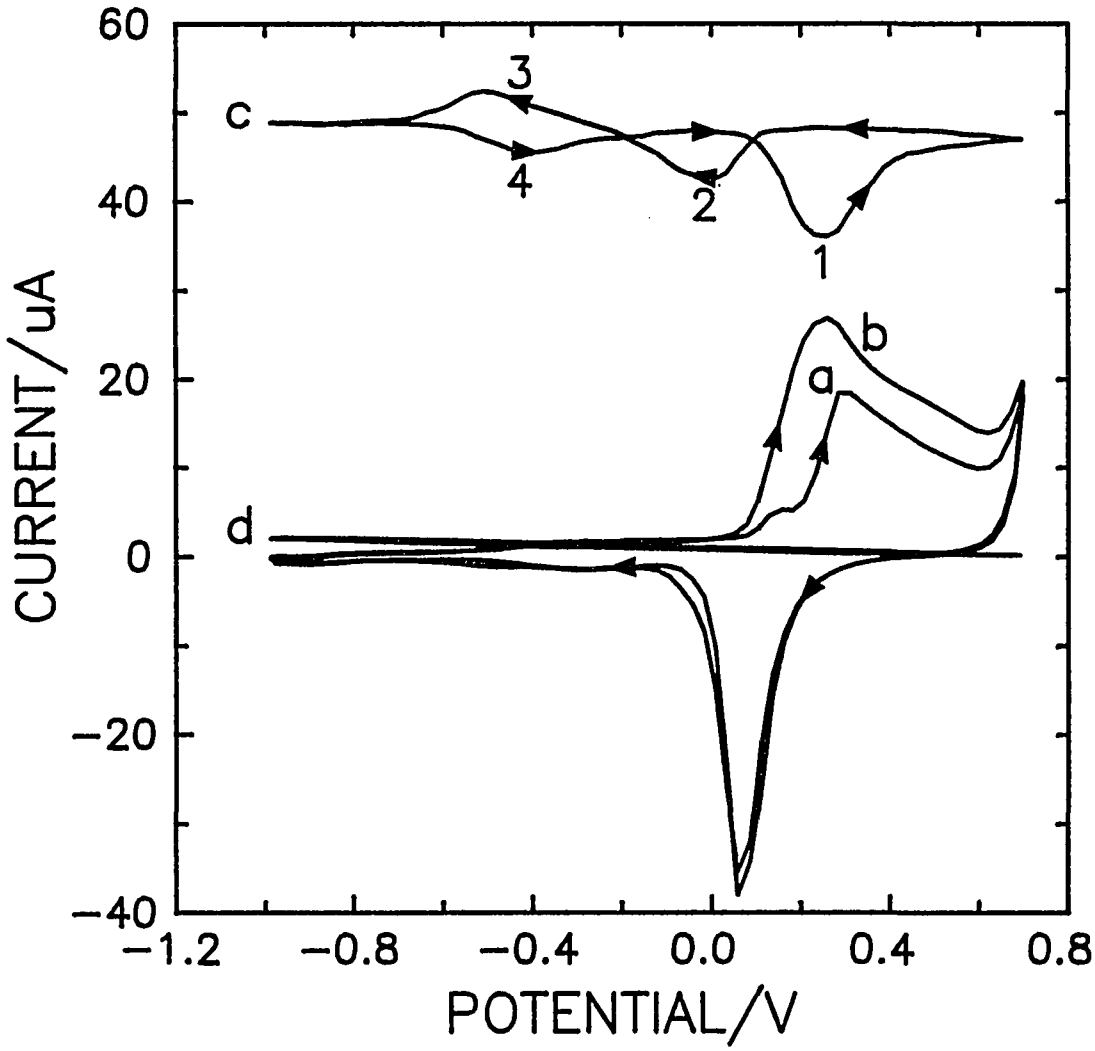

Figure 4. Voltammetric response for 40 μM ethylamine at Au in 0.1 M NaOH. Rotation rate: 900 rev min^{-1}. Disk scan rate: 50 mV s^{-1}. Curves: (a) disk, residual; (b) disk, 40 μM ethylamine; (c) ring (10x), 40 μM ethylamine, PED waveform: E_{DET} = 0.2 V, t_{DET} = 350 ms, t_{DEL} = 300 ms; E_{OXD} = 0.8 V, t_{OXD} = 60 ms; E_{RED} = -0.8 V, t_{RED} = 90 ms, (d) ring (10x), 40 μM ethylamine, CPD with a detection potential of 0.2 V.

Curve **a** again represents the residual response of the Au disk in 0.1 M NaOH. The disk response for 40 μM ethylamine is shown as curve **b**. As the disk potential is scanned positive of 0.1 V, the oxidation of ethylamine occurs concurrently with the formation of AuO. Oxidation of both ethylamine and Au continues until the positive scan limit is reached, and terminates upon initiation of the negative potential scan. The reaction of ethylamine at the Au disk behaves as would be expected for a process that is predominantly under surface control, with the resulting anodic current being much less than what would be seen for a mass-transport limited reaction. However, at concentrations less than 100 μM, the ethylamine signal does vary somewhat with both concentration and rotation speed, indicating that at low concentrations, the oxidation of ethylamine is under both mass-transport and surface control.

The ring response for the PED of ethylamine is shown as curve **c** of Figure 4. In the absence of any disk reaction affecting ethylamine flux, the ring signal would appear to be constant at all disk potentials. However, the ring response for ethylamine is not constant, and instead exhibits both shielding and collection phenomena. There are four distinct regions of ring response for ethylamine as the disk potential is scanned. Region 1 begins at E_d = 0.1 V and continues to the positive scan limit. Of the four regions, this region is the simplest to explain based upon the apparent behavior of ethylamine at the disk. As ethylamine is oxidized at the disk, the flux of ethylamine to the ring is reduced, resulting in the decrease (shielding) of ring current. The ring data can provide further insight into the oxidation of ethylamine at the disk. At potentials between 0.3 V and 0.5 V, disk current generated from the oxidation of ethylamine is fairly uniform, and so,

based upon disk response, it might be concluded that ethyalmine is adsorbing to the disk surface at a consistent rate in this potential region. If so, the ring current should also exhibit a relatively consistent shielding response. Instead, the ring's shielding response reaches a maximum at E_d = 0.2 V and then decreases at more positive potentials. This suggests that at potentials greater than 0.2 V, much of the disk current for ethylamine is not from analyte that is being concurrently transported to the electrode surface, but instead is due to ethylamine previously adsorbed at less positive potentials.

Upon initiation of the negative disk scan at 0.7 V, the oxidation of ethylamine at the disk ceases and a constant current for ethylamine is displayed by the ring. The currents remain stable until about 0.1 V. At this point, AuO is stripped from the disk, and a second shielding of ring current is evident in region 2. Unlike the shielding response in region 1, the shielding exhibited by the ring cannot be due to ethylamine oxidation at the disk, because there is no evidence for such a reaction from the disk response. Instead, the shielding peak is attributable to adsorption of ethylamine at the Au disk, and the adsorption occurs with negligible charge transfer. Since the adsorption takes place only as AuO is reduced at the disk, it appears that amines preferentially interact with a reduced Au surface that is relatively free of oxide.

As the disk potential is scanned negative of -0.4 V, the ring exhibits an increase in the current in region 3 that can be attributed to the collection of ethylamine being desorbed from the disk. As in region 2, there is no evidence of any faradaic reaction at the disk, and so the desorption of ethylamine from the disk is occurring without charge transfer. Apparently, some of the ethylamine adsorbed at the disk in region 2 undergoes

desorption as the disk potential is scanned into region 3, indicating that surface coverage is potential dependent.

A final shielding of ring current occurs in region 4 on the positive scan of the disk potential. The shielding occurs at almost the same potential as the collection of region 3 took place, and, indeed, the two regions are almost mirror images of each other. It follows that this decrease in ring current may be attributed to re-adsorption of ethylamine on the positive scan at disk sites where ethylamine had been desorbed on the negative scan in region 3.

The adsorptive behavior of ethylamine at a Au electrode appears to be rather complex. Ethylamine seems to preferentially adsorb to a reduced Au surface, as is evident by the ring shielding seen as disk surface oxide is being stripped at 0.1 V. At potentials negative of E_d = -0.5 V, some of the ethylamine is desorbed, resulting in the collection peak of region 3. When the disk is again scanned positive of E_d = -0.5 V, the ethylamine is re-adsorbed in region 4. Therefore the ethylamine adsorption appears to be potential-dependent, and maximized between -0.5 V and the onset of oxide formation at about 0.1 V. Since desorption and adsorption of ethylamine in regions 3 and 4 occur at virtually identical potentials, the interaction of ethylamine also is concluded to be, at least in part, reversible.

The adsorption/desorption couple exhibited by ethylamine at E_d = -0.5 V was investigated further by repeating the ring-disk experiment for ethylamine with the disk's positive scan limit changed from 0.7 V to 0.0 V. Changing the positive scan limit to 0.0 V ensured that no ethylamine would be oxidized during the entire disk scan, and any

observed ring phenomena would be due to processes occurring independently of AuO formation and dissolution. The disk potential was cycled several times between -1.0 V and 0.0 V, and, for each scan, the shape and size of the shielding and collection peaks at -0.5 V were consistent with the data shown in curve **c** in Figure 4.

Several other n-alkylamines were studied under the similar conditions. The ring-disk results for n-propylamine, n-butylamine, n-pentylamine and n-hexylamine were virtually identical to those for ethylamine, indicating a similar adsorption mechanism. There was almost no signal at either the ring or disk electrode for the aliphatic n-amines in acidic media, and so we conclude that the adsorption (and subsequent oxidation) of small aliphatic n-amines at Au requires the amine moiety to be in the deprotonated (RNH_2) form.

To determine whether CPD at the ring is capable of providing the same analytical information as PED, attempts were made to monitor ethylamine at the RRDE with CPD applied to the ring, which is shown as curve **d** in Figure 4. A detection potential of 0.2 V was used to facilitate comparison to the PED data shown in curve **c**. However, there is no CPD response for the ethylamine in solution, supporting the premise that aliphatic amines are not electroactive at Au under these conditions. Several other choices for the CPD potentials were tried with similar results.

Another compound investigated using PED at the ring of an RRDE was ethanolamine (2-amino-1-ethanol). The results are shown in Figure 5. The disk response for ethanolamine differs significantly from the response for ethylamine, especially at potentials less than 0.1 V. Oxidation of ethanolamine begins at about -0.5 V, and

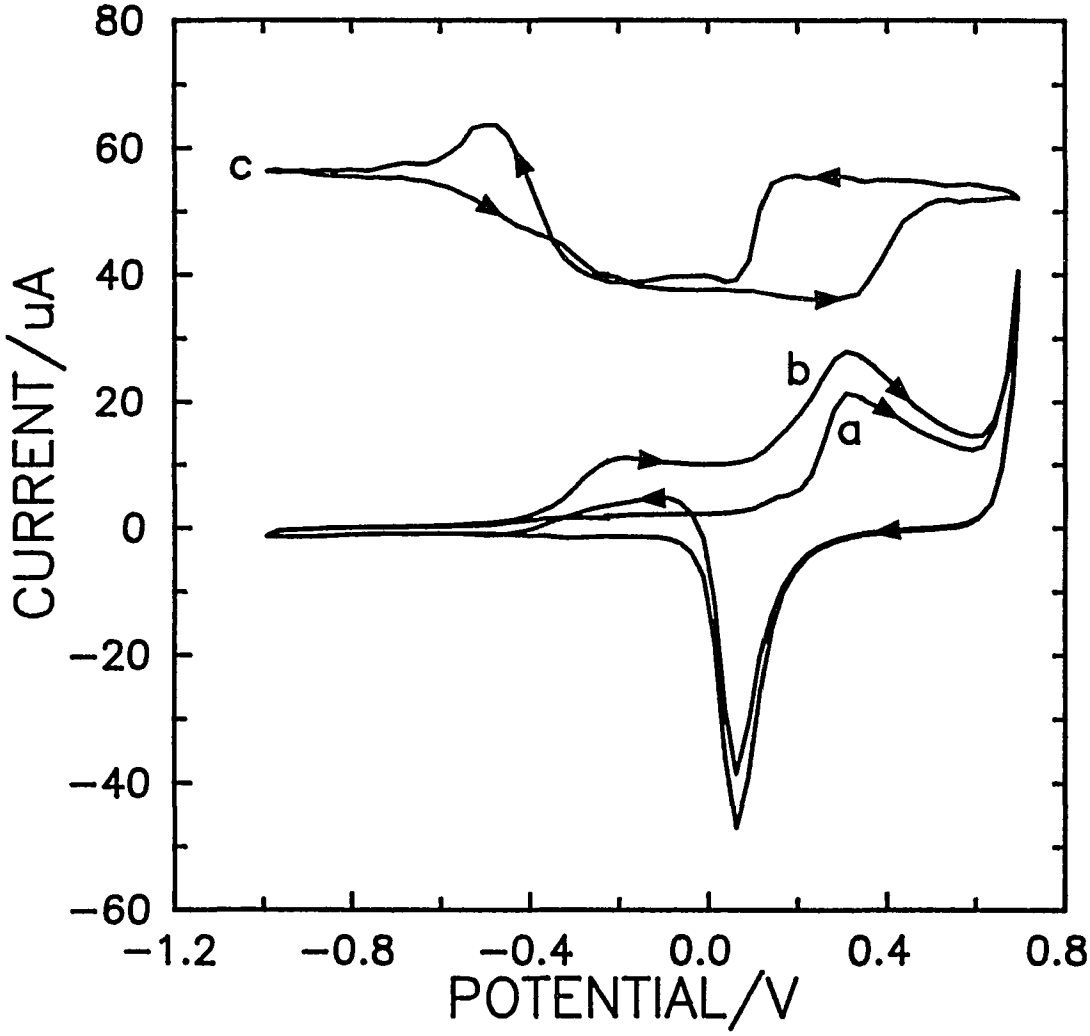

Figure 5. Voltammetric response for 20 μM ethanolamine at Au in 0.1 M NaOH. Rotation rate: 900 rev min^{-1}. Disk scan rate: 50 mV s^{-1}. Curves: (a) disk, residual; (b) disk, 20 μM ethanolamine; (c) ring (10x), 20 μM ethanolamine, PED waveform: E_{DET} = 0.2 V, t_{DET}= 350 ms, t_{DEL} = 300 ms; E_{OXD} = 0.8 V, t_{OXD} = 60 ms; E_{RED} = -0.8 V, t_{RED} = 90 ms.

continues for the remainder of the positive scan. Upon initiation of the negative scan, the anodic current for ethanolamine ceases until onset of AuO reduction. Once surface oxide is reduced, the oxidation of ethanolamine again commences and continues until the potential is scanned negative of -0.5 V. Jackson *et al.* concluded that the signal for ethanolamine at an Au electrode could be separated into two distinct regions [39]. At potentials less than 0.3 V, the majority of the anodic current is derived from conversion of the alcohol group to the carboxylic acid, so that the primary product of ethanolamine oxidation at Au is glycine. It also was shown that in comparison to simple alcohols, amino alcohols generate a much larger anodic current at Au. This was attributed to the beneficial effect of the amine group adsorbing to the Au surface, thus increasing surface residence times and allowing complete conversion of the amino alcohol to the amino acid. At low concentrations (less than 10 mM), the anodic current for ethanolamine at potentials less than 0.3 V was found to be mass-transport limited.

At potentials greater than 0.3 V, anodic current for ethanolamine is believed to be generated by the oxidation of the amine group, and the reaction in this region is no longer mass-transport limited. Instead, the signal for ethanolamine, like ethylamine, appears to be surface-controlled and dependent upon the formation of surface oxide. The ring response with PED clearly delineates where the oxidation of ethanolamine at the disk is mass-transport limited. As the disk is scanned positive, the shielding of ring current begins at about -0.6 V. This shielding increases until it reaches a plateau at a disk potential of about -0.3 V. The plateau of ring shielding, much as the plateau of the disk current, indicates that the oxidation of ethanolamine at the disk is limited only by the rate

at which analyte is transported to the electrode surface. As the disk is scanned positive of 0.3 V, the shielding decreases (ring current increases), and so the reaction at the disk is no longer mass-transport limited. On the negative scan, the ring response shows no shielding until the disk is scanned negative of 0.1 V, whereupon AuO is reduced and the oxidation of ethanolamine resumes. A shielding plateau is again seen at the ring, indicating that the oxidation of ethanolamine has resumed at a mass-transport limited rate.

On the negative scan near -0.5 V, oxidation of ethanolamine at the disk ceases and the ring current increases accordingly. However, before returning to a steady-state value, the ring shows a collection peak at E_d = -0.5 V. The ethanolamine collection peak occurs at virtually the same potential as the collection peak observed for ethylamine. On the positive scan, there is also a shielding of ring current at about the same potential, just prior to the onset of ethanolamine oxidation at the disk. The similarity of ring results for both ethanolamine and ethylamine in this potential region suggests that alkanolamines also adsorb to the Au surface through the amine moiety. The alcohol group, while responsible for the majority of the anodic signal, does not appear to influence the adsorption process. Ethanol was studied under similar conditions to determine if it undergoes adsorption in a manner similar to ethanolamine. No evidence was found for ethanol adsorption. It is perhaps not coincidental that the anodic current for ethanol is much smaller than that obtained for ethanolamine. The RRDE results tend to support the conclusions of Jackson *et al.*, who concluded that the response of alkanolamines in alkaline conditions benefits form the adsorption of the amine group [39]. It is speculated that, as with ethanol and ethanolamine, adsorption may be the primary factor in

determining the magnitude of the signal obtained for many aliphatic compounds at noble metal electrodes.

The RRDE results for 500 μM glycine are shown in Figure 6. The disk response is fairly similar to what was seen in Figure 3 for ethylamine, but at a much larger glycine concentration. Like ethylamine, glycine is oxidized at the disk concurrently with the formation of catalytic AuO. The ring response for glycine at disk potentials positive of 0.0 V also appears very similar to that of ethylamine, with shielding exhibited on the positive scan at $E_d > 0.1$ V, and on the negative scan at $E_d < 0.1$ V. However, the ring response for glycine is quite different than ethylamine at $E_d = -0.5$ V. In this region, the ring data for glycine show no evidence of the adsorption/desorption couple seen for both ethylamine and ethanolamine, indicating that the adsorption of glycine differs from the other amine compounds studied. As stated earlier, both ethylamine and ethanolamine are believed to adsorb primarily through the amine group. Because the RRDE results for glycine differ from the other amine compounds studied, we conclude that glycine's carboxylate group, unlike the alcohol group of alkanolamines, participates in the adsorption of glycine in alkaline solutions. This conclusion is supported by the previous work of other authors, who also found evidence for carboxylate's involvement in the adsorption of glycine on metal surfaces [5, 6, 19, 23].

HPLC-PED of aliphatic amines. The primary application of pulsed electrochemical detection is for the determination of aliphatic compounds separated by HPLC [1 - 4]. Typically, optimization of the PED waveform has concentrated on the

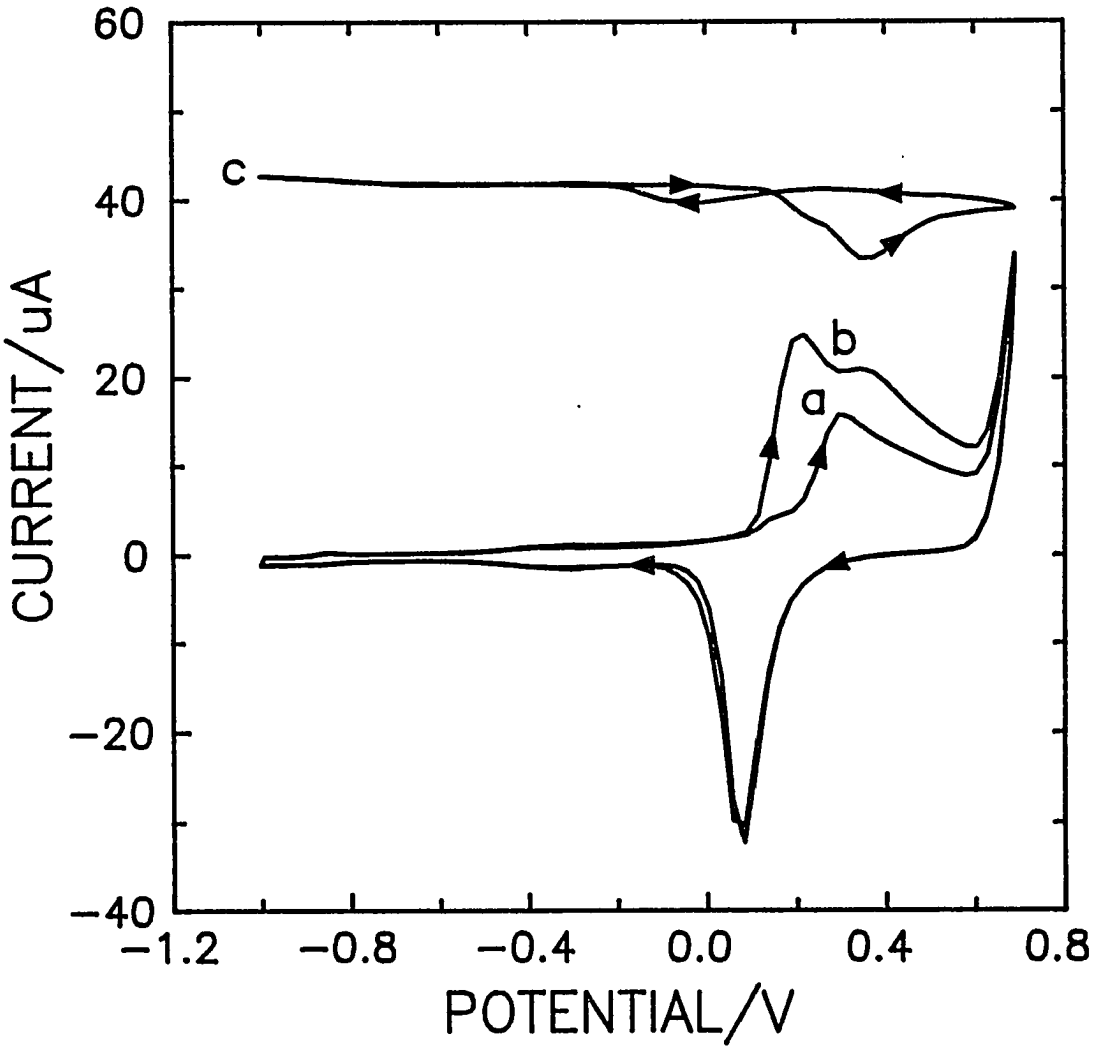

Figure 6. Voltammetric response for 500 μM glycine at Au in 0.1 M NaOH. Rotation rate: 900 rev min^{-1}. Disk scan rate: 50 mV s^{-1}. Curves: (a) disk, residual; (b) disk, 500 μM glycine; (c) ring (10x), 500 μM glycine, PED waveform: E_{DET} = 0.2 V, t_{DET} = 350 ms, t_{DEL} = 300 ms; E_{OXD} = 0.8 V, t_{OXD} = 60 ms; E_{RED} = -0.8 V, t_{RED} = 90 ms.

detection potential (E_{DET}), with the best E_{DET} determined empirically by ascertaining where signal for the analyte(s) is maximized relative to the background noise. For the detection of amines on Au in alkaline conditions, the optimum E_{DET} is about 0.2 V. Little attention usually is given to the oxidative cleaning (E_{OXD}) or reductive regeneration (E_{RED}) potential steps, and their possible effect on the PED response. As their names suggests, these potentials typically have been chosen simply to assure oxide formation at the working electrode during E_{OXD} and its subsequent dissolution during E_{RED}, thus providing a clean electrode surface when the potential is stepped to E_{DET}. However, if the value of E_{RED} is chosen to promote amine adsorption, then it can also serve to concentrate any amine in the chromatographic effluent. Thus, when the potential then is stepped to E_{DET}, a larger concentration of the amine will be present at the working electrode's surface, resulting in a larger analytical signal. Since the adsorption of aliphatic amines at Au is potential-dependent and maximized between -0.4 V and 0.0 V, choosing E_{RED} = -0.4 V should promote amine adsorption while still reducing AuO.

To determine if the choice of E_{RED} had any effect on the PED response for amines, a 50 μM ethylamine standard was prepared and its PED signal measured as a function of E_{DET} in an HPLC system. Separation was provided by a multimodal cation-exchange/reverse-phase column, and detection was done at an Au working electrode in a commercially-available flow-through cell. The results for a series of ethylamine injections are shown in Figure 7, with the first three injections made at E_{RED} = -0.4 V, and the last three injections made at E_{RED} = -0.8 V. All other conditions were identical

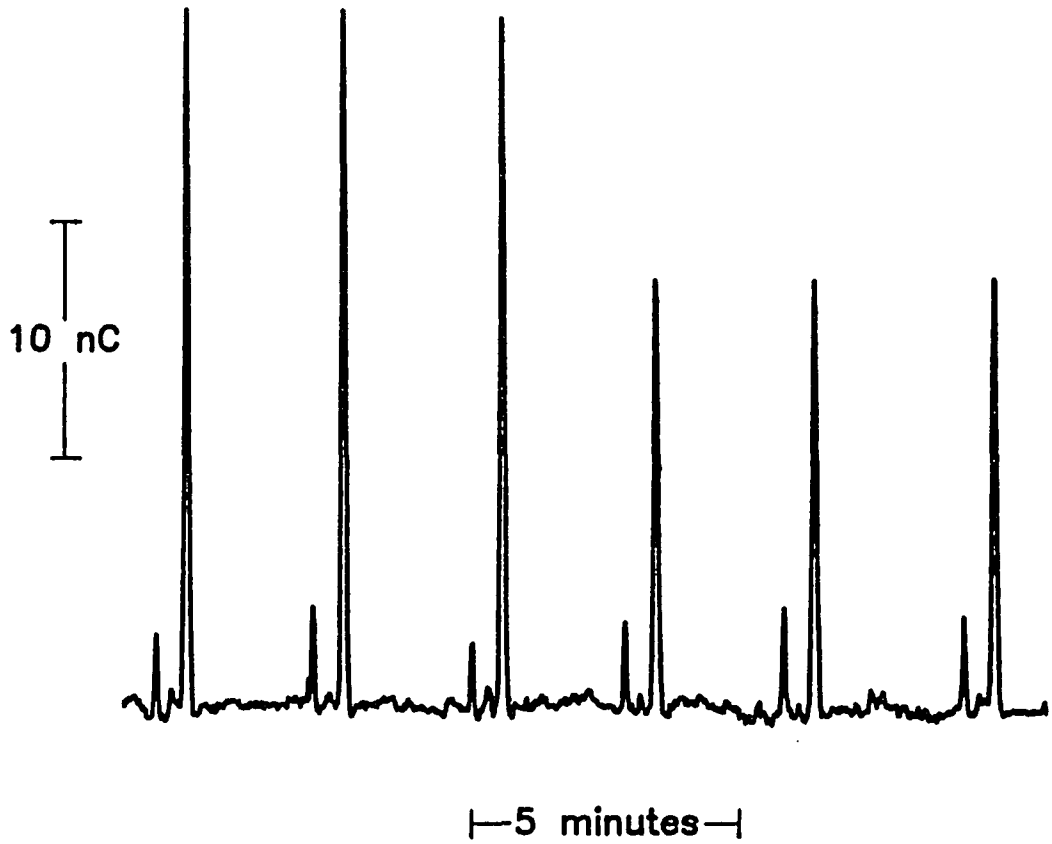

Figure 7. HPLC-PED of ethylamine. Analyte: 50 μM ethylamine. Column: Dionex PCX-500 (4 x 50 mm). Eluent: 20 mM HOAc/120 mM NaOAc at 1 mL min^{-1}. Post-column addition of 0.3 M NaOH at 0.6 mL min^{-1}. PED waveform: E_{DET} = 0.2 V, t_{DEL}= 250 ms, t_{INT} = 50 ms; E_{OXD} = 0.8 V, t_{OXD} = 120 ms; E_{RED} = -0.4 V, (first 3 injections) / -0.8 V (last 3 injections), t_{RED} = 380 ms.

for the six injections. With E_{RED} = -0.4 V, a larger response is obtained, which can be attributed to the beneficial effect of using the E_{RED} to promote adsorption. Therefore, these results support the conclusions from the RRDE data that indicated the adsorption of amines is potential-dependent. However, under these conditions, there is only about a 50% increase in the PED signal, which, though significant, is certainly not a large improvement in PED response.

Under more typical separation conditions, the effect of promoting adsorption during E_{RED} is more evident. The separation of a series of amines is shown in Figure 8 using a mobile phase containing 10% acetonitrile, which is necessary to elute many of the amines from the column. Again, the experimental conditions for the two sets of data were identical except in the choice of E_{RED}, which was -0.4 V for chromatogram **A**, and -0.8 V for chromatogram **B**. For the first four peaks representing ethylamine through pentylamine, there is an average five-fold improvement in the HPLC-PED signal when the more positive E_{RED} is used. The results are most dramatic for hexylamine (peak **e**), which is readily apparent in Figure 8A, but not detected in Figure 8B. Acetonitrile has been shown to adsorb to Au [40], and it is concluded that its presence in the eluent can affect the ability of amines to also undergo adsorption to the Au working electrode. Using an E_{RED} = -0.4 allows amines to more effectively compete with acetontrile for adsorption sites on the Au surface, and thus results in a larger PED response. A further benefit of having E_{RED} = -0.4 V is its effect on noise, which decreases, on average, by a factor of two relative to when E_{RED} = -0.8 V. We speculate that with the more positive reduction potential, there is less charging current when the potential is stepped to E_{DET}

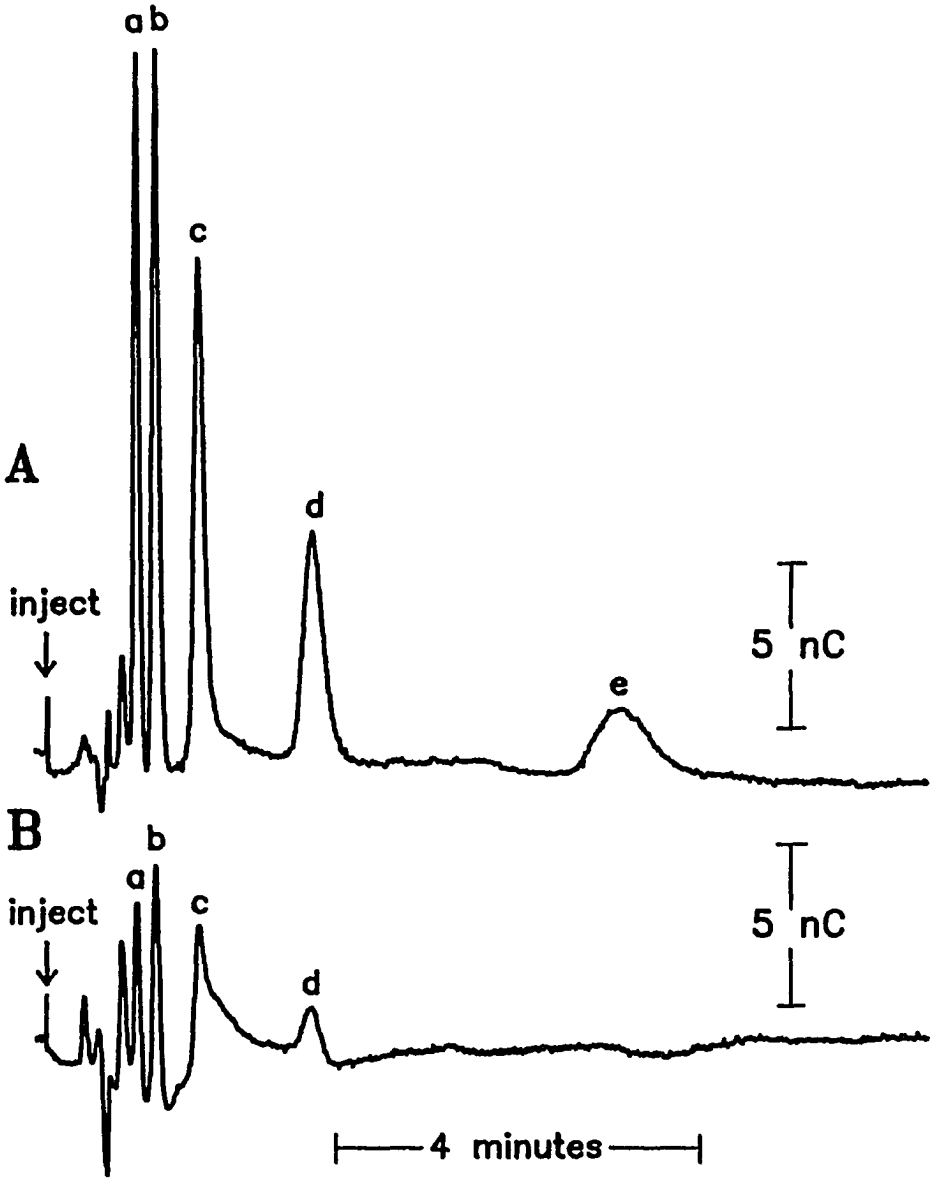

Figure 8. HPLC-PED of aliphatic amines. Column: Dionex PCX-500 (4 x 50 mm). Eluent: 30 mM HOAc/80 mM NaOAc/10% (v/v) acetonitrile at 1 mL/min^{-1}. Post-column addition of 0.3 M NaOH at 0.6 mL min^{-1}. Chromatograms: (A) PED waveform: E_{DET} = 0.2 V, t_{DET} = 300 ms, t_{DEL}= 250 ms, t_{INT}= 50 ms; E_{OXD} = 0.8 V, t_{OXD} = 120 ms; E_{RED} = -0.4 V, t_{RED} = 180 ms. (B) PED waveform: E_{DET} = 0.2 V, t_{DEL}= 250 ms, t_{INT} = 50 ms; E_{OXD} =0.8 V, t_{OXD} = 120 ms; E_{RED} = -0.8 V, t_{RED} = 180 ms. Peaks (50 μM): (a) ethylamine, (b) n-propylamine, (c) n-butylamine, (d) n-pentylamine, (e) n-hexylamine.

and signal is sampled. When the average gain in signal is factored in with the decrease in noise, there is an order-of-magnitude improvement in the detection limits for the HPLC-PED of aliphatic amines.

CONCLUSIONS

A new application of pulsed detection has been demonstrated in which PED is applied to the ring of an RRDE. The technique was characterized using ferrocyanide as a model compound, and the experimental results are in good agreement with both calculated and experimental results for constant potential detection. PED at the ring then was used to monitor the electrochemical behavior of aliphatic amine compounds at the disk. Simple amines and amino alcohols were shown to undergo potential-dependent adsorption at the Au disk in alkaline solutions. The adsorption appears to be reversible, and maximized at potential between -0.5 V and -0.1 V. The similar results for amines and alkanolamines suggests that, for alkanolamines, the alcohol group does not affect the adsorption process. The RRDE results for glycine at Au differ from the other amines studied, suggesting that glycine adsorption is not controlled solely by the amine group, but is influenced by the carboxylate moiety as well.

Understanding the potential dependence of amine adsorption allows optimization of the PED waveform parameters used with an HPLC system. By choosing the reduction potential to promote adsorption, ethylamine effectively is concentrated at the electrode surface, so that when the detection step is made, more ethylamine is oxidized and a larger PED signal is obtained. The benefits of promoting adsorption during E_{RED} are most dramatic in the presence of acetonitrile, with an average five-fold improvement in the signal obtained from the optimized PED waveform versus a non-optimized waveform. A concurrent reduction in noise for the optimized PED waveform resulted in an order-of-

magnitude improvement in the detection limits for the HPLC-PED of small aliphatic amines.

We anticipate that PED at the ring of an RRDE will have further application for monitoring adsorption at electrode surfaces. Current work in our laboratories continues to investigate the adsorption of both amines and sulfur compounds. Since the RRDE is already established as a tool for determining unstable electrode intermediates and reaction kinetics, we also expect that PED at the ring will have benefits in these areas as well.

ACKNOWLEDGEMENTS

This work was supported by the National Science Foundation under grants CHE-8914700 and CHE-9215963, and by Dionex Corporation.

REFERENCES

1. Polta, J. A.; Johnson, D. C. *J. Liquid Chromatogr.* **1983**, *6*, 1727-1743.
2. Johnson, D. C.; LaCourse, W. R. *Anal. Chem.* **1990**, *62*, 589A-597A.
3. Johnson, D. C.; LaCourse, W. R. *Electroanalysis* **1992**, *4*, 367-380.
4. Johnson, D. C.; Dobberpuhl, D.; Roberts, R.; Vandeberg, P. *J. Chromatogr.* **1993**, *640*, 79-96.
5. Lange, W.; Jirikowsky, M.; Benninghoven, A. *Surf. Sci.* **1984**, *136*, 419-436.
6. Ernst, K. H.; Christmann, K. *Surf. Sci.* **1989**, *224*, 277-310.
7. Bigelow, R. W.; Salaneck, W. R. *Chem. Phys. Letters*, **1982**, *89*, 430-434
8. Liedberg, B.; Lundström, I.; Wu, C. R.; Salaneck, W. R. *J. Colloid and Interface Sci.* **1985**, *108*, 123-132.
9. Uvdal, K.; Bodö, P.; Ihs, A.; Liedberg, B.; Salaneck, W. R. *J. Colloid Interface Sci.* **1990**, *140*, 207-216.
10. Ihs, A.; Liedberg, B.; Uvdal, K.; Törnkvist, C.; Bodö, P.; Lunström, I. *J. Colloid Interface Sci.* **1990**, *140*, 192-206.
11. Carlsson, C.; Liedberg, *B. Mikrochim. Acta* **1988**, *1*, 149-152.
12. Silin, V.; Talaikyte, Z.; Grigaliunas, R. *Liet. Fiz. Rinkinys* **1991**, *31*, 435-440.
13. Bogdanovskaya, V. A.; Safronov, A. Yu.; Tarasevich, M. R.; Chernyak, A. S. *J. Electroanal. Chem.* **1986**, *202*, 147-167.
14. Safronov, A. Yu.; Tarasevich, M. R.; Bogdanovskaya, V. A.; Chernyak, A. S. *Élektrokhimiya* **1983**, 19, 421-424.

15. Tarasevich, M. R.; Safronov, A. Yu.; Bogdanovskaya, V. A.; Chernyak, A. S. *Élektrokhimiya* **1983**, 19, 167-173.

16. Safonova, T. Yu.; Kidirov, S. S.; Petrii, O. A. *Élektrokhimiya* **1984**, *20*, 1666-1669.

17. Bockris, J. O'M.; Swinkels, D. A. J. *J. Electrochem. Soc.* 1964, 111, 736-743.

18. Horányi, G.; Orlov, S. B. *J. Electroanal. Chem.* **1991**, *309*, 239-249.

19. Bogdanovskaya, V. A.; Horányi, G. *Eletrokhimiya* **1989**, *25*, 1649-1651.

20. Horányi, G.; Rizmayer, E. M. *J. Electroanal. Chem.* **1989**, *264*, 273-279.

21. Horányi, G.; Rizmayer, E. M. *J. Electroanal. Chem.* **1988**, *251*, 403-407.

22. Horányi, G.; Rizmayer, E. M. *J. Electroanal. Chem.* **1986**, *198*, 393-400.

23. Horányi, G.; Rizmayer, E. M. *J. Electroanal. Chem.* **1975**, *64*, 15-19.

24. Bruckenstein, S.; Napp, D. T. *J. Am. Chem. Soc.* **1968**, *90*, 6303-6309.

25. Johnson, D. C.; Bruckenstein, S. *J. Electrochem. Soc.* **1970**, *117*, 460-467.

26. Johnson, D. C. *J. Electrochem. Soc.* **1972**, *119*, 331-339.

27. Gonz, Il; Vasil'ev, Y. B.; Bagotskii, V. S. *Élektrokhimiya* **1970**, 6, 325-328.

28. Filinosvsky, V. Yu.; Pleskov, Yu. V. In *Comprehensive Treatise of Electrochemistry*; Yeager, E.; Bockris, J. O'M.; Conway, B.; Sarangapani, S. Eds.; Plenum Press: New York, 1984, Vol. 9, p 293.

29. Opekar, F.; Beran, P. *J. Electroanal. Chem.* **1976**, *69*, 1-105.

30. Levich, V. G. *Physicochim. URSS*, **1942**, *17*, 257-307.

31. Levich, V. G. *Physiochemical Hydrodynamics*; Prentice-Hall: Englewood Cliffs, New Jersey, 1962, pp 60-72.

32. Levich, V. G. *ibid*, pp 102-108.

33. Albery, W. J. *Trans. Faraday. Soc.* **1966**, *62*, 1915-1919.

34. Albery, W. J.; Bruckenstein, S. *Trans. Faraday. Soc.* **1966**, *62*, 1920-1931.

35. Blaedel, W. J.; Schieffer, G. W. *J. Electroanal Chem.* **1977**, *80*, 259-271.

36. Daum, P. H.; Enke, C. G. *Anal. Chem.* **1969**, *41*, 653-656.

37. Angell, D. H.; Dickinson, T. *J. Electroanal. Chem.* **1972**, *35*, 55-72.

38. Kawiak, J.; Jedral, T.; Galus, Z. *J. Electroanal. Chem.* **1983**, *145*, 163-171.

39. Jackson, W. A.; LaCourse, W. R.; Dobberpuhl, D. A.; Johnson, D. C. *Electroanalysis* **1991**, *3*, 607-616.

40. Faguy, P. W.; Fawcett, W. R.; Liu, G.; Motheo, A. J. *J. Electroanal. Chem.* **1992**, *339*, 339-353.

PAPER 4

A STUDY OF ETHYLAMINE AT A GOLD ROTATING RING-DISK ELECTRODE WITH PULSED ELECTROCHEMICAL DETECTION*

*From D. A. Dobberpuhl and D. C. Johnson, *Electroanalysis*, to be submitted.

ABSTRACT

Linear scan (cyclic) voltammetry at the disk and pulsed electrochemical detection (PED) at the ring of a rotating ring-disk electrode are used to characterize the electrochemical behavior of ethylamine at Au. In 0.10 M NaOH, the oxidation of ethylamine at Au is found to be under both mass transport and surface control (mixed control), and limited by rate at which catalytic surface oxide is formed. The ethylamine signal at the disk can be divided into two parts: (1) current from ethylamine mass-tranported to the electrode concurrently with the oxidation process, and (2) current from ethylamine pre-adsorbed to the electrode surface at potentials negative of where oxidation occurs. At a concentration of 40 μM, 65% of the total disk signal is derived from ethylamine mass-transported to the electrode surface during the oxidation process. The other 35% of the disk signal is due to pre-adsorbed ethylamine. The pre-adsorbed ethylamine corresponds to a surface coverage of less than one monolayer. Approximately three-fourths of the total surface coverage is from ethylamine reversibly co-adsorbed with hydroxide, with the remaining one-fourth of the surface coverage is from ethylamine chemisorbed directly to the reduced Au surface.

INTRODUCTION

Because of their biological and industrial importance, the electrochemistry of amine compounds has been studied at a variety of metal electrodes, including Cu [1 - 3], Pt [4 - 6], Au [7 - 9], Ag [10 - 13], and the oxides of Co, Cu, and Ni [13 - 16]. A primary goal for many of these studies has been to determine the mechanism by which amines are oxidized at the electrode surface, and the resulting product(s) of the reaction. For the oxidation of aliphatic amines in aqueous media, the products were found to depend upon the electrode material and experimental conditions. Barnes and Mann studied the oxidation of primary amines at Pt, and found that the product was an aldehyde [6]. Based on their results, they proposed a mechanism in which the cleavage of the C-N bond to form the aldehyde occurred via the following (abbreviated) series of steps.

$$RCH_2NH_2 \rightarrow RCH_2NH_2^+ + e^- \quad (1)$$

$$RCH_2NH_2^+ \rightarrow RCHNH_2 + H^+ \quad (2)$$

$$RCHNH_2 \rightarrow RCH{=}NH_2^+ + e^- \quad (3)$$

$$RCH{=}NH_2^+ + H_2O \rightarrow RCHO + NH_3 + H^+ \quad (4a)$$

However, the predominant oxidation product for primary amines at most electrodes is the nitrile [17]. Hampson *et al.* [12] proposed a mechanism for nitrile formation at Ag in which the first steps were similar to steps 1 - 3 of the above mechanism, but with an imine formed at Step 4 instead of an aldehyde. The imine eventually was converted to the nitrile through the following (abbreviated) mechanism.

$$RCH{=}NH_2^+ \rightarrow RCH{=}NH + H^+ \quad (4b)$$

$$RCH{=}NH \rightarrow RCH{=}NH^+ + e^- \quad (5)$$

$$RCH{=}NH^+ \rightarrow RCH{=}N: + H^+ \quad (6)$$

$$RCH{=}N: \rightarrow RCH{=}N:^+ + e^- \quad (7)$$

$$RCH{=}N:^+ \rightarrow RCH{\equiv}N: + H^+ \quad (8)$$

In our laboratories, there is strong interest in the detection of amine compounds at noble metal electrodes, and in a previous paper the voltammetric basis for alkanolamine signal at Au was investigated [18]. The response for ethanolamine at Au was found to be much larger than that of ethanol, despite signal for both compounds resulting from the conversion of the alcohol moiety to the carboxylic acid. The larger ethanolamine response was attributed to the beneficial effect of amine adsorption. Adsorption was believed to increase the surface residence time of the individual ethanolamine molecules, and ultimately result in a reaction that was mass-tranport limited. A more general study of amine adsorption at Au followed, using results from a rotating ring-disk electrode (RRDE) [19]. Because the response for amines quickly decays to negligible values at noble metal electrodes when using constant potential (DC) detection, pulsed electrochemical detection (PED) was applied to the ring electrode, thus maintaining the conditions responsible for providing signal. The adsorption of aliphatic amines, alkanolamines and an amino acid, glycine, was described as a function of applied potential. The similarity of amine and alkanolamine behavior indicated that both classes

of compounds adsorb through the amine functional group. supporting previous speculation that the alkanolamine signal at Au benefits from amine adsorption.

In this paper, the electrochemistry of one amine compound, ethylamine, is further investigated using linear scan voltammetry at the disk and PED at the ring of a Au RRDE. By using data from both ring and disk electrodes, a more thorough characterization of ethylamine's electrochemical behavior at Au is possible, especially with respect to determining the role of adsorption in the oxidation process. Specifically, the goals of this paper are: (1) to qualitatively describe the behavior of ethylamine at the disk, and correlate the response to the formation of catalytic hydroxide/oxide on the Au surface; (2) to determine the fraction of signal at the Au disk that is attributable to ethylamine pre-adsorbed at potentials negative of where its oxidation takes place, as opposed to the fraction signal due to ethylamine mass-transported to the disk surface concurrently with the oxidation process; (3) to estimate the surface coverage of ethylamine on Au, identifying two possible adsorption states and their dependence on the condition of the electrode surface; and (4) determine the number of electrons transferred in the oxidation of ethylamine. Ultimately, we hope to provide a complete description of the processes that result in the oxidation of ethylamine at Au.

EXPERIMENTAL

Reagents. All chemicals were used as received. Ethylamine (Kodak, Aldrich) was a practical grade of 70% (w/w) in water. Sodium hydroxide used as the supporting electrolyte was prepared either from reagent grade pellets (Fisher Scientific) or a commercially available 50% w/w NaOH solution (Fisher Scientific). Deionized water was purified with a Milli-Q system (Millipore) after passing through two D-45 deionizing tanks (Culligan). All solutions used in the voltammetric experiments were deaerated with nitrogen gas before and during the experiments.

Voltammetric apparatus. All RRDE data were obtained using a AFRDE4 bi-potentiostat, AFMSR rotator, and AFMT28AUAU gold ring-disk electrode (Pine Instrument). The outer diameter of the disk was 0.457 cm. The ring had an inner diameter of 0.493 cm and an outer diameter was 0.538 cm. A saturated calomel electrode (SCE; Fisher Scientific) was used as the reference electrode, and a coiled Pt wire was used as the counter electrode. The electrochemical cell was made of pyrex, with porous glass frits separating the individual compartments for the working, reference and counter electrodes. The potentiostat was interfaced to a personal computer (Jameco) via a DT2801-A data acquisition board (Data Translation) and ASYST version 4.0 software (Keithley/Asyst).

Voltammetric procedure. The procedure has been described previously [19], and only a summary will be presented here. For most experiments, the disk potential was scanned as a PED waveform was applied to the ring electrode of a RRDE. Control of

the disk potential was maintained exclusively by the bi-potentiostat. The PED waveform applied to the ring electrode was provided by the computer interfaced to the bi-potentiostat. All PED parameters (see Figure 1) could be selected independently through programs written in ASYST software. During the detection time (t_{DET}), ring current, disk current and disk potential were sampled through the computer interface. The total time necessary for one complete PAD waveform determined how often signal was measured. For a typical PAD waveform with a total time of 500 ms, the sampling frequency was 2 Hz.

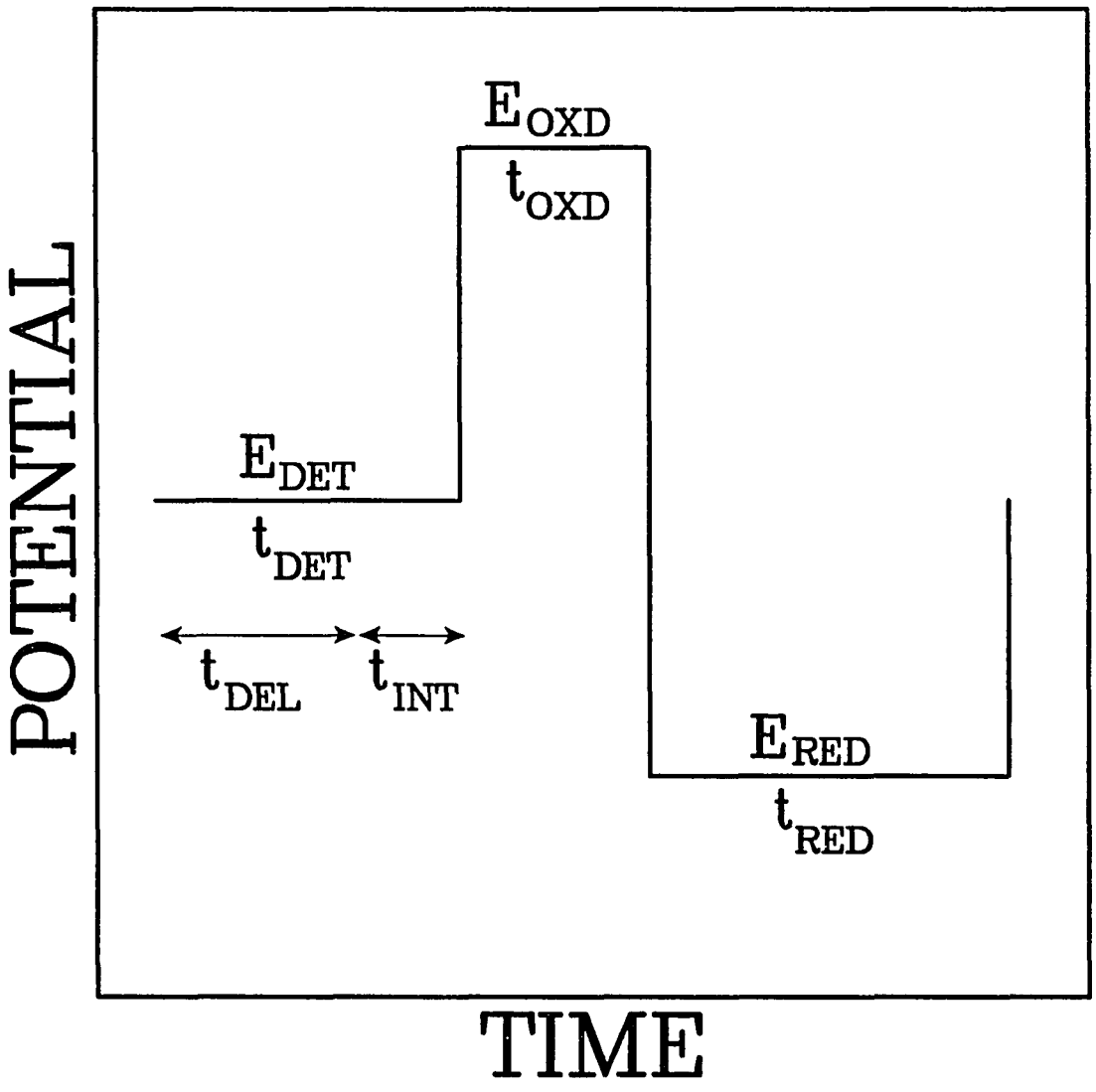

Figure 1. Potential versus time for a PED waveform. E_{DET} = detection potential; t_{DET} = detection time; t_{DEL} = delay time; t_{INT} = current integration or averaging time; E_{OXD} = oxidation potential; t_{OXD} = oxidation time; E_{RED} = reduction potential; t_{RED} = reduction time.

RESULTS AND DISCUSSION

Ethylamine behavior at a Au RDE. Based upon observed electrochemical behavior, there are two general classifications for reactions that occur at the surface of electrodes: those under surface control, and those under mass-transport control. Surface-controlled reactions are limited by slow heterogeneous kinetics for one or more of the reaction steps occurring at the electrode surface, with the rate-limiting step perhaps related to adsorption, electron transfer or oxygen transfer. Conversely, a reaction with fast heterogeneous kinetics is limited only by the rate that species are convectively and diffusionally transported from the bulk solution to the electrode surface, and such a reaction is said to be under mass-transport control. Linear scan (cyclic) voltammetry at a rotating disk electrode (RDE) is an excellent means for studying reactions at metal surfaces, because a controlled hydrodyanic flow is maintained through simple rotation of the electrode body. Thus, a quantitative description of the mass-transport process is possible. The Levich equation describes the current (i, Amps) for a mass-transport limited reaction at an RDE [20]:

$$i = 0.62nFAD^{2/3}\omega^{1/2}\nu^{-1/6}C^{b} \qquad (9)$$

where n is the number of electrons transferred in the reaction (eq/mol), F is Faraday's constant (C/eq), A is the area of the electrode (cm^2), ω is the electrode's rotational velocity (rad/s), ν is the kinematic viscosity of solution (cm^2/s), and C^b is the concentration of the analyte in solution (mol/cm^3). The Levich equation predicts that the response for a mass-transport limited reaction should be proportional to both C^b and $\omega^{1/2}$,

but independent of the potential scan rate (ϕ) when using linear scan voltammetry.

Conversely, for a reaction under surface control, the signal is not limited by mass-transport, and so is independent of the parameters defining analyte flux, C^b and $\omega^{1/2}$. Instead, the current shows linear dependence upon the voltammetric scan rate. This is because charge, which is the integral of current (i) multiplied by time (t), remains constant with increasing scan rate for a surface-controlled reaction. Therefore, as the scan rate is increased, the charge must be generated over a shorter amount of time, and so the current for a surface-controlled reactions increases accordingly.

Reactions also can be under both mass-transport and surface control. Such a reaction is said to be under "mixed control," and the current obtained for such a reaction at a RDE will vary with C^b, $\omega^{1/2}$ and ϕ, depending upon experimental conditions.

Figure 2 shows the linear scan voltammetric (i-E) response of a Au RDE in the absence of any electroactive species. On the positive scan between -1.0 and -0.5 V, the relatively small current that is generated is attributable to double-layer charging. As potential is scanned positive of -0.5 V, an increase in the anodic current is observed. This increase has been attributed adsorption of hydroxide [OH^-] in alkaline solutions [21 - 26] with possibly co-adsorption of water, especially in neutral and acidic solutions [27 - 29]. The exact nature of the adsorbed hydroxide has not been conclusively determined. Some authors have concluded that the adsorption is accompanied by partial or complete charge transfer resulting in the formation of the hydroxide radical, while other authors suggested that the hydroxide anion is adsorbed, as other anions, through electrostatic attraction to the Au surface when potential is positive of the point-of-zero-charge (PZC).

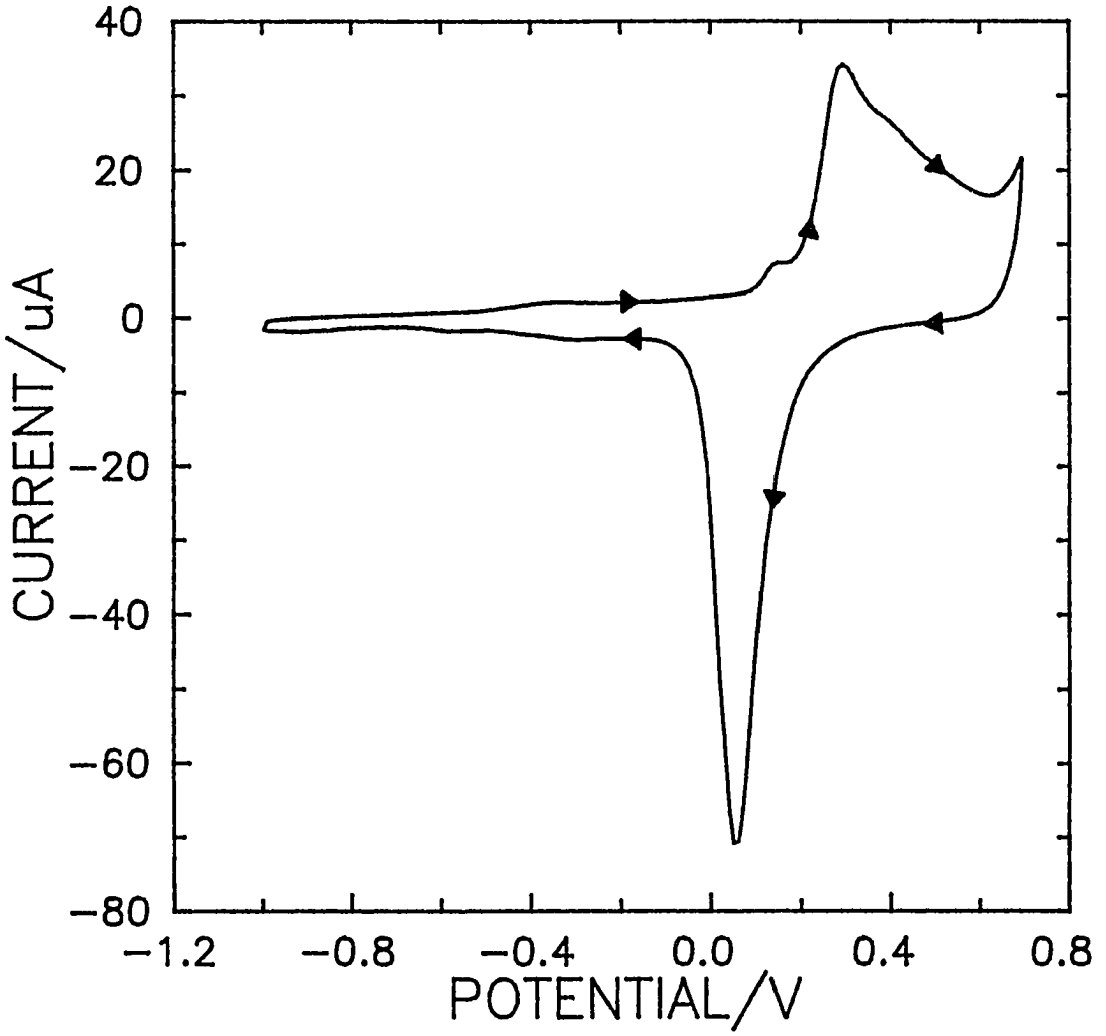

Figure 2. Residual voltammetric response at the Au RDE in 0.10 M NaOH. Rotational velocity: 900 RPM. Scan rate: 100 mV s^{-1}.

Whatever form hydroxide assumes upon adsorption, its importance for catalyzing the oxidization of many compounds at Au has been documented in previously studies [30 - 34].

As the potential is scanned positive of 0.1 V, there is a small pre-wave that has been associated with the formation of low-stoichiometry surface oxides, followed by a larger anodic wave beginning at 0.2 V representing the formation surface oxide (AuO). Oxide formation continues to the positive scan limit of 0.7 V, where an increase in anodic current results from oxygen evolution occurring through solvent break-down. Upon initiation of the negative scan, the signal for oxide formation and oxygen evolution diminishes, and the current at the Au disk approaches zero. As the disk is scanned negative of 0.2 V, a large cathodic peak results from the reduction of the surface oxide that had been formed on the positive scan. Once oxide reduction is completed, the negative scan is relatively featureless, and showing only current from hydroxide adsorption and double-layer charging. Because all of the processes contributing to the residual response are surface-controlled, the residual current is a linear function of scan rate.

The response for several concentration of ethylamine at Au in 0.10 M NaOH is shown in Figure 3. As the disk potential is scanned positive of 0.1 V, current is generated from both the formation of AuO and the oxidation of ethylamine. Current for ethylamine is generated throughout the entire oxide formation region, and, indeed, AuO apparently catalyzes the oxidation of ethylamine. Upon initiation of the negative scan at 0.7 V, the oxidation of ethylamine, like the formation of surface oxide, ceases.

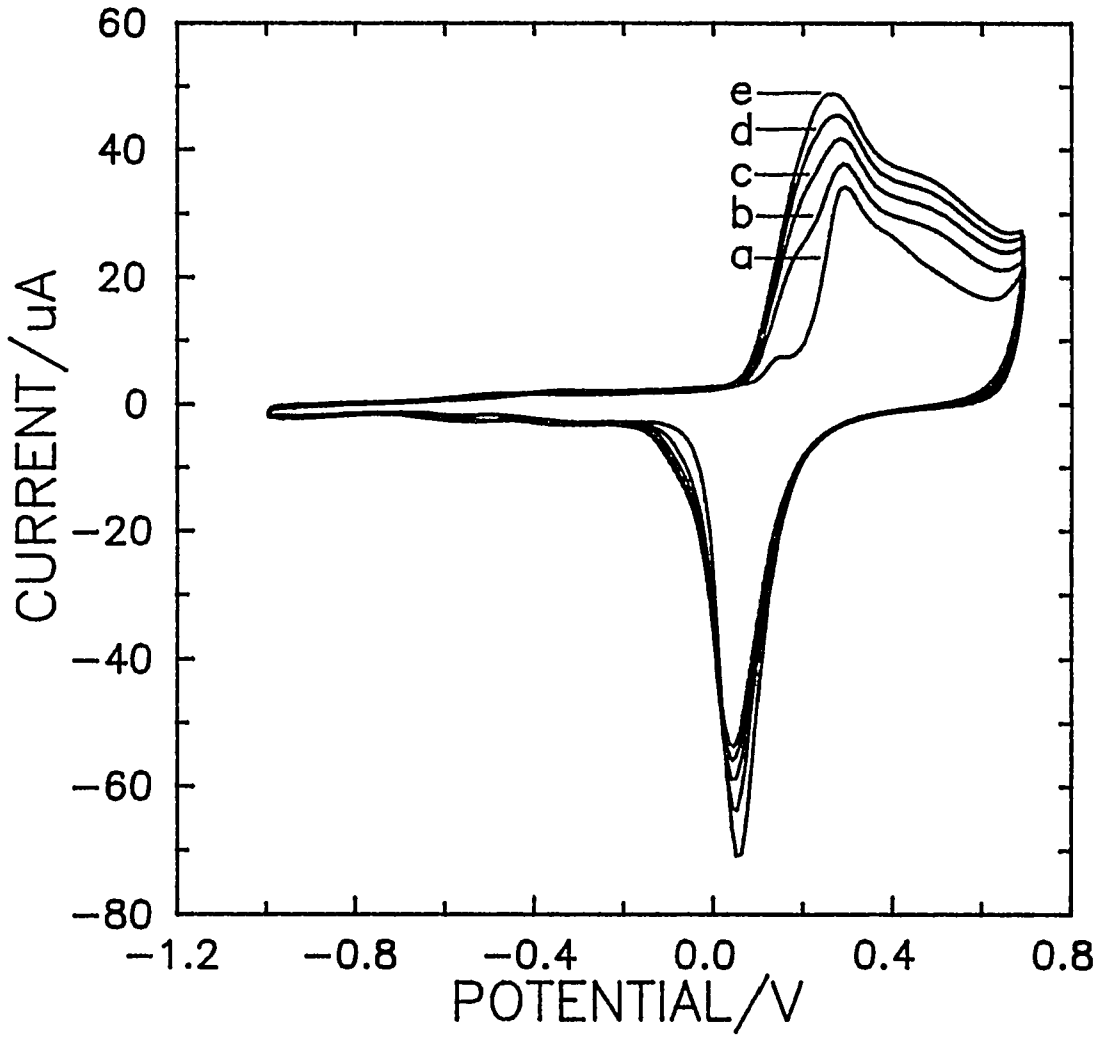

Figure 3. Voltammetric response for ethylamine at the Au RDE as a function of concentration. Rotational velocity: 900 RPM. Scan rate: 100 mV s^{-1}. Curves: (a) 0 μM, (b) 20 μM, (c) 40 μM, (d) 60 μM, and (e) 80 μM ethylamine.

At low concentrations, the current for ethylamine appears to be almost a linear function of C^b, as predicted by the Levich equation. However, this linear relationship is not observed at concentrations greater than 100 μM under the conditions described in Figure 3. The oxide reduction peak obtained on the negative scan also is sensitive to ethylamine concentration. As the ethylamine concentration increases, a part of the cathodic peak is shifted to more negative potentials. This shift in the reduction peak might be indicative of ethylamine adsorbed to the electrode surface. By adsorbing to the Au surface, the ethylamine may stabilize the AuO formed during the positive scan, and thus make oxide reduction thermodynamically less favorable. Though this is not definitive evidence for ethylamine adsorption, it is perhaps an indication that adsorption does occur.

The relationship between ethylamine signal and electrode rotation speed is shown in Figure 4. At an ethylamine concentration of 100 μM, the response is a linear function of $\omega^{1/2}$ at low rotation speeds, but not at high rotation speeds. The results indicate that the oxidation of ethylamine adheres to the Levich equation at small values of C^b and $\omega^{1/2}$, indicating that the reaction is mass-transport limited only at relatively low levels of ethylamine flux.

Since the oxidation of ethylamine did not appear to be entirely under mass-transport control, the relationship between signal and scan rate was used to investigate the extent of surface control. The dependence of ethylamine signal on scan rate are shown in Figure 5. A linear relationship is exhibited between current and scan rate, confirming that the oxidation of ethylamine is largely surface-controlled under the given experimental

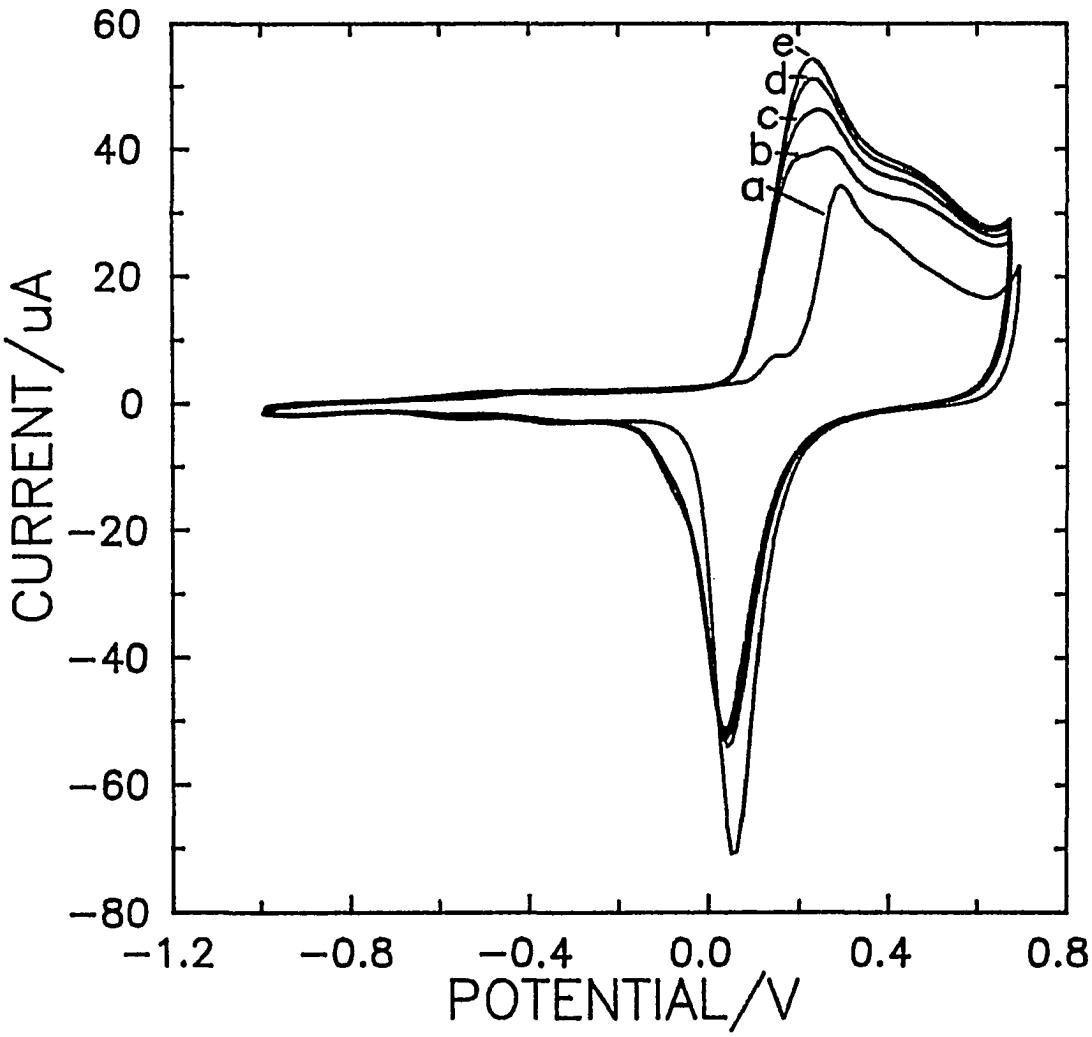

Figure 4. Voltammetric response for 40 μM ethylamine (EAM) at the Au RDE as a function of rotational velocity. Concentration: 100 μM. Scan rate: 100 mV s^{-1}. Curves: (a) residual; (b) EAM, 100 RPM; (c) EAM, 400 RPM; (d) EAM, 900 μM; (e) EAM, 1600 RPM.

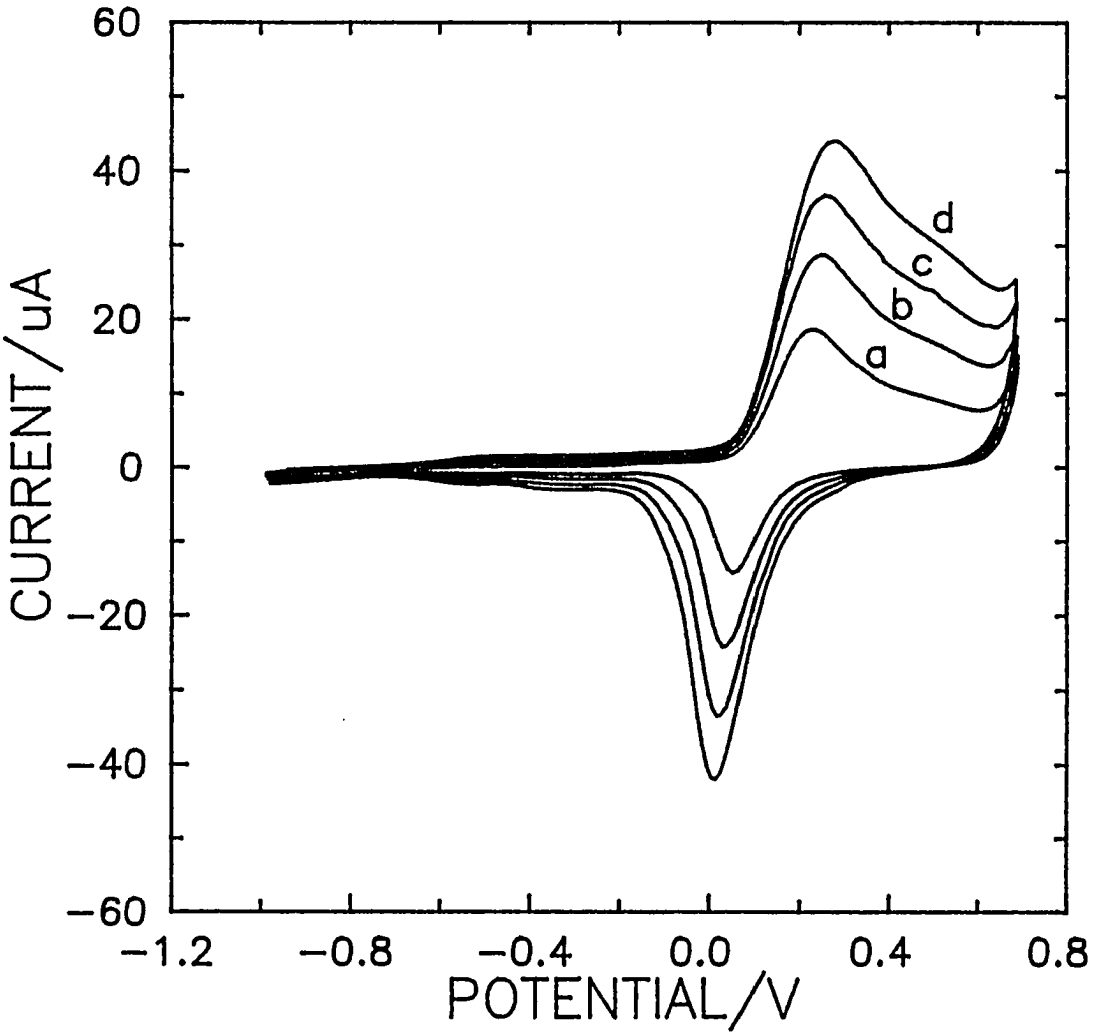

Figure 5. Voltammetric response for ethylamine at the Au RDE as a function of scan rate. Concentration: 100 μM. Rotational velocity: 900 RPM. Curves: (a) 25, (b) 50, (c) 75, and (d) 100 mV s^{-1}.

conditions. However, at higher scan rates ($\phi > 100$ mV s^{-1}), the linear relationship is not maintained. Instead, anodic current for the reaction of ethylamine becomes more dependent upon the rate of flux, and almost independent of scan rate.

The voltammetric results for ethylamine at a RDE indicate that the oxidation of ethylamine at Au in alkaline solutions is under mixed-control. At low ethylamine flux or high scan rates, the reaction is primarily under mass-transport control, because catalytic oxide is generated at a rate sufficient to oxidize all ethylamine that is transported to the surface of the electrode. At higher flux or lower scan rates, the reaction is under surface-control, and limited by the rate of AuO formation. In the next section, the potential dependence of ethylamine adsorption is studied, using PED at the ring electrode.

Ethylamine adsorption using PED at the ring of a RRDE. For a heterogeneous reaction that is partially under surface-control, there is a strong possibility that adsorption of the analyte to the electrode surface is a part of the overall reaction mechanism. If the adsorption is accompanied by charge transfer, then its diagnosis is possible using cyclic voltammetry the disk. However, when charge transfer is negligible or absent, it is difficult to determine adsorption based solely upon the results obtained with a disk electrode. Instead, other experimental techniques are better suited to monitor adsorption. In a recent paper, the ring electrode of a Au-Au rotating ring disk electrode (RRDE) was used to monitor the adsorption of amine compounds at the disk electrode [19]. This was possible because the ring of a RRDE is essentially downstream from the disk electrode. This makes the ring sensitive to disk processes that affect the local concentration of ethylamine in solution. Pulsed electrochemical detection (PED) at the ring of the RRDE

was used to maintain ring activity for amine compounds, which are electrochemically inactive at noble metal electrodes under constant potential (DC) detection conditions. Using PED at the ring, the adsorption of aliphatic amines, amino alcohols, and the amino acid, glycine was determined as a function of applied disk potential. Here, a more detailed analysis of the RRDE results are presented for ethylamine.

Figure 6 shows the response for 40 μM ethylamine using cyclic voltammetry at the disk and PED at the ring of a RRDE. The disk current (i_d) and ring current (i_r) are both plotted versus the disk potential, which was scanned at 50 mV s^{-1}. The ring response was obtained using PED and a detection potential (E_{DET}) of 0.20 V, which provides the largest signal-to-background ratio for ethylamine. Region 1 of the ring response is the most readily explained based upon the apparent disk response. Because ethylamine is being consumed by the disk in this potential region, the flux of ethylamine to the ring is reduced. The ring current decreases accordingly, and results in the shielding response evident at 0.1 V $< E_d <$ 0.7 V.

The ring phenomena observed in region 2 is not at a potential where amine oxidation is believed to occur at Au, and so is not readily explained by the apparent disk response. Instead, region 2 corresponds to potentials where oxide reduction occurs at the disk electrode, and the shielding of ring current is attributable to the adsorption of ethylamine on the reduced Au surface. The magnitude of disk cathodic peak also slightly decreases in the presence of ethylamine. This is perhaps because the presence of ethylamine at the Au surface suppresses the formation of oxide on the positive scan. However, it also may be the result of ethyalmine adsorbing to the reduced Au disk

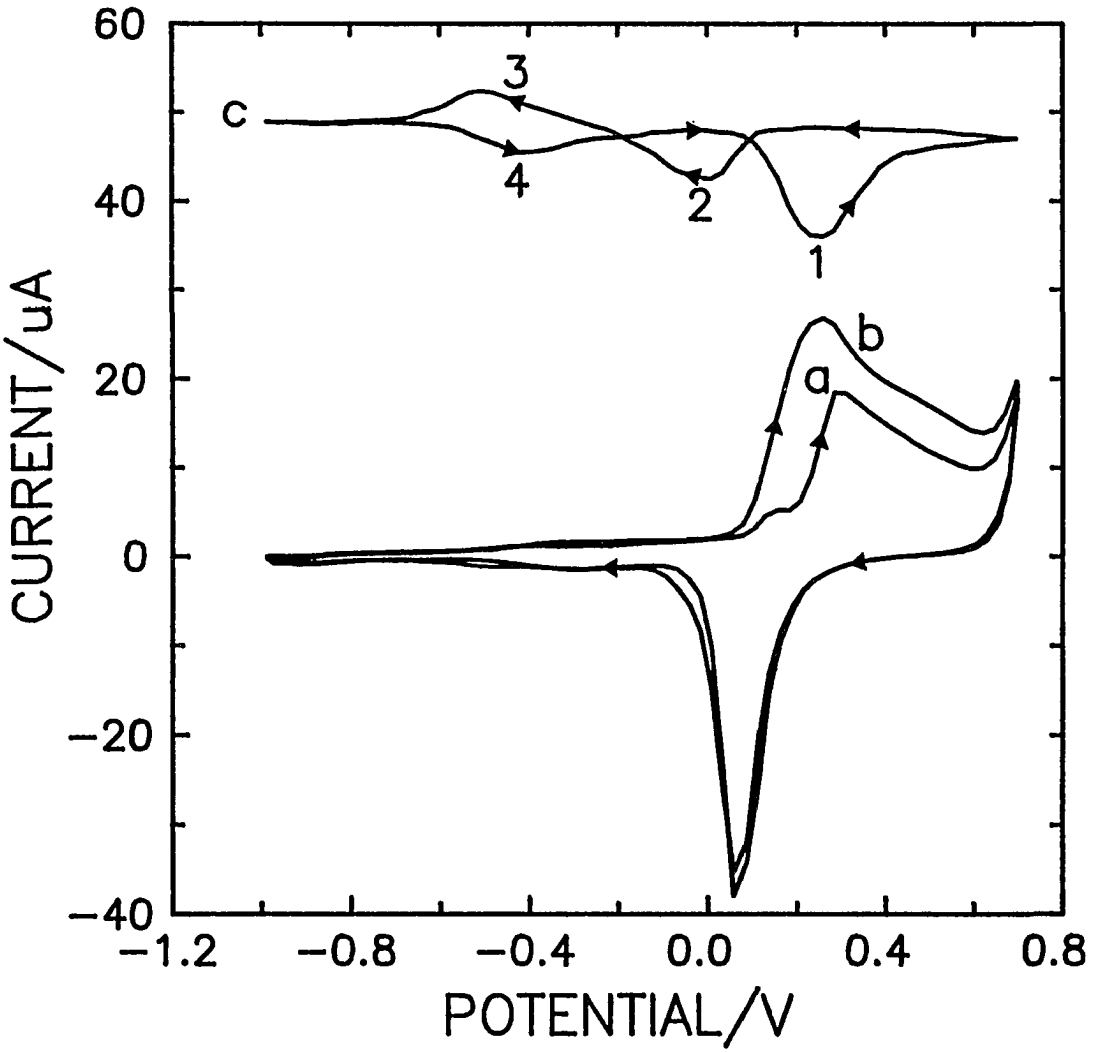

Figure 6. Voltammetric response for 40 μM ethylamine at Au in 0.1 M NaOH, with PED at the ring electrode. Rotational velocity: 900 rev min^{-1}. Disk scan rate: 50 mV s^{-1}. Curves: (a) disk, residual; (b) disk, 40 μM ethylamine; (c) ring (10x), 40 μM ethylamine; PED waveform: E_{DET} = 0.2 V (t_{DET} = 300 ms, t_{DEL} = 250 ms, t_{INT} = 50 ms); E_{OXD} = 0.8 V (t_{OXD} = 60 ms); E_{RED} = -0.8 V (t_{RED} = 90 ms).

with charge transfer.

At potentials corresponding to regions 3 and 4, the disk response is relatively featureless, both in the presence and absence of ethylamine in the solution. However, a change in the surface morphology is believed to occur at E_d = -0.5 V, which corresponds to the PZC for Au at pH 13. The change in the residual current observed at the disk at -0.5 V has been attributed to be the result of hydroxide adsorption in alkaline media. It is apparent that the adsorption of hydroxide promotes some form of interaction between ethylamine and the Au surface, and this results in the ring phenomena observed in regions 3 and 4. We speculate that ethylamine co-adsorbs with hydroxide ion to Au, and the increase in ring current exhibited in region 3 during the negative disk scan is the result of ethylamine desorbed with hydroxide as the disk potential is scanned negative of the PZC. On the positive disk scan, the ethylamine is re-adsorbed with hydroxide as the potential is made positive of the PZC, resulting in the shielding of ring current observed in region 4. Because the collection and shielding phenomena of regions 3 and 4 occur at the same potential, the co-adsorption of hydroxide and ethylamine is believed to be reversible.

The relative size of the ring shielding peaks in regions 2 and 4 provide for the possibility of more than one type of ethylamine adsorption occurring on the Au disk. The shielding of ring current in region 2, representing the maximum ethylamine adsorption, is larger than the shielding in region 4, representing reversible amine adsorption. Comparison of these two ring phenomena allows for a semi-quantitative description of the adsorption states. To accurately quantify the data, the ring response

was normalized to the response in the absence of any disk. This was done by acquiring the ring response with the disk at open-circuit, and then subtracted this current from ring response shown in Figure 6. The results are shown in Figure 7. Region 4, the ring shielding resulting from the reversible adsorption of ethylamine with hydroxide anion, is somewhat smaller than the shielding observed in region 2, representing total ethylamine adsorption. In quantitative terms, reversible adsorption accounts for only three-fourths of the total adsorption. The remaining 25% of the total adsorption is due to a second adsorption state, again perhaps the result of ethylamine chemisorbed directly to the Au surface.

The relative size of the ring shielding peaks in regions 1 and 2 can be used to divide the disk signal for ethylamine into two parts: (1) current from ethylamine mass-tranported to the electrode concurrently with the oxidation process on the positive disk scan (ETH_{MT}), and (2) current from ethylamine pre-adsorbed to the electrode at potentials negative of where oxidation occurs (ETH_{ADS}), but also oxidized when the disk potential is made positive of 0.10 V. Ring shielding in region 1 represents the contribution from ETH_{MT}, and the ring shielding of region 2 again represents the contribution from ETH_{ADS}. The relative size of the two regions shows that at a concentration of 40 μM, 35% of the total signal derived from the oxidation of ethylamine is from pre-adsorbed species, while 65% of the signal is the result of analyte mass-transported to the Au disk during the oxidation process. At lower concentrations, pre-adsorbed ethylamine is responsible for an increasing fraction of the total signal, whereas at higher concentrations, the percentage of disk response from ETH_{ADS} decreases. The size of the

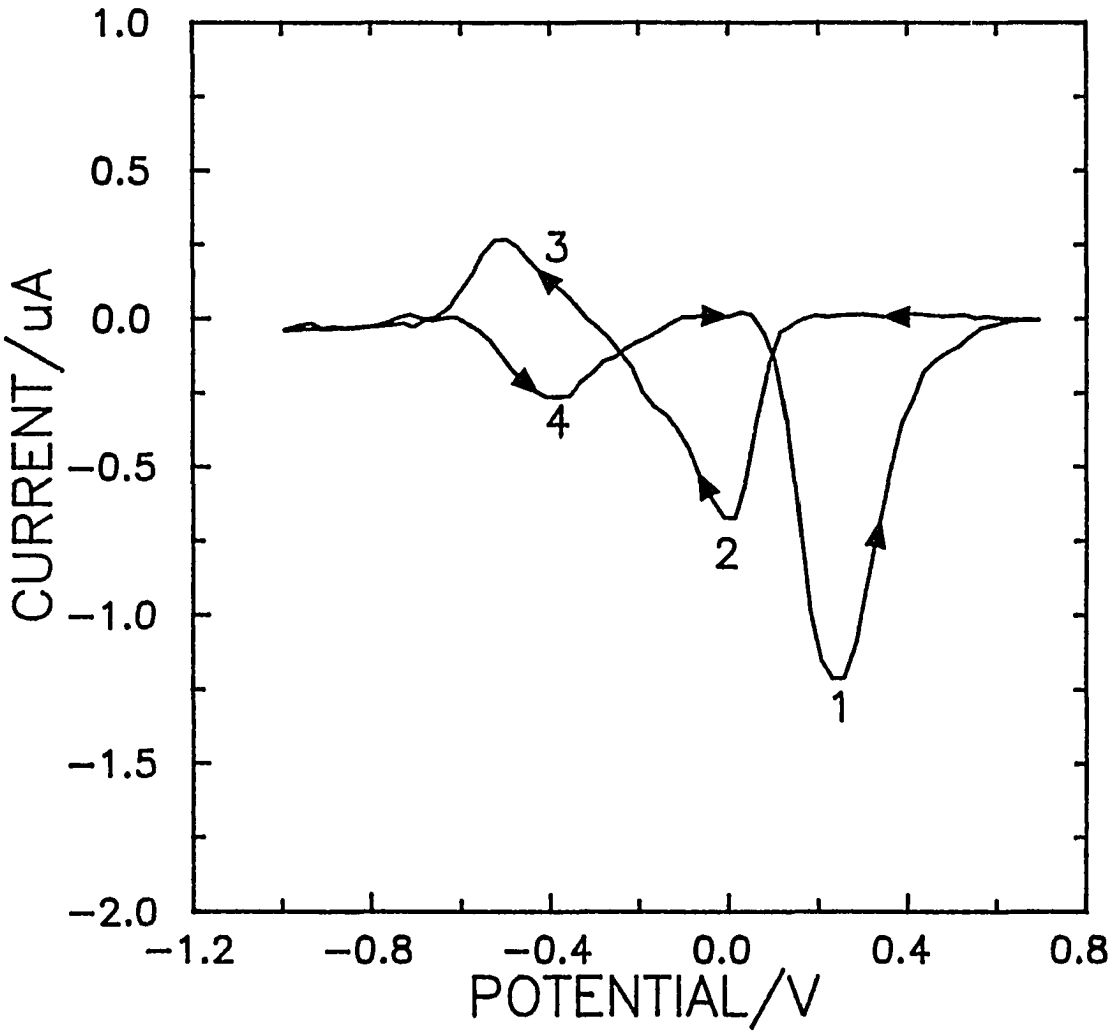

Figure 7. Normalized response for 40 μM ethylamine at the Au ring electrode in 0.1 M NaOH, versus disk potential. Reponse normalized to the current obtained for 40 μM ethylamine at the ring with the disk at open-circuit. Rotational velocity: 900 RPM. PED waveform: E_{DET} = 0.2 V (t_{DET} = 300 ms, t_{DEL} = 250 ms, t_{INT} = 50 ms); E_{OXD} = 0.8 V (t_{OXD} = 60 ms); E_{RED} = -0.8 V (t_{RED} = 90 ms).

shielding peak in region 2, while somewhat affected by the ethylamine concentration, reaches a maximum at concentrations less than 100 μM. This suggests that ethylamine adsorption is limited by the availability of suitable surface sites on the Au disk.

The RRDE data in Figures 6 and 7 indicates that during the positive scan between 0.1 and 0.7 V, maximum shielding of the ring current occurs at about the same potential, 0.2 V, where the maximum disk response for ethylamine is observed. However at potentials between 0.4 and 0.7 V, the shielding of the ring current diminishes, despite significant current still being generated from the oxidation of ethylamine at the disk. Therefore, the contribution from ETH_{MT} to the overall disk signal varies with the applied potential. Figure 8 shows the total disk current (curve **a**) for ethylamine (residual response subtracted), and the disk current due to ETH_{MT} (curve **b**), plotted versus applied potential. The difference between the two curves represents the portion of disk current from ETH_{ADS}. Ethylamine that is mass-transported to the disk surface at 0.1 V $< E_d <$ 0.7 V accounts for the majority of the disk current, especially at potentials between 0.25 - 0.30 V. However, at potentials greater than 0.40 V, virtually all of the ethylamine signal is from species adsorbed at less positive potentials.

The potential-dependent behavior of the disk response is perhaps better illustrated by Figure 9, which shows the fraction of integrated disk response attained as a function of disk potential. Curve **a** represents the total response for ethylamine at the disk, which by definition, reaches unity at the positive potential scan limit of 0.70 V. Curve **b** represents the fraction of integrated signal from ETH_{MT}, and curve **c** represents the

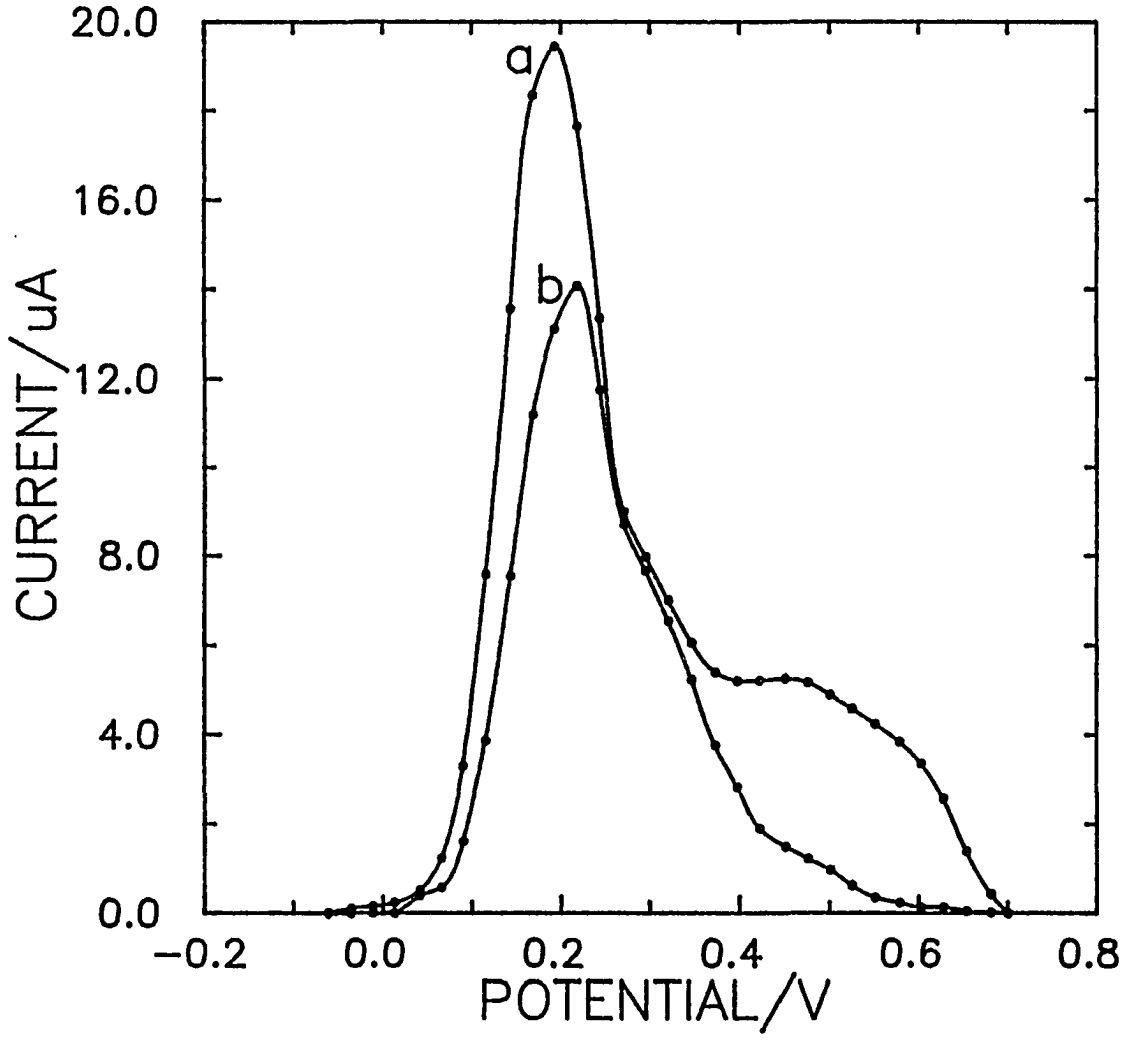

Figure 8. Disk signal for 40 μM ethylamine, with residual current subtracted, versus disk potential. Rotational velocity: 900 rev min^{-1}. Disk scan rate: 50 mV s^{-1}. Curves: (a) total disk current for ethylamine; (b) portion of disk current attributable to ethylamine that is mass-transported to the surface concurrently with the oxidiation process (ETH_{MT}).

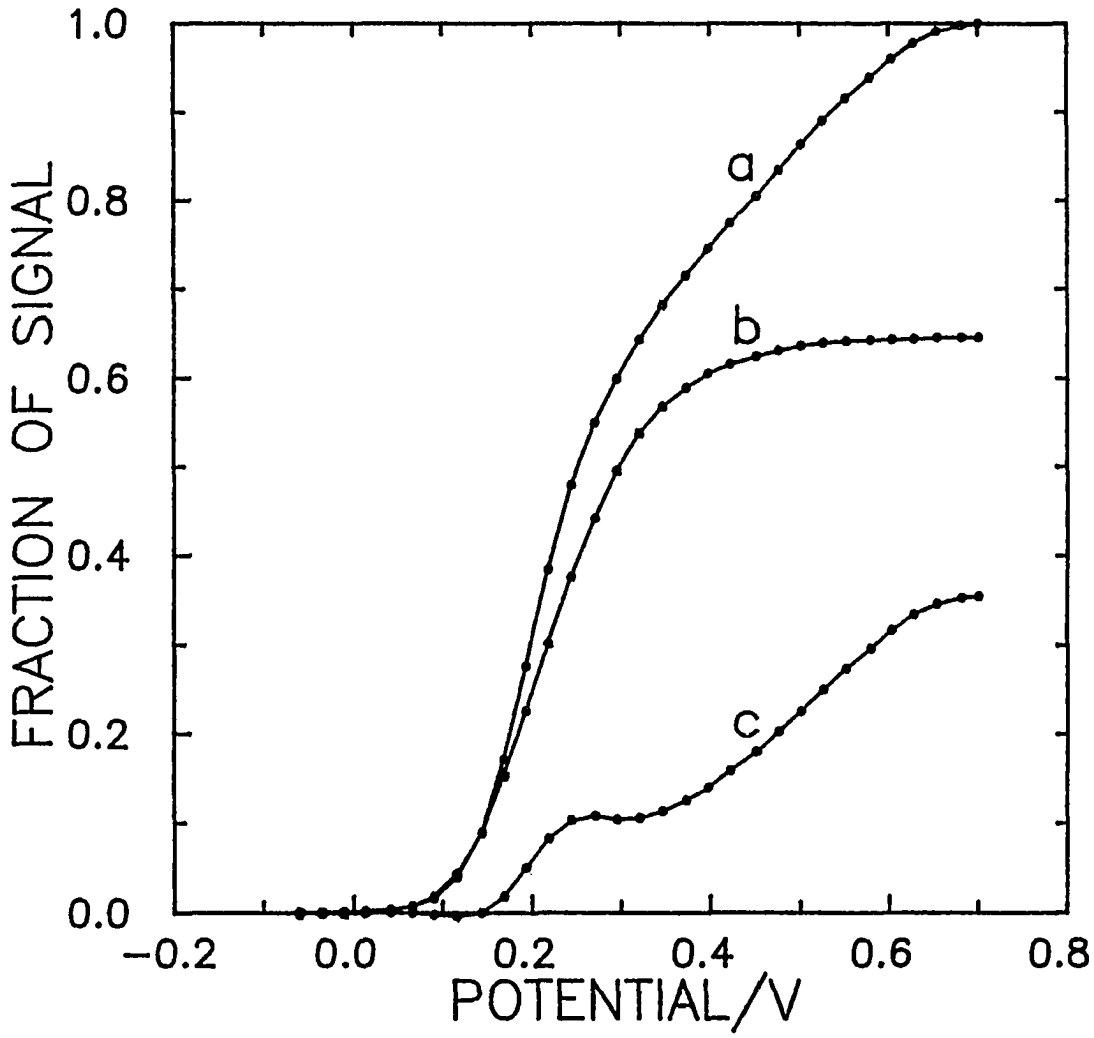

Figure 9. Integrated disk response, as a fraction of the total response, versus disk potential. Rotational velocity: 900 rev min^{-1}. Disk scan rate: 50 mV s^{-1}. Curves: (a) total disk response for ethylamine; (b) disk response due to ETH_{MT}; (c) disk response due to ETH_{ADS}.

fraction due to ETH_{ADS}. The data represented by curves **b** and **c** indicate that at $E_d <$ 0.40 V, only a small fraction of the disk response is due to ethylamine that had been pre-adsorbed at potentials negative of where ethylamine oxidation begins. However, at disk potentials between 0.40 and 0.70 V, the majority of the disk signal is provided by pre-adsorbed ethylamine.

Determination of n and possible reaction products. As shown by the results from cyclic voltammetry at the disk, the response for ethylamine at Au is a linear function of concentration and electrode rotational velocity under certain conditions. This is also true when PED is used instead of cyclic voltammetry, with the advantage that the PED response is linear over a larger range of C^b and $\omega^{1/2}$. The linear relationship between i and $\omega^{1/2}$ may be used with the Levich equation to calculate the value of n, the number of electrons transferred in the reaction, if the values of the other equation variables are known.

Figure 10 shows PED disk current versus the square root of rotational velocity for three different ethylamine concentrations. For each concentration, there is a region where current shows a linear dependence on $\omega^{1/2}$. Rearranging the Levich equation to yield

$$\frac{i}{\omega^{1/2}} = 0.62nFAD^{2/3}\nu^{-1/6}C^{b} \qquad (10)$$

allows the linear region of i-$\omega^{1/2}$ plots to be used to calculate n. The slope of the line representing $\Delta i/\Delta\omega^{1/2}$ was determined for several concentrations of ethylamine using

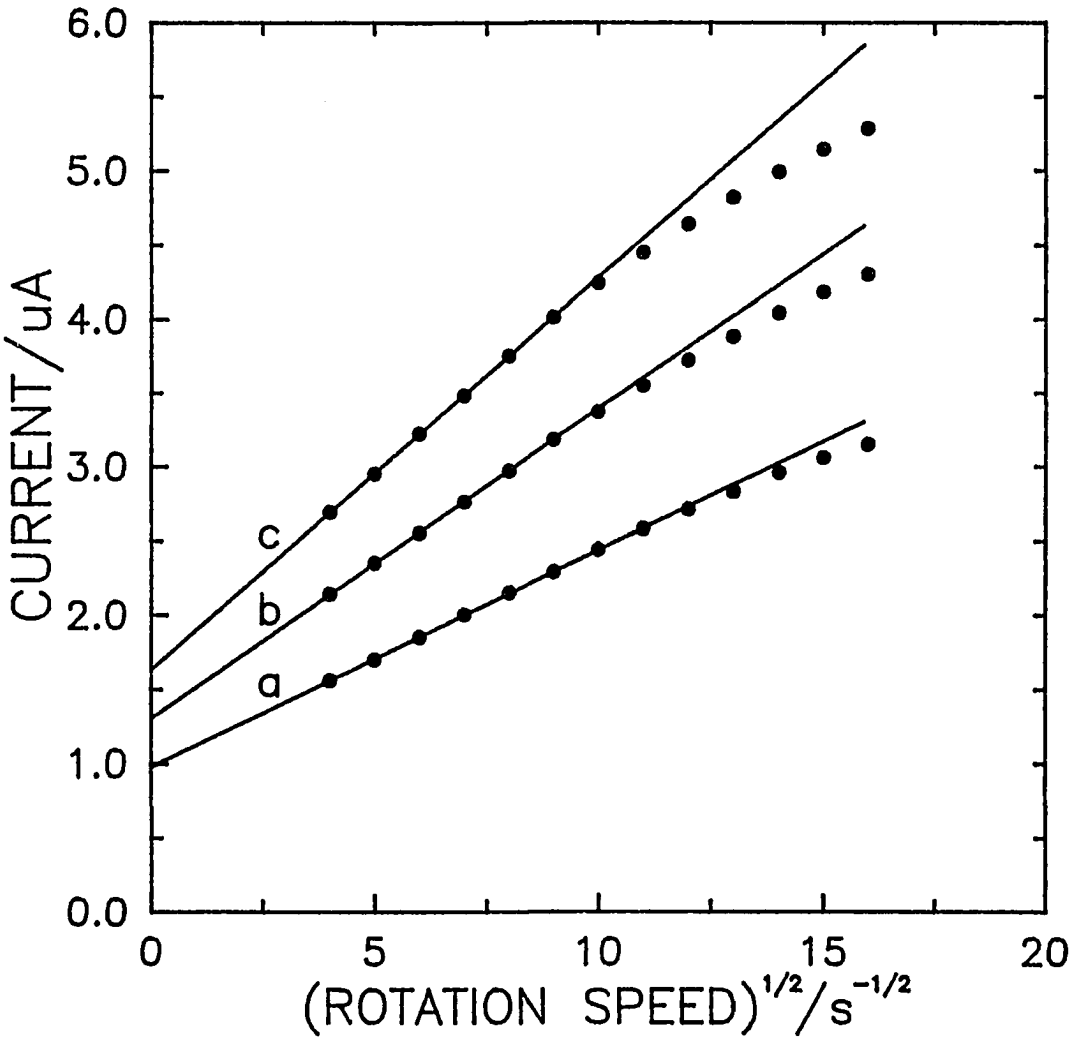

Figure 10. Ethylamine signal at Au disk with PED versus rotational velocity. PED waveform: E_{DET} = 0.2 V (t_{DET} = 300 ms, t_{DEL} = 250 ms, t_{INT} = 50 ms); E_{OXD} = 0.8 V (t_{OXD} = 120 ms); E_{RED} = -0.8 V (t_{RED} = 380 ms). Curves: (a) 5 μM ethylamine; (b) 10 μM ethylamine; (c) 20 μM ethylamine.

linear regression analysis. The value of A was the geometrical area of the disk electrode, and F had its usual value of 96,487 C eq^{-1}. The kinematic viscosity (ν) for a 0.1 M solution of NaOH is 0.0104 cm^2 s^{-1} [35]. Based upon the work by Cambell and Lam, the diffusion coefficient for ethylamine at low concentrations is approximately 1.3 * 10^{-5} cm^2 s^{-1} [36]. The average value of n for four different ethylamine concentrations is shown in Table 1.

Table 1. Experimentally determined n for the oxidation of ethylamine at Au in 0.1 M NaOH, using PED at an RRDE. PED waveform: E_{DET} = 0.2 V (t_{DET} = 300 ms, t_{DEL} = 250 ms, t_{INT} = 50 ms); E_{OXD} = 0.8 V (t_{OXD} = 60 ms); E_{RED} = -0.8 V (t_{RED} = 90 ms).

Concentration (μM)	n (eq mol^{-1}) $\pm$ std. dev.	number of trials
5	4.02 $\pm$ 0.29	3
10	3.16 $\pm$ 0.22	4
20	2.07 $\pm$ 0.11	4
40	1.64 $\pm$ 0.22	3

Although only regions where a linear relationship between i and $\omega^{1/2}$ were used to calculate n, the experimental values of n were dependent upon the concentration of the ethylamine. Therefore, it must be concluded that linear regions of i-$\omega^{1/2}$ do not necessarily indicate a mass-transport limited response for ethylamine, and so it becomes difficult to determine n by this method. However, the maximum value of n calculated by the method was approximately 4 eq mol^{-1}, at an ethylamine concentration of 5 μM.

The data in Table 1 can be used with the results of other studies to allow speculation as to the product of ethylamine oxidation in alkaline solutions. Based upon previous work by others at various metal and metal oxide electrodes [6, 12, 17], there are two possible products for the oxidation of ethylamine at Au, acetaldehyde (CH_3CHO) and acetonitrile ($CH_3C\equiv N$). Acetaldehyde appears to be an unlikely choice for the reaction product, because it involves only a two-electron transfer. As Table 1 shows, n values up to 4 eq mol^{-1} were obtained for ethylamine. Acetaldehyde also is unlikely to be the final product because aldehydes are highly reactive at Au in alkaline solutions, and provide a mass-transport limited response over a large potential region extending from -0.50 V to 0.10 V. Further evidence against acetaldehyde was provided by the RRDE. An RRDE experiment similar to that shown in Figure 2 was done using 40 μM ethylamine, but with a PED detection potential of -0.20 V at the ring. Using this detection potential, the ring shows no response for ethylamine, but is very sensitive for any aldehyde present in solution. No evidence of aldehyde was detected at the ring for several successive scans of disk potential between -1.00 and 0.70 V, and so we conclude that acetaldehyde cannot be the final product of ethylamine oxidation at Au in 0.10 M NaOH.

Therefore, the oxidation of ethylamine at Au tentatively is concluded to involve a four-electron transfer resulting in the production of acetonitrile. The formation of acetonitrile may explain some of the differences observed between ethylamine and ethanolamine signal at Au. The oxidation of ethanolamine results in the conversion of the alcohol functional group to the carboxylic acid. The product, glycine, is not believed to strongly adsorption to the Au surface, and thus would not foul the electrode surface.

This perhaps explains why the reaction of ethanolamine at Au in 0.10 M NaOH is mass-transport limited over a large potential region. Conversely, the likely product of ethylamine oxidation, acetonitrile, has been well-documented as being strongly adsorbed to metal electrodes, and because of this is used in competitive adsorption studies. We speculate that the formation of acetonitrile ultimately poisons the Au surface towards the oxidation of ethylamine, and thus necessitates potential excursions into oxide formation and dissolution to desorb the acetonitrile and reactivate the electrode surface for the oxidation of ethylamine.

Estimation of surface coverage. The RRDE data can be used to estimate both the total and reversible surface coverage of ethylamine at the Au disk. For a 40 μM concentration of ethylamine, the ring results (region 2) indicate that approximately 35% of the total disk current is due to contributions from pre-adsorbed ethylamine. Multiplying the total amount of current generated for ethylamine at the disk by 35% therefore yields the fraction of disk signal due to pre-adsorbed ethylamine. Once the current from pre-adsorbed ethylamine is integrated to yield charge, it can be converted into moles of ethylamine using

$$N = Q/nF \tag{11}$$

where Q is charge (Coulombs) and N is moles. Futhermore, by multiplying the moles of pre-adsorbed ethylamine by Avogadro's number ($N_A = 6.023 * 10^{23}$) the number of molecules of pre-adsorbed ethylamine is obtained. Surface coverage, defined here as the number of adsorbed molecules divided by the total number of Au atoms present on the disk surface, can be estimated by assuming the Au surface has a roughness factor near

unity [37]. Thus, the true area of the disk is approximated by the geometric area (cm^2). By multiplying the geometric area by an estimated Au surface density of 10^{15} atoms cm^{-2}, the total number of disk surface sites is found. Using data from three separate trials, the total coverage of adsorbed ethylamine on Au was estimated to be approximately 0.7 monolayers. As stated above, about three-fourths of this is reversibly adsorbed with hydroxide, and will desorb at potentials less than -0.5 V. Thus, the reversibly adsorbed ethylamine accounts for about 0.5 monolayers of surface coverage. Though the data from the RRDE experiments allows only for calculation of only an approximate surface coverage, the results were relatively consistent for the three trials (less than 0.1 monolayers difference). The calculated surface coverage depended slightly upon the concentration of ethylamine in solution. However, the maximum calculated surface coverage never exceeded one monolayer.

CONCLUSIONS

The electrochemical behavior of ethylamine at Au was studied using cyclic voltammetry at the disk and PED at the ring of an RRDE. The disk results indicate that the oxidation of ethylamine at Au is not entirely under either mass-transport or surface control. Instead, the reaction is under mixed control, and dependent upon the formation of catalytic surface oxide. The ring response permits a more complete characterization of the processes responsible for the oxidation of ethylamine at the disk, especially as to the role adsorption plays in the oxidation process. Using the RRDE about one-third of the total disk response was found to be from ethyalmine pre-adsorbed at potentials negative of where ethylamine oxidation occurs, with the remaining two-thirds due to ethylamine mass-transported to the disk surface concurrently with its oxidation. The ring data also indicated that there are two types of adsorption occurring on Au. Approximately 75% of the ethylamine adsorbed on the Au surface is reversibly co-adsorbed with hydroxide anion. The remaining 25% is the result of ethylamine chemisorbed to the reduced Au surface. The maximum surface coverage for ethylamine on Au was estimated to be less than one monolayer.

ACKNOWLEDGEMENTS

This work was supported by the National Science Foundation under grants CHE-8914700 and CHE-9215963.

REFERENCES

1. K. Stulík, V. Pacáková, K. Le, and B. Hennissen *Talanta* 35 (1988) 455.
2. J. S. Banait, G. Singh, and P. K. Pahil *J. Electrochem. Soc. India* 33 (1984) 173.
3. N. A. Hampson, J. B Lee, and K. I. MacDonald, *J. Electroanal. Chem. 34* (1972) 91.
4. G. Horanyi and E. M. Rizmayer *J. Electroanal. Chem. 198* (1986) 393.
5. C. K. Mann *Anal. Chem. 36* (1964) 2424.
6. K. K. Barnes and C. K. Mann *J. Org. Chem. 32* (1967) 1474.
7. V. A. Bogdanovskaya, A. Yu. Safronov, M. R. Tarasevich, and A. S. Chernyak *J. Electroanal. Chem. 202* (1986) 147.
8. B. Malfoy and J. A. Reynaud *J. Electroanal. Chem. 114* (1980) 213.
9. A. Yu. Safronov, M. R. Tarasevich, V. A. Bogdanovskaya, and A. S. Chernyak *Elektrokhimiya 19* (1983) 421.
10. N. A. Hampson, J. B. Lee, and K. I. MacDonald *Electrochim. Acta 17* (1972) 921.
11. N. A. Hampson, J. B. Lee, J. R. Morley, K. I. MacDonald, and B. Scanlon *Tetrahedron 26* (1970) 1109.
12. N. A. Hampson, J. B. Lee, J. R. Morley, and B. Scanlon *Can. J. Chem. 47* (1969) 3729.
13. M. Fleishmann, K. Korinek, and D. Pletcher *J. Chem. Soc. Perkin Trans. II 10* (1972) 1396.

14. P. Cox and D. Pletcher *J. Appl. Electrochem. 21* (1991) 11.

15. D. Pletcher, M. Fleishmann, and K. Korinek *J. Electroanal Chem. 33* (1971) 478.

16. A. Mohammad and I. Haque *Pak. J. Sci. Res. 29* (1977) 50.

17. R. C. Reed and R. M. Wightman in *Enclyclopedia of Electrochemistry of the Elements* Vol. XV, A. J. Bard and H. Lund (Eds.), Marcel Dekker Inc., New York, 1984 pp. 1-165.

18. W. A. Jackson, W. R. LaCourse, D. A. Dobberpuhl, and D. C. Johnson *Electroanalysis 3* (1991) 607.

19. D. A. Dobberpuhl and D. C. Johnson *Anal. Chem.* to be submitted.

20. V. G. Levich, *Physiochemical Hydrodynamics*, Prentice-Hall, Englewood Cliffs, New Jersey, 1962, pp. 60-72.

21. D. W. Kirk, F. R. Foulkes, and W. F. Graydon *J. Electrochem. Soc. 127* (1980) 1069.

22. G. N. Van Huong, C. Hinnen, and J. Lecoeur *J. Electroanal. Chem. 107* (1980) 185.

23. L. D. Burke, M. E. Lyons and D. P. Whelan *J. Electroanal. Chem. 139* (1982) 131.

24. S. Bruckenstein and M. Shay *J. Electroanal. Chem. 188* (1985) 131.

25. J. Desilvestro and M. J. Weaver *J. Electroanal. Chem. 209* (1986) 377.

26. H. Angerstein-Kozlowska and B. E. Conway *Electrochim. Acta 31* (1986) 1051.

27. G. N. Van Huong, C. Hinnen, J. Lecoeur, and R. Parsons *J. Electroanal. Chem. 92* (1978) 239.

28. C. Hinnen, G. N. Van Huong, A. Rousseau, and J. P. Dalbera *J. Electroanal. Chem. 106* (1980) 175.

29. J. S. Gordon and D. C. Johnson *J. Electroanal. Chem.* in press.

30. L. D. Burke and V. J. Cunnane *J. Electroanal. Chem. 210* (1986) 69.

31. J. E. Vitt, L. A. Larew, and D. C. Johnson *Electroanalysis 2* (1990) 21.

32. L. D. Burke and K. J. O'Dwyer *Electrochim. Acta 35* (1990) 1829.

33. L. D. Burke and B. H. Lee *J. Electroanal. Chem. 330* (1992) 637.

34. L. D. Burke and J. F. O'Sullivan *Electrochim. Acta 37* (1992) 585.

35. *CRC Handbood of Chemistry and Physics*, 59th Ed., R. C. Weast (Ed.) CRC Press, Inc., Boca Raton, Florida, 1979, p. D-303.

36. A. N. Cambell and S. Y. Lam *Can. J. Chem. 51* (1973) 4005.

37. J. F. Rodriguez, T. Mebrahtu, and M. P. Soriaga *J. Electroanal. Chem. 233* (1987) 283.

GENERAL CONCLUSIONS

Separations of amines and alkanolamines were performed on a multimodal high performance liquid chromatography (HPLC). The separation relied upon both cation-exchange and reverse-phase retention mechanisms of the mixed-bed column, and permitted baseline resolution of isomers using only isocratic elution. Diamines were not capable of being eluted off the multimodal column. This was attributed to their divalency in acidic eluents, which caused excessive adsorption onto the high-capacity multimodal stationary phase. Therefore, a low-capacity cation-exchange column functionalized with a carboxylic acid was used instead.

The response for each class of amine compounds differs at a Au electrode, and so voltammetry was used to optimize the pulsed electrochemical detection (PED) waveform used with HPLC. For alkanolamines, the optimum detection potential was less than 0.2 V. For the amines, cyclic and pulsed voltammetry showed that the optimum detection potential depended upon the concentration of acetonitrile in the mobile phase. The best signal-to-noise ratios were obtained for amines at a detection potential of 0.2 V, but more positive detection potentials also provided reasonable response. For diamines, a detection potential of between 0.4 V and 0.6 V was indicated, especially in solutions containing more than 10% acetonitrile. The effect of acetonitrile on the signal obtained for amine compounds at Au was attributed to the ability of acetonitrile to compete with the amines for adsorption sites on the Au surface.

Coupled with pulsed electrochemical detection (PED), the determination of

alkanolamines, amines and diamines was shown to be both sensitive and reproducible. Limits of detection (S/N = 3) using a 25 μL injection loop were 20 nM (500 fmol) for alkanolamines, 100 nM (2.5 pmol) for amines, and 200 nM (5.0 pmol) for diamines. For both alkanolamines and amines, the relative standard deviation (RSD) for several successive injections was less than 0.5%.

To investigate the voltammetric basis for amine response at Au, a new application of pulsed detection was demonstrated in which PED was applied to the ring of an RRDE. Simple amines and amino alcohols were shown to undergo potential-dependent adsorption at the Au disk in alkaline solutions, with a large percentage of the total adsorption being reversible. Maximum amine surface coverage was found at potentials between -0.5 V and 0.1 V. The similar results for amines and alkanolamines suggests that, for alkanolamines, the alcohol group does not affect the adsorption process. The results for glycine at Au differ from the other amines studied, suggesting that glycine adsorption is not controlled solely by the amine group, but is influenced by the carboxylate moiety as well.

Understanding the potential dependence of amine adsorption allows the PED waveform parameters to be chosen such that surface coverage is maximized. By maximizing surface coverage, more analyte is concentrated near the electrode surface and a larger signal is possible for amines determined by HPLC-PED. The benefit of promoting adsorption is most dramatic in the presence of acetonitrile, where the optimized PED waveform provides an order-of-magnitude improvement in aliphatic amine detection relative to a non-optimized waveform.

Using PED at the ring of an RRDE, a quantitative description of amine adsorption was made, emphasizing the importance of adsorption to the overall response. About a third of the ethylamine response at the disk was attributed to species that were pre-adsorbed at potentials negative of where ethylamine oxidation occurs, with the remaining two-thirds due to ethylamine that mass-transported to the disk surface concurrently with its oxidation. Results showed that about 75% of the total adsorption was from ethylamine that is reversibly co-adsorbed with hydroxide anion. In terms of fractional surface coverage, this represent about 0.5 monolayers, with total surface coverage by all ethylamine species estimated at 0.7 monolayers.

We anticipate that PED at the ring of an RRDE will have further application for monitoring adsorption at electrode surfaces. Current work in our laboratories continues to investigate the adsorption of both amines and sulfur compounds. Since the RRDE is already established as a tool for determining unstable electrode intermediates and reaction kinetics, we also expect that PED at the ring will have benefits in these areas as well. By using voltammetry at a RRDE to elucidate the mechanism and conditions responsible for the oxidation of amine compounds at noble metal electrodes, it is hoped that superior PED waveforms will be devised for amine compounds separated by HPLC and other chromatographic techniques.

LITERATURE CITED

1. Adams, R. N. *Electrochemistry at Solid Electrodes*; Marcel Dekker: New York, 1969.
2. Malfoy, B.; Reynaud, R. A. *J. Electroanal. Chem.* **1980**, *114*, 213-223.
3. Stulík, K.; Pacáková V.; Le, K.; Hennissen, B. *Talanta* **1988**, *35*, 455-460.
4. Banait, J. S.; Singh, G.; Pahil, P. K. *J. Electrochem. Soc. India* **1984**, *33*, 173.
5. Hampson, N. A.; Lee, J. B.; MacDonald, K. I. *J. Electroanal. Chem.* **1972**, *34*, 91-99.
6. Fleishmann, M.; Korinek, K.; Pletcher, D. J. *Chem. Soc. Perkin Trans. II* **1972**, *10*, 1396-1403.
7. Hampson, N. A.; Lee, J. B.; MacDonald, K. I. *Electrochim. Acta* **1972**, *17*, 921-955.
8. Hampson, N. A.; Lee, J. B.; Morley, J. R.; MacDonald, K. I.; Scanlon, B. *Tetrahedron* **1970**, *26*, 1109-1114.
9. Hampson, N. A.; Lee, J. B.; Morley, J. R.; Scanlon, B. *Can. J. Chem.* **1969** *47*, 3729-3736.
10. Amjad, M.; Haque, I. *Pak. J. Sci. Res.* **1977**, *29*, 50-55.
11. Cox. P.; Pletcher, D. *J. Appl. Electrochem.* **1991**, *21*, 11-13.
12. Pletcher, D.; Fleishman, M.; Korinek, K. *J. Electroanal. Chem.* **1971**, *33*, 478-479.
13. Barnes, K. K.; Mann, C. K. *J. Org. Chem.* **1967**, *32*, 1474-1479.

14. Mann, C. K. *Anal. Chem.* **1964**, *36*, 2424-2426.

15. Reed, R. C.; Wightman, R. M. In *Enclyclopedia of Electrochemistry of the Elements*; Bard, A. J.; Lund, H. Eds.; Marcel Dekker Inc.: New York, 1984, Vol. XV, pp 1 - 165.

16. Jackson, W. A.; LaCourse, W. R.; Dobberpuhl, D. A.; Johnson, D. C. *Electroanalysis* **1991**, *3*, 607-616

17. Bogdanovskaya, V. A.; Safronov, A. Yu.; Tarasevich, M. R.; Chernyak, A. S. *J. Electroanal. Chem.* **1986**, *202*, 147-167.

18. Safronov, A. Yu.; Tarasevich, M. R.; Bogdanovskaya, V. A.; Chernyak, A. S. *Élektrokhimiya* **1983**, *19*, 421-424.

19. Horányi, G.; Rizmayer, E. M. *J. Electroanal. Chem.* **1989**, *264*, 273-279.

20. Horányi, G.; Rizmayer, E. M. *J. Electroanal. Chem.* **1988**, *251*, 403-407.

21. Horányi, G.; Rizmayer, E. M. *J. Electroanal. Chem.* **1986**, *198*, 393-400.

22. Horányi, G.; Rizmayer, E. M. *J. Electroanal. Chem.* **1975**, *64*, 15-19.

23. Horányi, G.; Orlov, S. B. *J. Electroanal. Chem.* **1991**, *309*, 239-249.

24. Bogdanovskaya, V. A.; Horànyi, G. *Eletrokhimiya* **1989**, *25*, 1649-1651.

25. Horányi, G.; Rizmayer, E. M.; Simon, E. P.; Szammer, J. *J. Electroanal. Chem.* **1992**, *328*, 311-315.

26. Nguyen Van Huong, C.; Hinnen,; C. Lecoeur, J. *J. Electroanal. Chem.* **1980**, *106*, 185-191.

27. Desilvestro, J.; Weaver, M. J. *J. Electroanal. Chem.* **1986**, *209*, 377-386.

28. Kirk, D. W.; Foulkes, F. R.; Graydon, W. F. *J. Electrochem. Soc.* **1980**, *127*, 1069-1075.

29. Angerstein-Kozlowska, H.; Conway, B. E.; Hamelin, A.; Stoicoviciu, L. *Electrochim. Acta* **1986**, *31*, 1051-1061.

30. Alonzo, C.; Gonzalez-Velasco, J. *Z. Phys. Chemie* **1988**, *269*, 65-75.

31. Sawyer, D. T.; Chooto, P.; Tsang, P. K. S. *Langmuir*, **1989**, *5*, 84-89.

32. Burke, L. D.; Cunnane, V. J. *J. Electroanal. Chem.* **1986**, *210*, 69-74.

33. Burke, L. D.; O'Dwyer, K. J. *Electrochim. Acta* **1990**, *35*, 1829-1835.

34. Burke, L. D.; and Lee B. H. *J. Electroanal. Chem.* **1992**, *330*, 637-661.

35. Burke, L. D.; and O'Sullivan, J. F. *Electrochim. Acta* **1992**, *37*, 585-594.

36. Vitt, J. E.; Larew, L. A.; Johnson, D. C. *Electroanalysis* **1990**, *2*, 21-30.

37. Hui, B. S.; Huber, C. O. *Anal. Chim. Acta* **1982**, 134, 211-218.

38. Krafil, J. B.; Huber, C. O. *Anal. Chim. Acta* **1982**, *139*, 347-352.

39. Alexander, P. W.; Haddad, P. R.; Low, G. K. C.; Maitra, C. *J. Chromatogr.* **1981**, *209*, 29-39.

40. Kok, T. Th.; Hanekamp, H. B.; Bos, P.; Frei, R. W. *Anal. Chim. Acta* **1982**, *142*, 31-45.

41. Xie, Y.; Huber, C. O. *Anal. Chem.* **1991**, *63*, 1714-1719.

42. Krull, I. S.; Selavka, C. M.; Duda, D.; Jacobs, W. *J. Liq. Chromatogr.* **1985**, *8*, 2845-2870.

43. Allison, L. A.; Mayer, G. S.; Shoup, R. E. *Anal Chem.* **1984**, *56*, 1089-1096.

44. Cox, R. L.; Schneider, T. W.; Koppang, M. D. *Anal. Chim. Acta* **1992**, *262*, 145-149.

45. Hughes, G.J.; Winterhalter, K. H.; Boller, E.; Wilson, K. J. *J. Chromatogr.* **1982**, *235*, 417-426.

46. Elkin, R. G.; Griffith, J. E. *J. Assoc. Off. Anal. Chem.* **1985**, *68*, 1028-1032.

47. LePage, J. N.; Rocha, E. M. *Anal. Chem.* **1983**, *55*, 1360-1364.

48. Moore, S; Spackman, D. H.; Stein, W. H. *Anal. Chem.* **1958**, *30*, 367-388.

49. Stein, S.; Böhlen, P.; Dairman, W.; Leimgruber, W.; Weigele, M. *Science* **1972**, *155*, 202-212.

50. Stein, S.; Undenfriend, S. *Anal. Biochem.* **1984**, *136*, 7-23

51. Boykins, R. A.; Liu, T. Y. *J. Biochem. Biophys. Methods* **1982**, *7*, 55-65.

52. Dong, M. W.; Gant, J. R. *J. Chromatogr.* **1985**, *327*, 17-25.

53. Jones, B. N.; Paabo, S.; Stein, S. *J. Liq. Chromatogr.* **1981**, *4*, 565-586.

54. Carisano, A. *J. Chromatogr.* **1985**, *318*, 132-138.

55. Jones, A. D.; Homan, A. C.; Favell, D. J.; Hitchcock, C. H. S. *J. Chromatogr.* **1986**, *353*, 153-161.

56. Bidlingmeyer, B. A.; Cohen, S. A.; Tarvin, T. L. *J. Chromatogr.* **1984**, *336*, 93-104.

57. Heinrickson, R. L.; Meredith, S. C. *Anal. Biochem.* **1984**, *136*, 65-74.

58. Cohen, S. A.; Strydom, D. J. *Anal. Biochem.* **1988**, *174*, 1-16.

59. Wilkinsin, J. M. *J. Chromatogr. Sci.* **1978**, *16*, 547-552.

60. Grego, B.; Hern, M. T. W. *J. Chromatogr.* **1983**, *255*, 67-77.

61. Lin, J.-K.; Lai, C.-C. *Anal. Chem.* **1980**, *52*, 630-635.

62. Knecht, R.; Chang, J.-Y. *Anal. Chem.* **1986**, *58*, 2375-2379.

63. Hughes, S.; Meschi, P. L.; Johnson, D. C. *Anal. Chim. Acta* **1981**, 132, 1-10.

64. Hughes, S.; Johnson, D. C. *Anal. Chim. Acta* **1981**, 132, 11-22.

65. Johnson, D. C.; LaCourse, W. R. *Anal. Chem.* **1990**, *62*, 589A-597A.

66. Johnson, D. C.; LaCourse, W. R. *Electroanalysis* **1992**, *4*, 367-380.

67. Johnson, D. C.; Dobberpuhl D.; Roberts, R.; Vandeberg, P. *J. Chromatogr.* **1993**, *640*, 79-96.

68. Polta, J. A.; Johnson, D. C. *J. Liq. Chromatogr.* **1983**, *6*, 1727-1743.

69. Polta, J. A.; Johnson, D. C.; Merkel, K. E. *J. Chromatogr.* **1985**, 324, 407-414.

70. Martens, D. A.; Frankenberger, W. T. *J. Liq. Chromatogr.* **1992**, *15*, 423-439.

71. Martens, D. A.; Frankenberger, W. T. *Talanta* **1991**, *38*, 245-251.

72. Welch, L. E.; LaCourse, W. R.; Mead, D. A.; Johnson, D. C. *Talanta* **1990**, *37*, 377-380

73. Vandeberg, P. J.; Johnson, D. C., *Anal. Chim. Acta*. **1994**, *290*, 317-327.

74. Jackson, W. A. M. S. Dissertation, Iowa State University, 1990.

75. LaCourse, W. R.; Jackson, W. A.; Johnson, D. C. *Anal. Chem.* **1989**, *61*, 2466-2471.

76. Cambell, D. L.; Carson, S.; Van Bramer, D. *J. Chromatogr.* **1991**, 546, 381-385.

77. Polta, J. A. Ph. D. Dissertation, Iowa State University, 1983.

ACKNOWLEDGEMENTS

I would like to begin by recognizing Dr. Johnson for all the support and guidance he has provided during my tenure at Iowa State University. In addition to his role as a research advisor, he is a friend, mentor and advocate. Dr. Johnson is also perhaps the most principled person that I have had the privilege of knowing, and it has been an honor to work and learn under his direction.

I would also like to thank the many members of the Johnson group, past and present. In particular, I would like to thank Joe Vitt, from whom I learned a great many things in my first years at Iowa State, both in the laboratory and on the basketball court. I've also benefitted from the help and friendship of Pete Vandeberg, Rich Roberts and James "Tiger" Gordon. Pete, Rich and I spent over two years working together in the laboratory, and I enjoyed every minute of it. From Tiger, I learned a great deal about chemistry, teaching, and life in general. Together, with the rest of the members of the Johnson group, you made research more fun and interesting, and I will miss you all.

I'd also like to acknowledge two former students at Iowa State who are (proudly) not chemists: Joel Elmquist and Clint Schmidt. Over the past three years, we had a lot of fun, whether it was on the golf course, on the basketball courts, or around a card table.

Finally, I would like to thank my family, especially my parents, Dale and Earlene Dobberpuhl, for all the support and love they have provided in my many years as a professional student. I'd also thank my brother, Bryan. If I ever needed an unbiased

opinion, he was the one to ask. Last but foremost, I would like to thank my wife, Annie. You will never know how much you mean to me, and I look forward to our many years together.